2011-01-01

Improved Joining Method For Segmental Prestressed Structures

Ralph Warren Jensen
University of Texas at El Paso, ralphjen@gmail.com

IMPROVED JOINING METHOD FOR SEGMENTAL PRESTRESSED STRUCTURES

An Introductory Study

Ralph W. Jensen

Department of Civil Engineering

APPROVED:

Louis J. Everett, Ph.D., Chair

Soheil Nazarian, Ph.D.

Gary Hart, Ph.D.

John Harvey, Ph.D.

_____

Patricia D. Witherspoon, Ph.D.
Dean of the Graduate School

IMPROVED JOINING METHOD FOR SEGMENTAL PRESTRESSED STRUCTURES

An Introductory Study

By

RALPH W. JENSEN

DISSERTATION

Presented to the Faculty of the Graduate School of

The University of Texas at El Paso

in Partial Fulfillment

of the Requirements

for the Degree of

Doctor of Philosophy

Department of Civil Engineering

THE UNIVERSITY OF TEXAS AT EL PASO

May 2011

Improved Joining Method for Segmental Prestressed Structures

An Introductory Study

Publication No._____

Ralph W. Jensen, Ph.D.

The University of Texas at El Paso, 2011

Supervisor: Louis J. Everett

This dissertation addresses the need for more robust and materially efficient structures, specifically structures that absorb higher levels of energy, can self-erect and which have variable reaction capabilities. These structures can take much higher levels of strain and loading compared to current technologies in reinforced concrete and carbon fiber composites. These structures are made using a novel method of joining segmental elements. A great advantage with this segmental structural system is it's survivability under overloaded conditions. During an impact, or concentrated pressure load, the structure will wrap around the impact zone thereby widely distributing the contact stresses. This function or joining-method can be adapted to vehicles, or aircraft frames and other structures such as landing strips, bridges and buildings.

Self-erecting structures are also a function achieved by this innovation. This may be accomplished through the process of post-tensioning. A structure that is in a collapsed state but linked with tendons is pulled into an erect state as the tendons are tensioned. One example is a tower, which would slowly pull itself into a standing position one segment at a time as the tendon tension increased. At a fully prestressed state the tendons

would be anchored. Additionally, variable reactivity to loading can be incorporated into each joint function.

The joint structures incorporate rubber layers and end caps which are at the ends of each segment. The rubber layers are similar in function to the hyaline cartilage found throughout animal skeletal structures.

Table of Contents

List of Tables

List of Figures

Chapter 1: Introduction

1.1 Overview

The primary objective of this dissertation is to maximize structural strength and resiliency while minimizing the amount of material, i.e. reduce cost, for a broad range of structures. The motivation being the development of higher resiliency structures that can withstand higher levels of loading without catastrophic failure and maintain economic practicability.

Structural systems which may withstand higher levels of loading are desirable for greater survivability against various hazards such as earthquakes, wind storms, impacts, explosions, or traffic overloading. Many lives and billions of dollars are lost yearly to structural failure associated with such disasters. To these ends new concepts in joining segmental structures were developed and are presented in this dissertation. The concepts are applicable to modular prestressed structures (the context of prestressing, in this thesis, is prior to the structure being in-service). Proposals will be developed and analyzed through two practical applications: A stop sign post and pavement construction.

From a cursory view the assemblies look similar to segmental post-tensioned bridges and columns however the joints between the segmental elements are different in function and geometry. The essential unique aspect is a method for integrating rubber and steel elements into the joint structure. In current post-tensioned structures key joints are used to join the modular elements together.

Key joints help minimize random cracking and provide proper load transfer from module to module. However typically key joints are trapezoidal and require grout to reduce stress concentrations upon high loading[1] (see fig 1). The geometry of the proposed joints, presented in this study, is composed of combinations of elastomeric and steel layers.

However various other material interfaces were considered in the investigative process. Segmental element materials other than concrete are considered as well. One proposed embodiment of a joint is composed of opposing cylindrical or spherical surfaces that are held together by post tensioning tendons (see fig 4). Another proposed joint structure includes connectors, such as steel end caps on the ends of the concrete modular segments. One critical objective of the proposed concept is to reduce stress concentrations in the segments, which for this study will be considered as primarily concrete. Another is allowing large joint rotations upon overloading.

Large rotations or displacements, depending upon the degree of rotation, can require additional costs and complexity. Means of allowing additional tendon strain must be provided. Much more strain may be required than is provided in current post-tensioned systems. Although more costly and difficult to achieve than a simpler conventional static structure (details in sections 2.2 and chapter 5) the high deflections are useful in specific applications such as: vehicles frames, crash barriers, etc. Additionally, lubricant can be provided between the joint surfaces to enhance relative surface movements.

Assemblies of elements, in the proposed structural systems, may be configured into pole or columnar structures, or into planar structural elements, or complex 3D forms (frames, monolithic or planar constructs). This study will explore a small number of possible geometries and configurations, primarily to determine feasibility and direction for future research. The focal study is of a pole structure: specifically a comparison between a conventional prestressed sign post and one composed of the proposed system.

Prior work was explored and surprisingly there is nothing very similar. Segmental concrete bridges are similar in a number of ways however the joint structures between the segments are mostly intended to facilitate permanent bonding with the aid of grout between the segments. Various other structures and mechanisms have been developed over the years that address the goals of: improved structural resiliency and costs (while

maintaining strength and stiffness requirements) but they are quite different from what is proposed here.

Various detailed joint geometries were explored but a great deal of investigation still remains. Optimization of shape, materials and assembly details could be developed for many other applications and classes of structures not covered in this dissertation.

The focal study was conducted comparing stop sign posts: posts using the new concepts, to another conventionally structured post. The primary performance measure for comparison was the Resistive Moments: the pole strength as measured by the maximum reactive moments each pole could generate under shear loading. The shear loading represents a wind load. At the conclusion of this study the new concept shows a significant advantage in strength relative to tendon steel cost. In other words the new concept needs less tendon steel than the conventional pole for the same strength. The tendon steel is one of the most costly components for prestressed concrete structures. Through the course of this study two joint structure types were developed:

1) Composed of square end concrete segments bonded to sheet metal - steel layers with an elastomeric layer being bonded to the sheet metal (see figure 2). The elastomeric layer transverse center is the center of the joint.
2) Composed of cylindrically ended concrete segments bonded to elastomeric layers with the elastomeric layer bonded to steel end caps. The steel end caps have opposing journal bearing lobes which mate at the joint transverse center (see figure 2).

In both joint types the elastomeric layer serves to cushion or help redistribute the compressive stresses and the steel serves to reduce the tensile or shear stresses. For convenience the first joint type will be referred to as Elastomeric Butt Joints (EB Joints). And the second proposed concept will be referred to as Mechanistic-Static Joints (MS Joints).

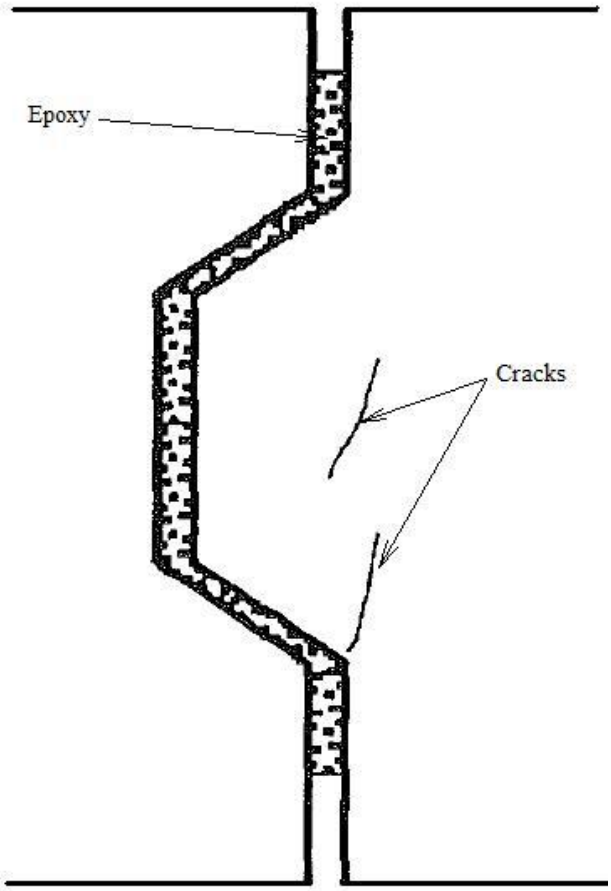

Figure 1. Typical Key Joint

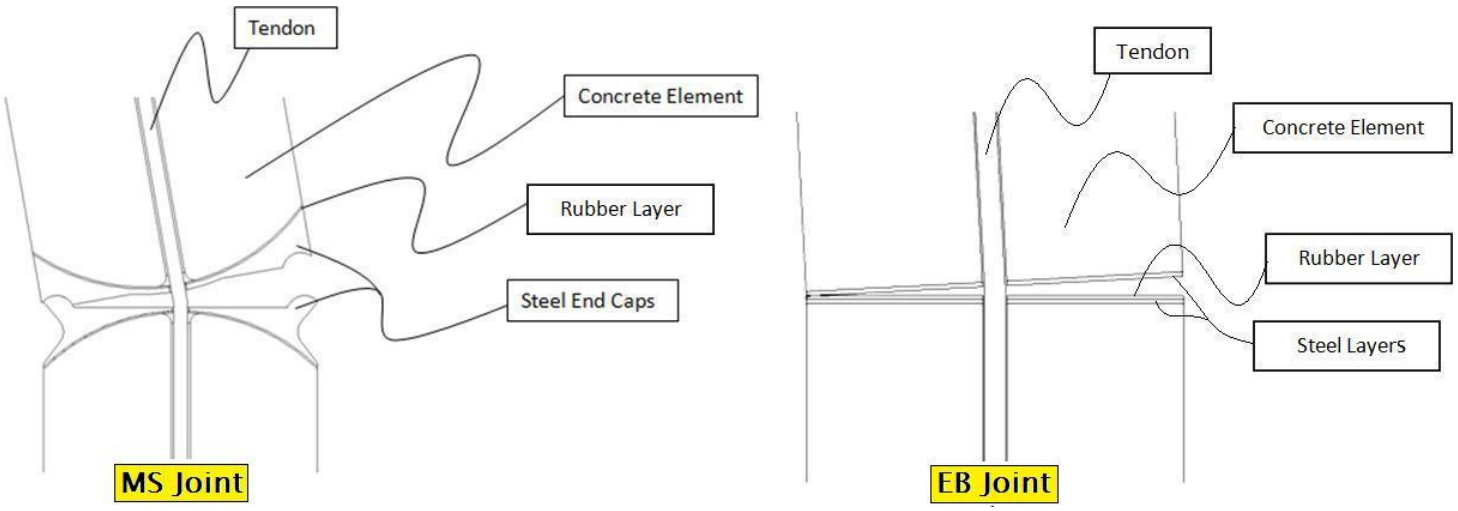

Figure 2. MS Joint and EB Joint, Cross Sections; Under High Deflection

There are two hypotheses that this dissertation will seek to prove:

1) That the new proposed joining structures can be made significantly stronger than the conventional prestressed monolithic structures, given the same sized structural dimensions, and steel costs; this is the over-strength comparison.

2) That less tendon steel is required to achieve an equivalent resistive moment for the proposed systems verses the conventional structure. The goal is to achieve the same strength, or stronger, structure for less cost; this is the reduced material comparison.

1.2 Investigation Method

The function of EB joints is to help minimize cracking and provide load transfer between segments. But unlike any kind of concrete on concrete joint, or crack, the compressive contact stresses are reduced through the cushioning action of the rubber layer. This cushioning effect appears to be somewhat complex in that the deformations of the rubber layer are a function of segment rotations and translations in multiple directions. Also because of the high value of an elastomer's Poisson's ratio very near 0.5, and the high level of ultimate strain, the rubber material flows away from areas of high compressive stress to areas of lower stress. For these reasons this cushioning effect is significant even with quite thin layers, such as 0.25mm. These effects are unlike that which occurs in a simple one dimensional compression of rubber between two relatively rigid objects; all objects being square in shape. This is essentially what occurs during the structure's pre-loading; when the rubber's cushioning affect is minimal.

The sheet metal layer acts to reduce tensile stresses at the terminal surfaces of the concrete segments. These tensile stresses are especially acute at the terminus of the crack, or joint openings, during high loading (see figure 3). Essentially the steel layer supports the concrete surfaces by absorbing the tensile stresses that would otherwise develop on the concrete surfaces. This property is evident in current steel encapsulated concrete[2].

The function of MS joints includes the same functionality as the EB joint system but with additional capabilities including: higher initial reactive moments, a fixed reactive lever arm (distance from journal pivots to tendon center line), relatively constant joint contact areas, and massive mechanistic structural deformations; as long as the tendon/(s) allow the additional strain required. Therefore there exist two domains for the MS joint concept: static and mechanistic.

In the static mode the MS joints act essentially the same as most other modular post stressed systems except that much larger rotational deflections can potentially occur

and the stress flow through the structural assemblies should be improved. The static domain is defined as the domain of linear deflections which are matched by the same domain of behavior seen in the conventional counterpart. Within the static domain there are some joint deflections which can occur in which the joints can open slightly, in a similar fashion as conventional structure cracks. In chapter 4 the detailed comparison is done between the new proposed systems and a conventional continuous concrete structure. The structure used in the comparison is a square cross sectioned pole. The conventional pole has a crack modeled into it at its base. As the pole is overloaded the crack lengthens until finally at a critical load the concrete cross section that is not cracked, catastrophically fails under compressive as well as tensile overload. This form of failure is the basis of Maximum Resistive Moment failure analysis of conventional prestressed concrete structures[10]. As the comparison in chapter 4 shows, the proposed concept will function in this domain of deflection and loading, and can potentially continue into a higher mode of deflection: the dynamic domain. Unlike the conventional prestressed concrete structure, either modular or monolithic, the joints will smoothly open up, which acts to prevent cracking. And unlike a crack, the MS joint concept acts as a journal bearing, potentially allowing large mechanistic movements. The dynamic mode involves mechanistic motions in which the structure acts as a multi-joint mechanism, potentially allowing for large deformations.

During very small deflections the stress fields at internal surface contacts and throughout the structural elements, can be affected strongly. This is because the stress flows are necked down thru smaller pathways as crack openings/angles increase. This is evident during crack formation in conventional concrete structures. Catastrophic failure can occur while crack openings are quite tiny; the maximum crack width in figure 3 (at failure) is only 0.25mm. If joint opening occurs within conventional trapezoidal key joints, stress concentrations can easily cause severe damage. Conventional key joints are

not designed to open up. To cope with intra-joint deformation under extreme loading epoxy grouts have proven to be helpful[1].

Grouted joints which are exposed to structural overloading will be damaged or destroyed when the joints open due to cracking, especially over repeated cycles. The proposed new types of joints are un-grouted and maintain relatively large contact areas as the joints react to external loading by opening. This is in contrast to either conventional key joints or random cracking.

The MS joint concept can take a wide variety of possible geometries however the common essential aspect is that the joint geometry is composed of opposing journal bearings. Figure 4 shows an early simple example of the basic concept implemented in a pole or column structure (developed by the author). In this example the joints are cylindrical and formed of male and female sides. Unfortunately this first concrete on concrete joint generated excessive tensile stresses and performed no better than a conventional monolithic concrete structure. However there is still potential for further development of this type of joint. It has the additional capability of allowing massive deformation. The high tensile stresses maybe mitigated through polymer injection surface strengthening.

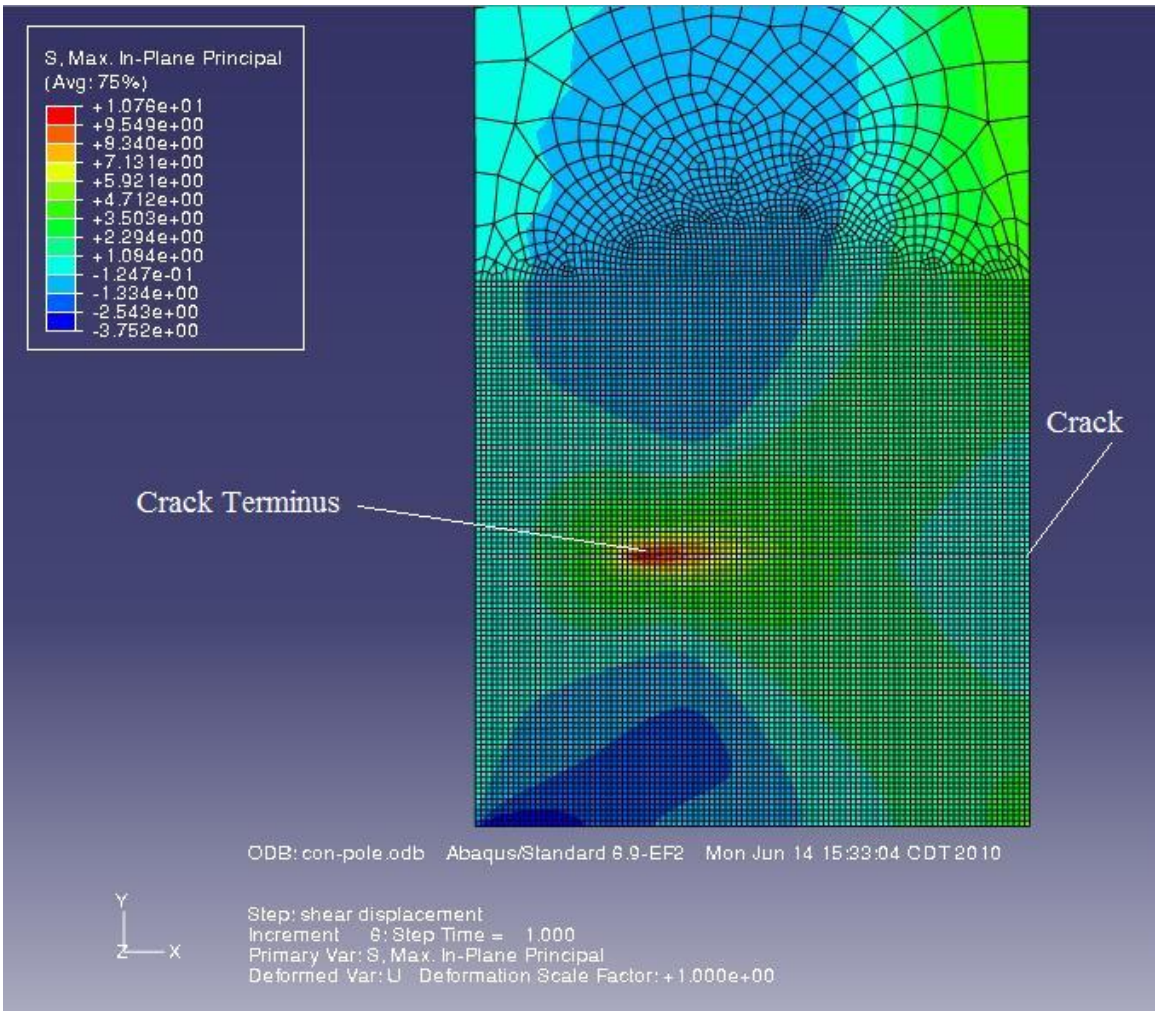

Figure 3. Conventional concrete pole under heavy loading (1.66E06 N-mm), with crack at base

A force diagram for the post model in figure 3 is illustrated in figure 21.

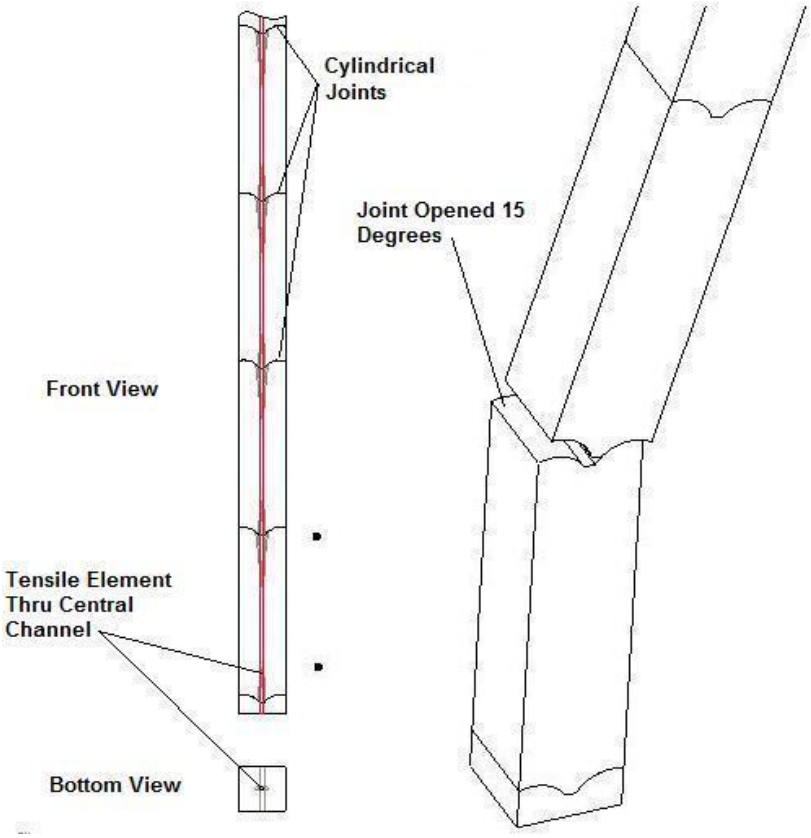

Figure 4. Simple two lobed pole structure

Figure 5 shows a pole structure with steel end caps at the compression element ends. This kind of MS joint shows much higher potential for load bearing than the concrete on concrete joints shown in figure 4.

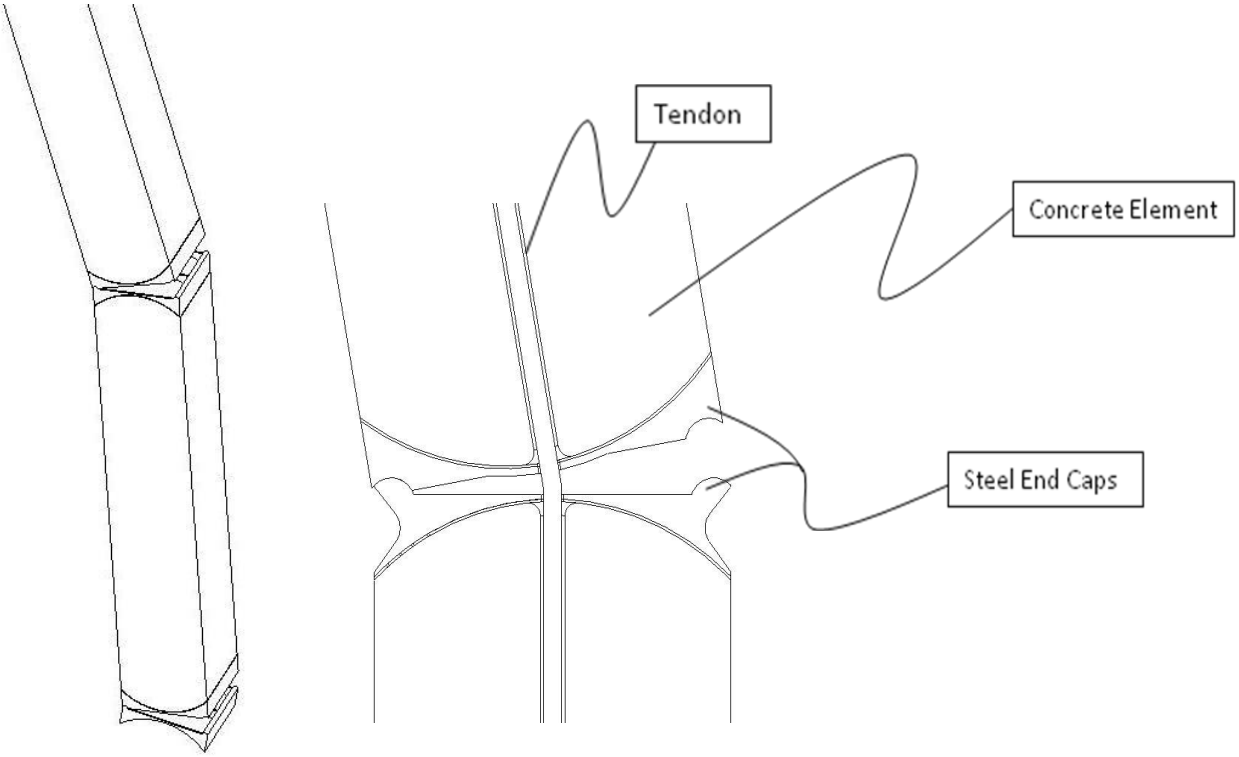

Figure 5. Pole structure, with two lobed steel end caps

As discussed above this study is on prestressed concrete structures, which are comprised of concrete for the compression elements (or bricks) and high tensile steel for the tension elements (or tendons), as well as lower grade steels for stirrup reinforcement; the stirrup reinforcement are only applicable to the conventional monolithic structures. In the MS joint end caps, or sheet metal layer, structures may use lower grade steels. The MS joint concept is not strictly limited to concrete and steel virtually any set of materials

can be considered (such as Carbon Fiber (CFRP) bricks and tendons, which might be used in aircraft designs). Other materials may prove to aid in many applications, such as fiber reinforcement, or polymer additives within the concrete.

1.3 Structure and Scope of Study

This dissertation presents an introduction of the MS and EB joint concepts. It starts with a general description, background and reasons for the study.

Chapter 4 is a comparison between the proposed structures to an equivalent conventional one. The structure used in the comparison study is a stop sign. The outer dimensions of the two comparison poles will be the same.

The comparison study is only within the static mode. This is because there is no dynamic or mechanistic mode possible for the conventional precast pole.

In chapters 3 through 6 classical methods of design and analysis of prestressed concrete poles/beams were applied. The primary calculation is for the Maximum Resistive Moment (M_R). And through Finite Element Analysis (FEA) the maximum principle stresses were determined. For the MS joint design, the geometry was evolved in order to keep the maximum principle stresses below yield and to simultaneously minimize the steel cost (i.e. minimize material). For both the EB and MS joint designs the material layers, material and arrangement, were varied in order to demonstrate the design optimization path. The process for optimizing the length of segments was also explored, for both joint systems.

In chapters 4 and 6 optimization of the proposed designs were conducted, in chapter 4 for the sign post and in chapter 6 for pavement structures. The method of shape optimization has primarily been manual, seeking to find at minimal a feasible configuration and shape. Feasibility is defined as achieving a joint which may match, or surpass the equivalent conventional structure's performance at acceptable cost. The

optimization was carried out as far as necessary in order to achieve a material cost which is the same or less than the conventional pole, while achieving a greater strength as compared to the conventional pole.

The results of the sign post comparison study will include design and maximum strength calculations for both the conventional pole and the proposals. Also included are iterative design methods for the MS and EB joint structures, and details of the FEA methodologies.

In chapter 6 concrete pavement applications will be explored. A series of proposed methods will be explored concerning the application of the EB joint in pavement construction. The focus will be on a post stressed design which seeks to minimize material cost as well as assembly complexity. This proposal will be looked at in the context of precast pavements, cast in place and rapid repair applications.

Overload behavior in the mechanistic mode is also discussed, for MS joints, as this presents a very interesting new field of study. The benefits and problems are investigated, as well as the different ways of solving the various problems with MS joint design. This field of study will also include new structural possibilities such as: vehicle frames with crash recovery capability, crash barriers with crash recovery, self erecting towers, new reactive structural systems, and practically any object in which the structural performance is critical.

The limitations of the studies in this dissertation are:

1) Extensive investigation into all the optimal elastomers for the new concepts was not performed (Neoprene or EPDM were used; very commonly used in construction).
2) There was no study into FEA optimization or degree of accuracy (for the most part Abaqus default parameters were used).
3) The study is purely numerical.

4) Modal analysis was not performed.

5) No dynamic FEA studies were done (only implicit FEA analysis).

6) FEA damage modeling was not included (Abaqus special damage elements or features).

7) No investigation into optimal lubrication for MS joints; although MoS_2 is a great candidate.

8) Final FEA comparison models did not include tendon elements or rebar.

9) The effects of vertical temperature gradients were not taken into consideration, in the pavement modeling and analysis.

10) 3D FEA modeling and analysis was not done for the pavement studies. So the Load Transfer Efficiencies (LTE) done for the 2D analysis should be considered too conservative, or on the low side (chapter 6).

11) The cost model for the sign post comparison did not include labor, manufacturing and construction costs. For the pavement studies no cost model was detailed.

12) Soil creep was no investigated; especially important for the retention dams in chapter 6.

The results will present comparison data from the simulation studies that show the potential capabilities of the new joint systems. There were two general capabilities explored for the new joints structures (within the sign post study): 1) to surpass the conventional structure in strength while using the same or less structural material: the "over strength" designs, 2) to match the strength of the conventional structure but with significantly less material used; the "reduced material" designs.

Chapter 2: Behavior Modes

2.1 Static

A crack in a conventional prestressed concrete structure is not controlled. Its geometry can vary unpredictably and typically will take a jagged path. In relation to classical prestressed concrete strength analysis, cracks are idealized as planar and perpendicular to the longitudinal direction of the structural body. As the external loading varies, the idealized crack creates a variable cross section for the longitudinal stress paths. As the crack width increases the compressive stresses reach yield and cause catastrophic failure. As will be discussed further in chapter 3 the steel index (the ratio of the tendon strength to the concrete strength) will generally be above 0.4 for the concrete to fail before the tendon. Otherwise for lower steel index ratios the tendon is relatively weak (too small in diameter) and will fail before the concrete fails[10]. So for a steel index of 0.4 the tendon and concrete are generally considered of equal strength. However with the MS joint concept the journal contact area remains relatively constant throughout loading, including after joint opening.

In the static structure domain, the MS and EB joints act like completely-controlled cracks, in that they offer tensile stress relief like cracks, but the surfaces are not random or jagged like cracks. Also for the MS joints depending upon internal forces such as friction, the joints can act as journal bearings. As the external loading increases, the internal compressive forces shift from equal loading on each opposing joint lobe, to one of the lobes, on one side of the joint. This in turn creates a reaction moment. The internal contact forces, in the journal or socket, act through the center of each bearing surface. As external loading increases at some point the contact forces of one side of each joint lobe pair becomes zero and at this point that side of the joint will begin to open up (see figure 34). Once the joint opens the reactive lever arm remains constant. As an MS

joint opens up due to external loading, internal frictional forces must be overcome. It is at this point that the structure may be considered a mechanism. However for purposes of comparison between MS joint and conventional prestressed concrete, the MS joint will be considered still within the Static domain until the range of movement, or rotation, surpasses that which an equivalent conventionally cracked concrete structure would rotate. Relative to a structure's width, or depth, these are very small deflections, or crack openings.

For the EB joint the opening is similar in action to the conventional structure's idealized crack. The reactive lever arm is variable throughout variations in loading. The lever arm being the distance between the tendon center line and the centroid of the reaction stresses at the joint boundary.

As discussed above both the EB and MS joints utilize elastomeric layers and steel structures, at the concrete segment ends. At these layers and their corresponding boundaries the stress fields can be fairly complex. Consequently any simplified analysis such as that utilized in classical strength of materials studies is not applicable, so FEA methods are required. Another consideration pertaining to the stress strain analysis is that for the conventional, EB and MS jointed structures, the areas under the closest scrutiny are the transition zones at and around the segment or crack boundaries.

For conventional prestressed concrete structures, such as the conventional pole in this study, modified beam equations are typically utilized for stress analysis. Because of the initial prestressing tendon load, the transverse cross section of the beam is under a uniform compressive stress. Subsequently after beam loading the stresses from classical beam equations are superimposed upon the initial stress field. As loading increases to the point that tensile stresses occur in the concrete, then it is assumed that a crack develops at the location where tension initiates.

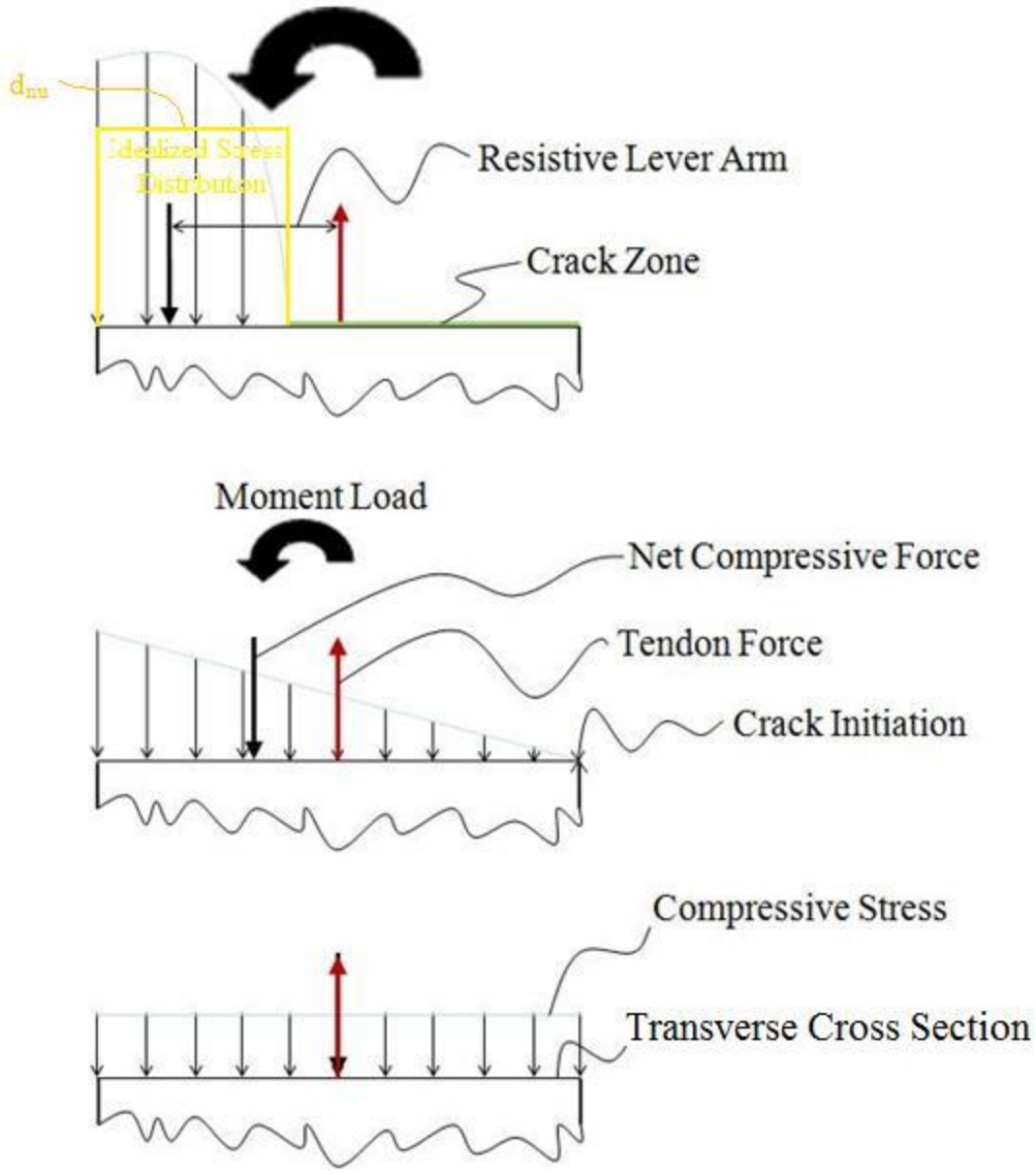

Figure 6. Transitional Stress Field for the Conventional Concrete Pole

Figure 6 illustrates the transition of the internal stress field through the cross section of the conventional concrete pole. At the bottom of the figure is shown the stress field with only the tendon preload. Then as the external shear load is applied a corresponding moment develops. As the loading increases the stress level drops to zero at one end of the cross section plane. Because it is assumed that any degree of tensile stress

at a location causes a crack to develop at that location, a crack will start to develop at the zero stress level point. This condition is shown in the middle of figure 6. Subsequently the crack grows as the external loading increases. Shown at the top of the figure is the state where the maximum compressive stress reaches yield within the uncracked zone at which point the concrete pole will completely fail. This idealization of the stress field, reacting moment and crack propagation have proven to be a fairly accurate approximation[10, 12, and 13]. However the actual stress fields are much more complex, because of the non-planarity of the actual cracks, including spider cracks.

What further complicates the stresses, and failure analysis of conventional reinforced concrete structures is the reinforcement that is not prestressed. This typically is composed of longitudinal, transverse as well as hoop steel bars or wire. This reinforcement helps hold the structure together after cracks develop, and are mandatory in most concrete structures. This reinforcement steel complicates the failure analysis and is often neglected with relation to analysis of conventional structures.

It is important to mention that repeated high load cycling in conventional reinforced concrete structures tends to degrade the structure's integrity. This occurs through the progressive concrete damage at the crack boundary zones. Through repeated cycles of loading the cracks can degenerate with spalling and aggregate debonding. Results obtained from testing reveal how cracks degrade. Three phases of damage occurs: First degradation of the fine particles occurs. Next the larger aggregate begins to bear against each other. Finally the aggregate cracks and debonds from the remainder of the concrete whereupon structural failure occurs[3]. Simulation results indicate that this type of failure is much less likely to occur in the EB or MS joints (shown in section 4.3.1). That presents a great advantage in terms of long term structural reliability.

A basic function of a great many structural elements is to provide as large a resistive moment (M_R) as possible given a certain amount of construction materials and dimensional requirements/restrictions. For the new joint concepts a main goal is to

maximize the M_R which a structure can generate. In order to do that the resistive lever arm between the longitudinal reaction force at the pivoting lobe/(s) and the tendon center must be maximized (see fig 15). The limitations to this lever arm length are: the width of the pole, and the limitation which are coupled to the material stress levels. That is when the journal surface is so small that it fails under a given loading. The smaller journal size allows a longer lever arm. The goal is to maximize the M_R representing a structure's strength.

In other words this becomes an optimization problem of maximizing the M_R (a function of the joint geometry), while remaining below the tensile and compressive yield stresses. The primary variable is the lever arm length, but a plethora of shape details as well as assembly alternatives affect the achievable maximum M_R. The detailed methods of calculating the M_R is discussed below in section 3.3.

There appear to be a few potential advantages with the proposed joints relative to conventional prestressed concrete structures, in the static domain.

1) The stress concentrations for the MS joint are relatively constant as a function of loading, while with conventional structures crack length varies along with corresponding stress concentrations.
2) Repeated cycling within a joint, or crack opening domain, is detrimental to conventional concrete while for EB or MS joint structures there can be expected to be little or no ill effects.
3) There are many more design options available for controlling maximum stresses with the proposed joints than are available with conventional prestressed concrete. That is through shape, and assembly optimization as well as material variations.
4) Depending upon maximum stress levels within an MS joint structure's static domain, an MS joint structure may continue its deflection behavior into a mechanistic mode, i.e. much larger rotations at each joint.

2.2 Mechanistic

Only the MS joint system has a mechanistic mode. In the mechanistic structural domain, the MS joints act like journal or ball joint bearings. As stated above additional costs and complexity may be required for an MS joint structure to act in the mechanistic mode. As a structure becomes sufficiently overloaded one joint will begin to open and continues to open with increases in external loading.

As any structure fails in overload the strain energy stored in the structure as well as the energy being added through external loading, will tend to drain into the weakest point - the point of failure: such as a crack, highest yield point, or highly deformed point. In the MS joint structure this would be the first joint to open up. For optimal structural efficiency in relation to minimal material usage, the maximum strain energy that a structure can absorb may be considered a good objective measure.

The overall MS joint structure can act much like a break-over mechanism in that subsequent to the first joint opening any additional loading will continue to open that joint up more and more. A break-over mechanism will hold a static structural shape until the loading exceeds a certain level, whereupon the structure will give way in a generally controlled collapse which may be fully recoverable. For some structural applications this kind of break-over function is desirable such as for the basketball goal post illustrated in figure 11. And the MS joint structure concept can provide this functionality when sufficient strain is provided to the tendon.

For most structural applications it is desirable for the structure to hold its original unloaded (externally unloaded) shape, or as close to this initial shape as possible. Up to the point of initial joint opening the MS joint structure will provide this capability much as a conventional prestressed structure does. And as explained more fully below, for a given amount of material, the MS joint will surpass a conventional structure in terms of maximum loading before collapse. In order to avoid the break-over event each joint

requires a rotation limiting device; or leash. This is so that the energy being loaded into a MS joint structure maybe distributed throughout any number of segmental elements and joints. The energy would also be more effectively distributed through the tendon, or network of tendons, by the use of leashes (rotation limiting devices). The structure would also maintain more of its static integrity as opposed to an extreme collapse of one particular joint (see figure 7).

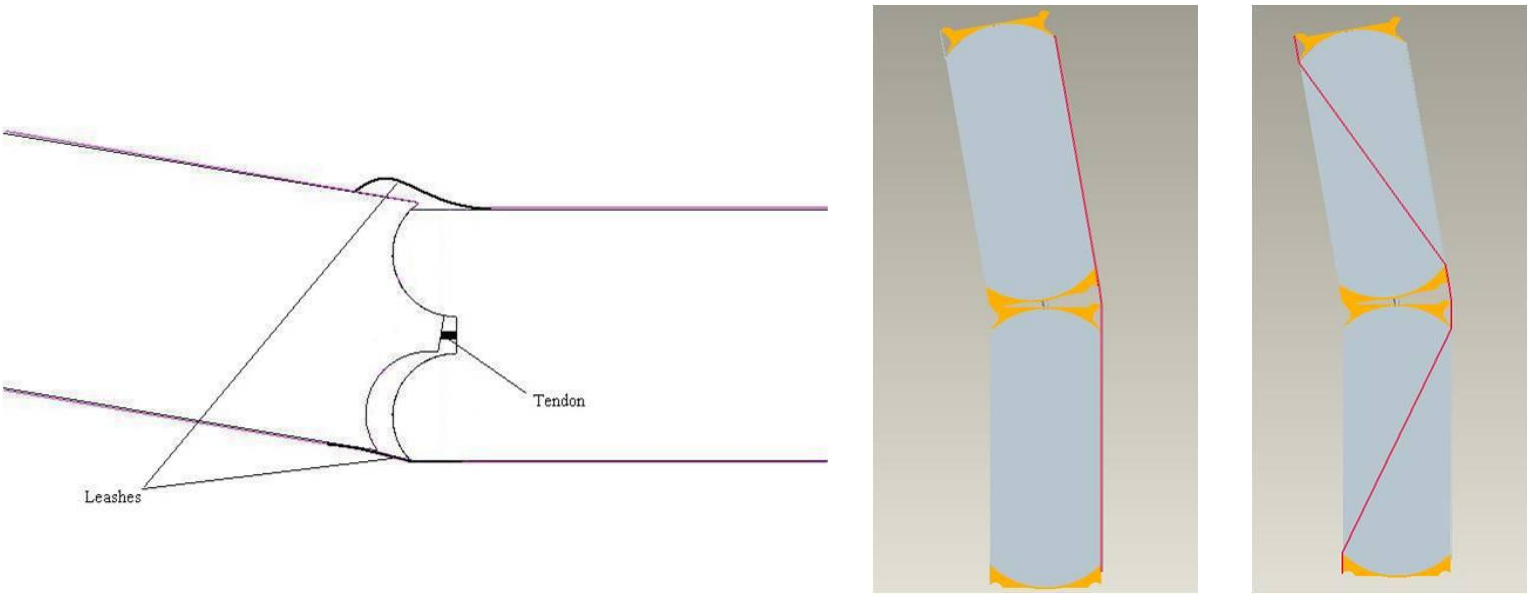

Figure 7. Leash Configurations

Once the mated male and female pivot lobes begin to have relative movement between them, friction will play a critical role in the mechanistic behavior. The friction may have beneficial effects, as well as detrimental ones depending upon the level of frictional forces and the structural application being considered. Friction can help dampen dynamic movement in a given structure. Also it can provide an additional counter-moment to the imposed loading. But it may cause jerky motion as a structure deforms

into the mechanistic mode. And it may cause locking of the joints when it is desirable for the structure to massively deform, or fully recover.

Dynamic dampening would be a great asset to have within a structure, for many overloading scenarios such as earthquakes. This may be achieved via the friction within each MS joint, as well as between tendons and their channels. Friction if too high will setup undesirable internal stress levels within the MS joints. Therefore the choice of a joint lubricant may be important. MoS_2 is a very good candidate as it has a low friction coefficient and is chemically stable. It could be applied as a powder during assembly or molded into the joint surfaces.

In order for an MS joint structure to operate in the mechanistic domain there must be some margin of stress available at the extreme end of the static domain otherwise either the concrete elements or tendons will be stressed beyond yield. The key component to the enabling of mechanistic behavior is that the tendons must allow additional strain above the levels reached at the end of the static domain. That is, when a joint opens, the gap that develops between the segments at the tendon axis can present an enormous strain to the tendon. Means for allowing this strain must be provided for the mechanistic mode to exist. Chapter 5 develops a number of detailed proposals for accomplishing this function.

Within a conventional prestressed concrete structure the tendon lengths are grouted within their respective channels, or cast in place after being prestressed, or, allowed to move relatively freely within their channels after post tensioning. In all these scenarios the tendons almost always terminate, or are anchored, at the ends of a structural component such as a beam, column, slab, or in the case of segmental bridges across entire bridge structures. In MS joint structures, the tendons must remain free to move after post tensioning, between anchors for the mechanistic mode operation.

The mechanistic mode of the proposed system introduces additional concrete stresses beyond those that exist at the terminus of the static domain. This is because of

accumulated moment build up required for successive joint openings. Therefore additional concrete strengthening must be provided or the stress levels at the end of the static domain must be held to considerably lower than yield. The strengthening can be done with either reinforcement: steel wire/rods or fibers, or with polymer surface impregnation, etc. The mechanistic mode includes: larger force vectors angles, friction forces, dynamics, tendon contact forces and leash forces, plus accumulated moment/shear loading to open higher successive joints. All these factors tend to increase the stress levels in the segments and tendons.

Chapter 3: Background And Approach

3.1 Prior Work and Current Practice

Robert Englekirk developed construction methods that achieved greater structural resiliency. His primary focus is in structures that resist earthquake damage. He uses a variety of techniques which involve the joining of precast members[4]. One technique is a joint structure which allows relatively large angular rotations between members; however in this arrangement structural compliance is achieved through grout deformation/damage (see figure 8). In large earthquakes the joint grout could be over stressed and need to be reapplied. Structural repair could also have to be done for tendons and reinforcement steel. However the structural damage would be minimal and only to grout sections, which would allow the reuse of all concrete precast components.

Englekirk's precast building structures have been shown to perform much better under earthquake loading relative to cast in place methods. The proposed joint structures of this dissertation should have the same advantages without as much structural rehabilitation required. Additionally the elastomer layers throughout the structural elements should provide additional damping that aids in earthquake response.

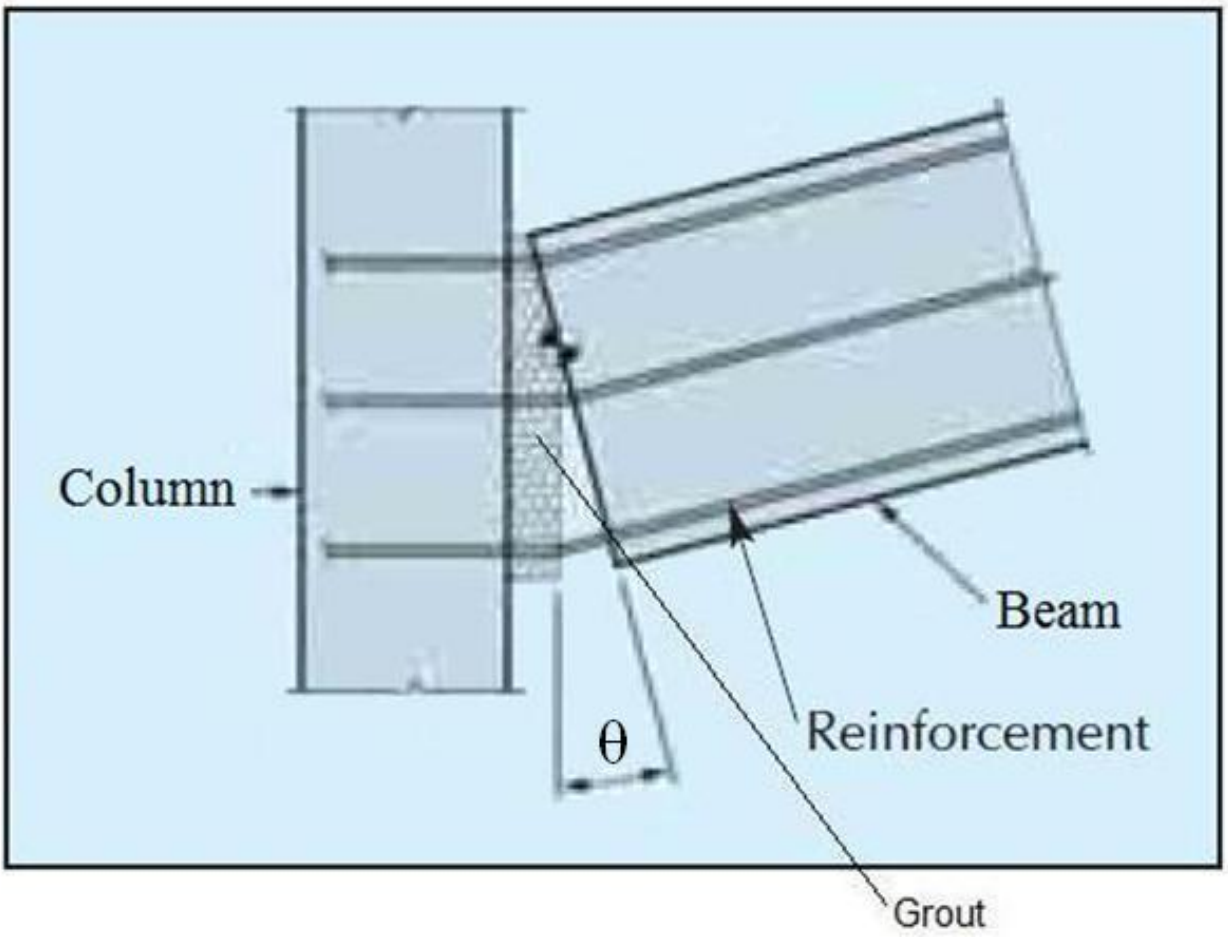

Figure 8. Englekirk's Precast Frame Joint[4]

Post-tensioned segmental bridges, in many ways, resemble the proposed joint concepts (see figure 9). The EB joint system is especially similar in that the ends of concrete segments are square and essentially butt joints. In fact through the elimination of the grout between the segment faces and replacing that with sheet metal and rubber layers, nearly the same bridge segment geometry could be used. The strength improvement however should be at least 54%, using the results from section 4.3.1. In

regard to the key joints in the conventional bridge segments they could also be eliminated.

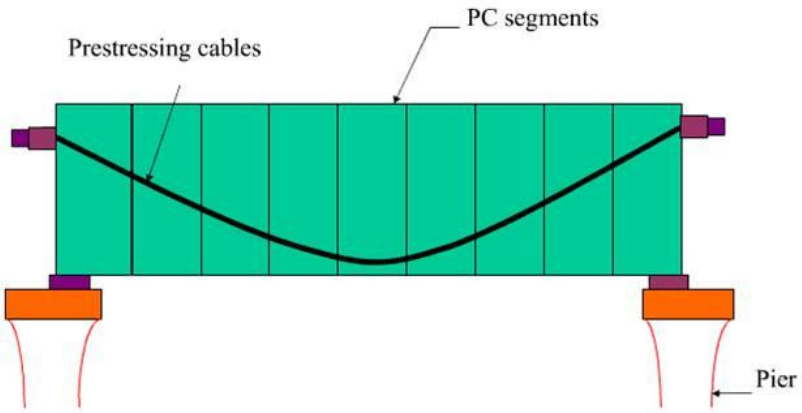

Figure 9. Segmental Bridges[34]

The question of how much shear displacement there is through the rubber layers needs to be answered. Conventional grouted joints have very little displacement across the grouted section. The shear displacement across the rubber sections of the simulated sign posts was determined to be tiny (0.04mm, from FEA studies shown in section 4.3). Scaling up the shear displacement to the appropriate size in a segmental bridge, with a concrete segment depth of 3.2 meters, indicates a shear displacement or step between segments of only 1.3 mm. This would be the maximum step at the highest structural loading before yield in the concrete. Functionally this step would be insignificant on a segmental bridge.

The MS joints can be thought of as a further potential enhancement to the technology of segmental bridges. In that even higher strength and stiffness can be achieved compared to the EB jointed system. The MS joint system should have at least a 73% improvement in strength in comparison to the conventional segmental bridge structure (detailed results in chapter 4). The MS jointed bridge also has the potential capabilities of a mechanistic mode that could better survive extreme loading such as seen during earthquakes.

Because the MS joint concept can be applied to a wide variety of structural applications a patent search was conducted to see if the concept had been developed before. Very little was found that even partially matched. The closest match was US Patent 6,766,562 – "Extendible Hinge". In this patent a cabinetry hinge was developed which is also a break-over mechanism. The primary similarity is the use of opposing cylindrical surfaces which create the joint between the door and the cabinet frame (see figure 10).

There are also a number of break-over mechanisms that can be found within the patent records. One application is that used in basketball goals. The similarity here, to the MS joint concept, is that the rim is a static structure but in order to avoid permanent damage, the mechanism will allow the collapse of the rim at a threshold loading. An

example of these break-over goals is: 7,214,148 – “Basketball breakaway goal release apparatus” (see figure 11).

Concerning the EB joint, the only patent found with some similarity is 6,409,423 that is used in pavement structures. This is discussed in detail in section 6.2.1.

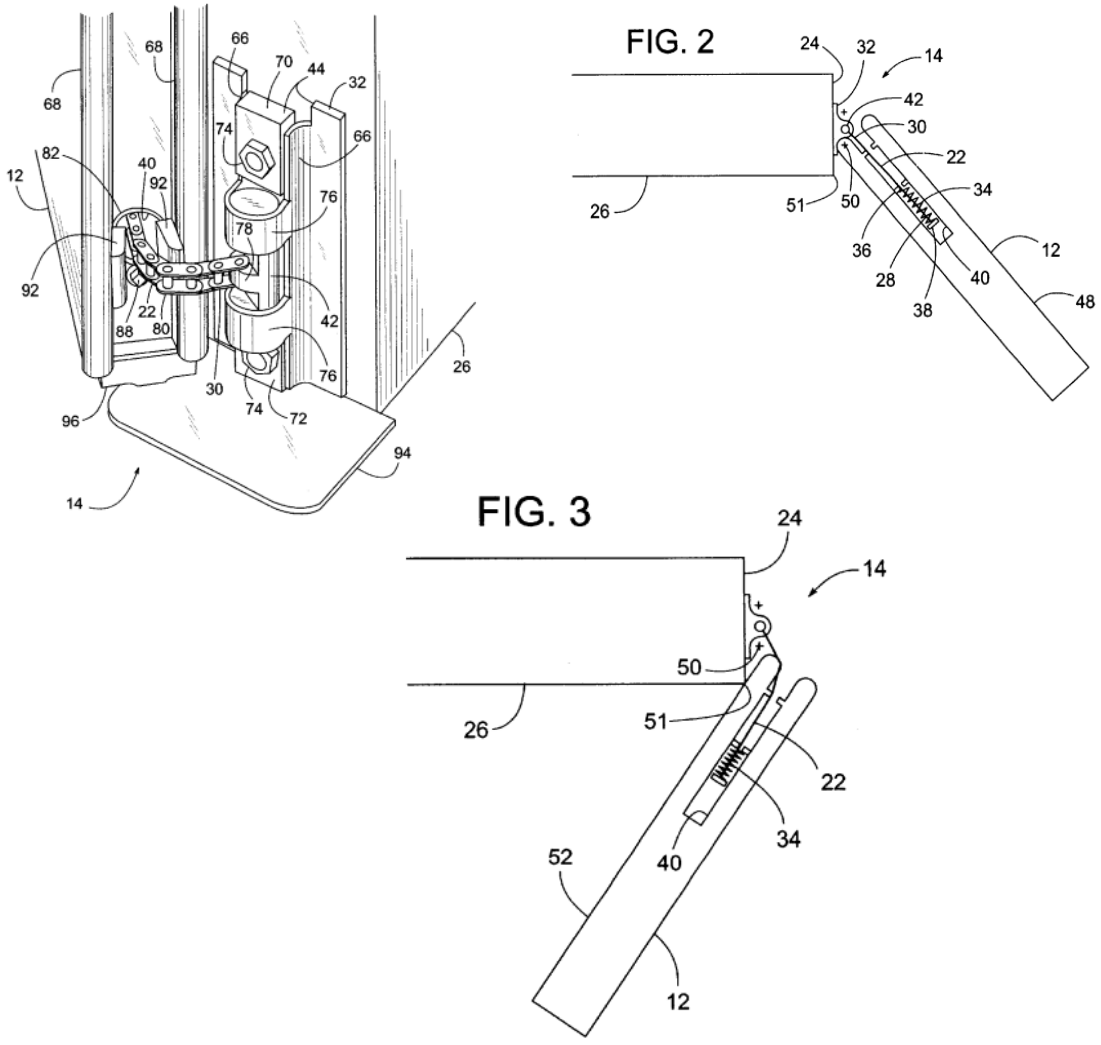

Figure 10. Patent 6,766,562 – “Extendible hinge”[35]

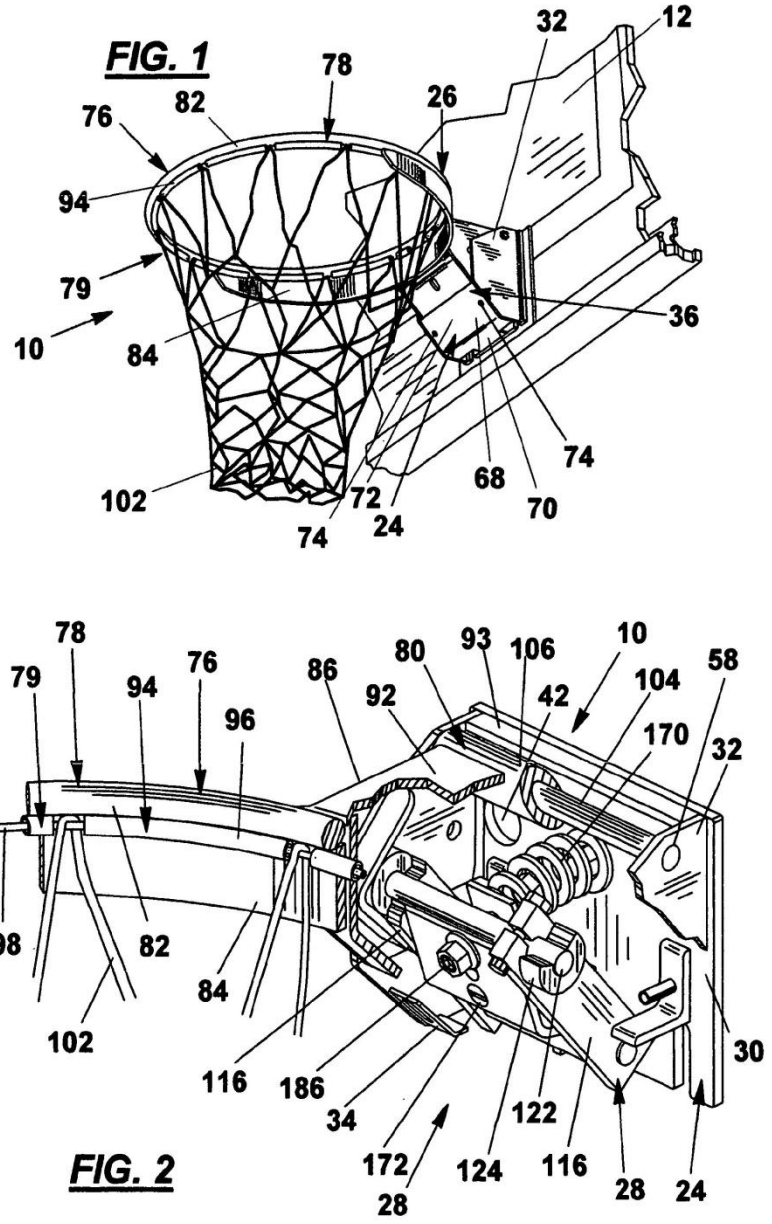

Figure 11. Patent 7,214,148 – "Basketball breakaway goal release apparatus"[36]

3.2 Bonded Versus Unbonded

Both of the proposed joint systems are ungrouted between the segment faces. However the bonding of the tendon to the concrete segments needs to be considered as it is an important factor. Typically after post tensioning and anchoring of the tendons, grout is pumped into the annular cavity between the tendon and the tendon channel. Some post-tensioned structures do not have their tendons grouted. There are advantages and disadvantages to either method.

Commonly post-tensioned structures are grouted around their tendons. Post-tensioned concrete refers to a method of applying compression after pouring concrete and the curing process. The concrete is cast around plastic, steel or aluminum curved duct, to follow the path where tension would occur in the concrete element. A set of tendons are fished through the duct before or after the concrete is poured. For segmental elements it would be after both pouring and curing. Once the concrete has hardened, the tendons are tensioned by hydraulic jacks. When the tendons have stretched sufficiently, according to the design specifications, they are wedged in position and maintain tension after the jacks are removed, transferring pressure to the concrete. It is at this point that the tendons may be grouted. For conventional concrete structures, the advantages of this system over unbonded post tensioning are:

1. Reduction in traditional reinforcement requirements as tendons cannot de-stress in accidents.
2. Tendons can be woven allowing a more efficient design approach.
3. Higher ultimate strength (relatively small increase) due to bond generated between the strand and concrete.
4. No long term issues with maintaining the integrity of the anchor/dead end.
5. The grout helps protect the tendons from corrosion.

Unbonded post-tensioned concrete differs from bonded post tensioning by allowing individual cables permanent freedom of movement relative to the concrete. To achieve this, each individual tendon is coated with grease (generally lithium based) and covered by plastic tubing, most often made of high density polyethylene. The transfer of tension to the concrete is achieved by the steel cable acting against steel anchors embedded in the perimeter of the slab, or element. The main disadvantage over bonded post tensioning is the fact that a cable can de-stress itself and burst out of the slab if damaged (such as during repair). The advantages of this system over bonded post tensioning are:

1. The ability to individually adjust cables based on poor field conditions (For example: shifting a group of cables around an opening to change the force vector).
2. The procedure of tendon grouting is eliminated. Also faster placement.
3. The ability to de-stress the tendons before attempting repair work.
4. Tendons have lower friction values, which aid in the prestressing process.
5. Tendons provide a larger maximum lever arm and drape due to the smaller diameter channels.

In the pole comparison study of this dissertation, the general assumption is that all the designs are grouted. In large part this is not relevant in the context of the sign post comparison study as the analysis and results are unaffected. For the MS joints to operate in the mechanistic mode requires that the tendons are ungrouted. If grouted joint opening will cause extensive damage to the grout and tendons, thereby preventing the recovery action of the structure as well as its rehabilitation. Also for the reduced material comparison study, because of the higher levels of deflection, standard grout may not be applicable. However if the grout strength is low enough it could fail well before the tendon thereby allowing the larger deflections.

3.3 Design Methodology, Initial Geometry Investigation

The design process of this dissertation was primarily inductive in nature. The development of the new joint concepts, and detailed designs, were accomplished through an iterative process. This iterative process revolved around design proposals, analysis and results; there were many progressive cycles. And although in the end a development path was found to reach the goal of the study it is apparent that more studies should be conducted in the future.

The MS joint was developed first to bring more insight into the overall scope of the project, since it is more complicated than the EB joint, it was felt that the EB joint development steps would be mostly subsumed by those of the MS joint.

In order to conduct a simple comparison study between conventional concrete post-tensioned structures and the new proposals a simple structure was chosen. For simplicity sake as well as to facilitate ease of prototyping later, a stop sign post was chosen (see Appendix A for an example of a detailed specification). The pole dimensions are 12 foot long and 4 inch square, with a quarter inch diameter tendon running through the middle. The conventional pole will consist of one solid prism. The new proposed designs will consist of a series of concrete segments and either EB or MS joint assemblies. Most often stop sign posts are not made of concrete but for the purposes of this study this practical application was picked to develop a comparison. A high speed wind loading at the centroid of the sign would be represented in the analysis as the external loading.

In order to establish an initial design domain the degree of preloading must be established. This was done by using the tendon preloading that an equivalent conventional post-tensioned pole would use. First a steel index value was chosen, then the tendon preload. For the 4 inch square sign post the tendon preload was initially set at 80% of the tendon tensile strength, which is 45,550N, for the ¼ inch diameter tendon

(equivalent cross sectional area). Using this established preloading, various joint geometries and concrete element lengths were then proposed and evaluated for the sign post, in developing the MS joint concept.

The simplest approach to the MS joint is for all surfaces to be composed entirely of concrete. However preliminary investigations showed that no gain in M_R could be gained in this initial MS joint post verses the conventional post; while maintaining the same post dimensions and tendon steel. There were serious problems with high tensile stresses at the joint's female surfaces (see fig 12 and 13). As can be seen in the figures, tensile stresses became excessive. This was the case for the concrete on concrete joints even after the journal geometry was optimized. In figure 12 is illustrated the state of Maximum Principle stress (tensional stress, in MPa) at the point where joint opening just starts to occur (maximum opening is 0.17mm). For a concrete with compression strength of 4ksi the maximum tensile strength is approximately 0.53ksi, or 3.66Mpa; 13% of the compressive strength[12]. In figure 13 the joint opening is at 15 degrees. For both cases of joint opening the maximum principle stress is too high, approximately 7MPa in figure 12 and 11MPa in figure 13.

Even before a shear load was imposed the female surfaces were near the tensile limit (assuming an isotropic material of 4ksi concrete). Therefore the concrete on concrete joints do not look promising, at least not at 80% tendon preload. Higher strength concrete, fiber reinforced, and variable internal reinforcement structures could make the concrete and concrete designs more attractive. Given the above findings other geometries and material combinations were investigated.

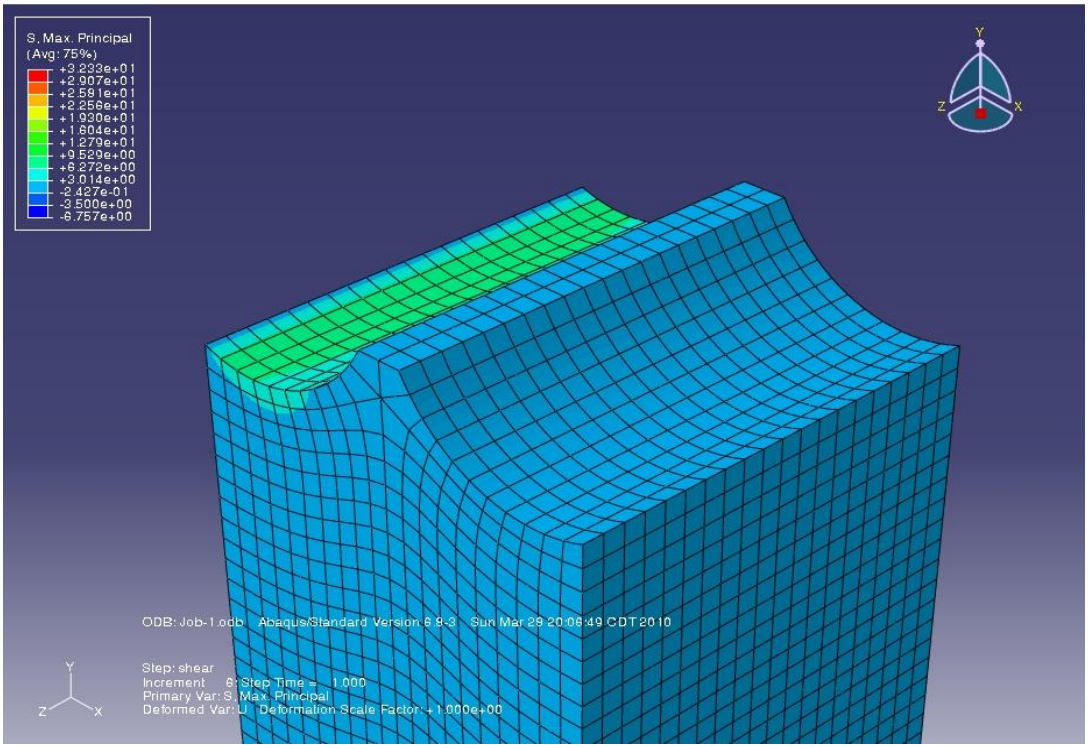

Figure 12. Concrete on concrete joint, start of opening, maximum principle stress (MPa)

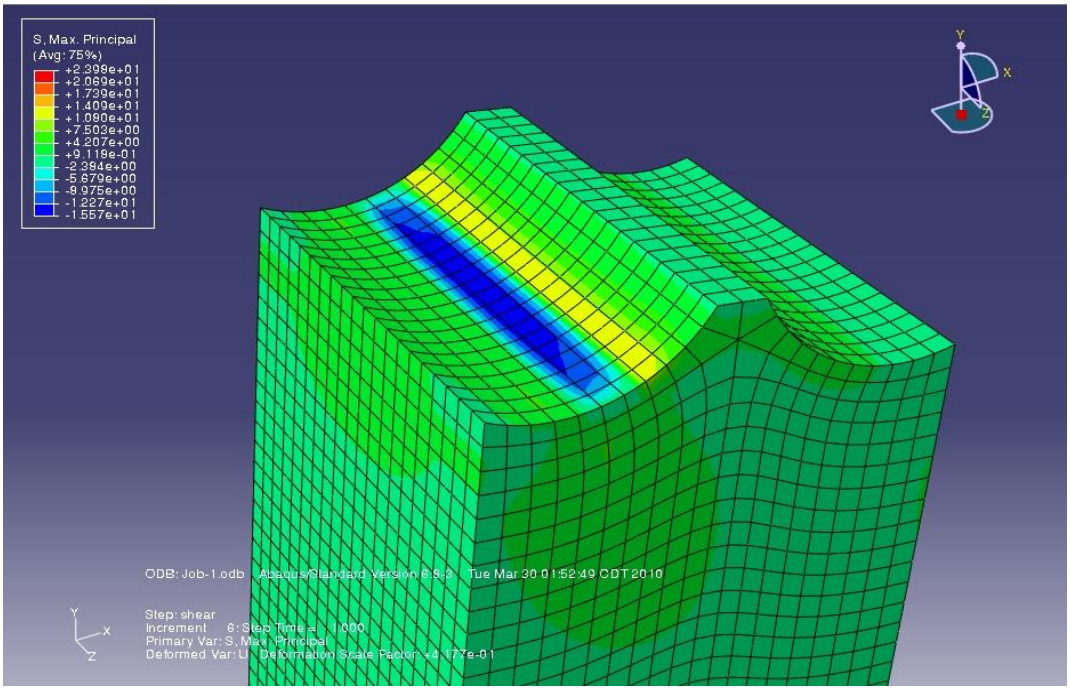

Figure 13. Concrete on concrete joint, 15 degree opening, maximum principle stress (MPa)

It was at this point that steel end caps were conceived as a possible solution. Various shapes and configurations were tried. A wide variety of end cap configurations were studied. The profile of the concrete element end, which interfaces with the steel cap, was varied between: flat, circular arc, symmetrical exponential arcs, and symmetrical cycloidal arcs. The goals sought in the process of developing the various end cap geometries was: maximizing the M_R, minimizing the steel quantity, and minimizing the stress levels. It was quickly discovered that square ended concrete elements, in conjunction with steel end caps, were not optimal in comparison to curvilinear profiles. A square ended profile for the most part simply transmitted the forces from the center of the pivot lobes directly into the concrete without much stress spreading. Circular arcs were shown to perform the best. Exponential curves worked nearly as well as circular. For future optimization the exponential end profiles should be looked into because they lead to shorter steel end caps that would reduce the amount of steel needed. The cycloidal profiles did not work well. A ninety degree circular arc was chosen to use for the continuation of the studies. Next the method of bonding the end caps to the concrete was investigated.

Fully bonded end caps to concrete, were tried. Also unbounded end caps, with both zero friction, through various levels of friction, between the steel and concrete. Little was gained in terms of reducing the stress levels, or stress concentrations. It was at this point that an elastomeric layer was tried between the steel end caps and the concrete.

The initial idea for an elastomeric layer originated from current bearing pads used in various prestressed concrete construction. These types of pads are often made of laminated stacks of alternating sheet metal and rubber layers. They are used in bridge construction and buildings[5, 30].

The bearing pads help absorb, and cushion, shear movement and rotation between horizontal and vertical members. They also serve to dampen earthquake loading (see figure 14).

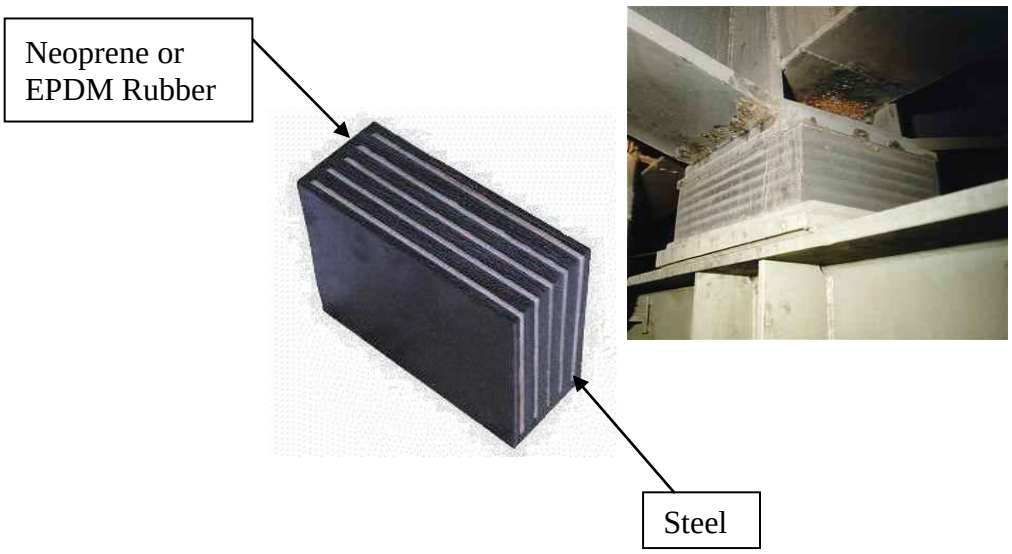

Figure 14. Bearing Pads[34]

The elastomeric layer helped tremendously! It worked especially well in conjunction with curvilinear concrete end profiles. This layer could be very thin and still offer a tremendous benefit. One quarter millimeter through 1 millimeter thick layers were tried. The one millimeter thick rubber layer worked best, and for this initial feasibility study it was chosen for the rest of the analysis.

The steel end caps not only improved the stress field in the concrete but also facilitate the lengthen of the Lever Arm associated with the M_R generation, both of which contribute to maximizing the M_R. As previously stated, extensive or automated shape optimization was not conducted in this study, but rather just a manual trial and error method for the purposes of establishing a feasible solution. One of the primary variables to improving the M_R is the diameter of the pivot lobes. The smaller the journal diameter the longer the lever arm can be, however the smaller the pivot diameter the higher the

stresses in the pivot as well as in the concrete directly beneath it. These stress levels limit how small the diameter may be. It turns out that the concrete stresses are the limiting factor. Figure 15 illustrates how the level arm is a function of the pivot lobe diameter and the minimum outside arc length of the lobe; for the male end cap. For this study fifty degrees was chosen for the minimum outside arc length. If the arc length is too small, or zero, the male and female mated lobes will cease to act as a journal bearing and tip onto the outer most edge, which would cause an over stressed condition, and failure in the lobes.

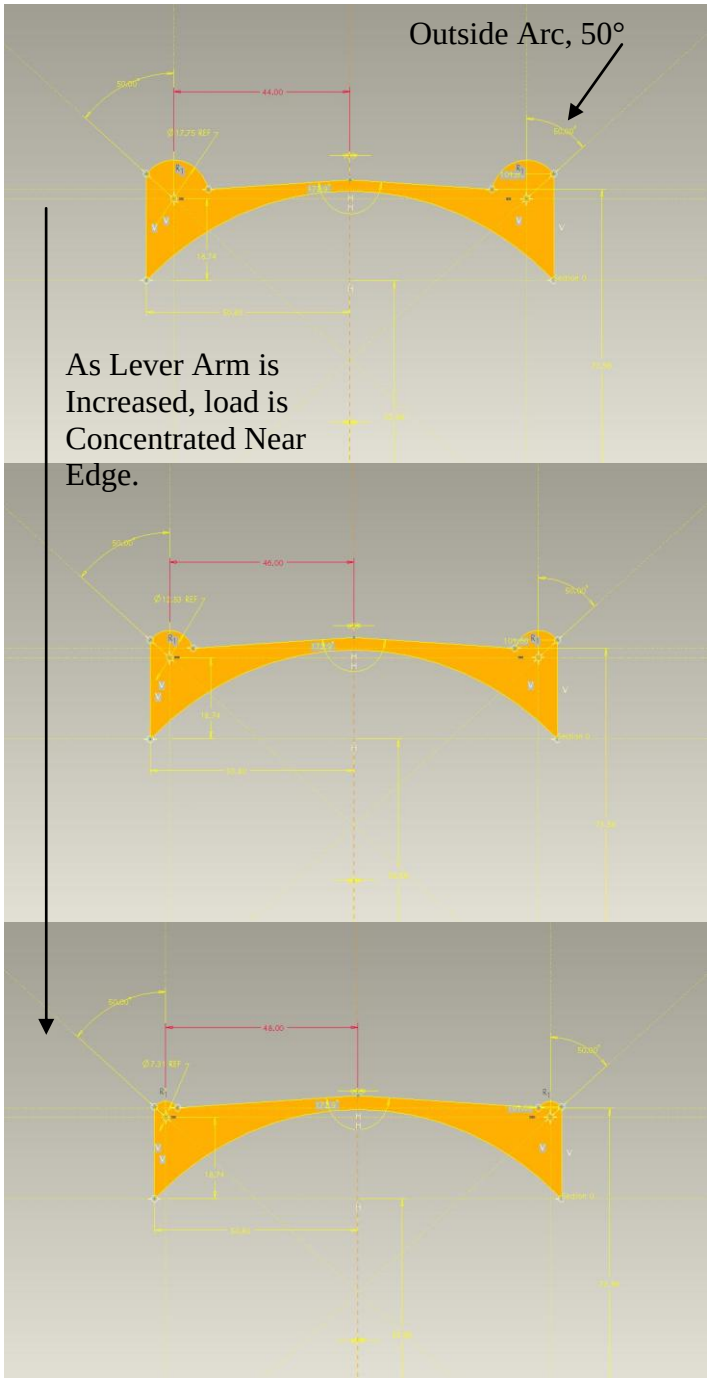

Figure 15. Pivot Lobe Geometry (Male)

For much of the initial end cap development a simplified assembly was used. In figure 16 is a picture of the setup and of an analysis step. This assembly simplified the loading by placing a concentrated load at a point above the proposed pivot center. This greatly facilitated the iterative design process. Later stress levels and corollary M_R's were verified in the more complete pole assemblies.

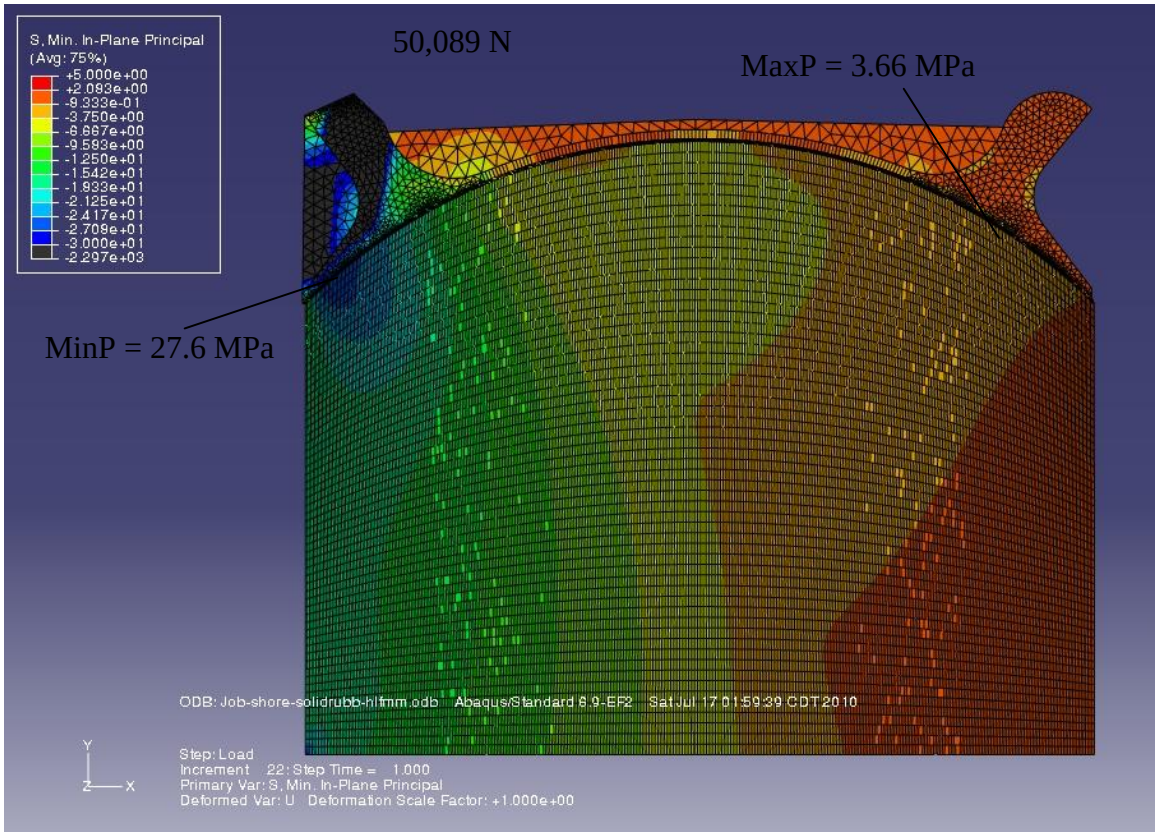

Figure 16. Simplified Assembly for End Cap Development

The steel end caps may be considered a kind of “connector”. The use of steel connectors of various sorts for precast concrete joints has been practiced over many years in many forms. Amongst the various RC systems that use steel connectors are: bolted, dowels and lapped bars. For the most part aside from bolted connections most steel connectors for concrete are grouted in place. The MS joint concept could incorporate grout, around the tendons, but then the dynamic mode would not be optimal.

This is the list of design parameters which maybe varied in seeking an optimized MS joint post design, with steel end caps (in the context of this study):

1. Number and lengths of concrete segments
2. Profile of concrete end
3. Overall shape of steel end caps
    - 3.1. Diameter of pivot lobes
    - 3.2. Position of pivot lobes
    - 3.3. Outside arc length
    - 3.4. Webbing profile
    - 3.5. Webbing density
4. Elastomeric layer between steel and concrete
    - 4.1. Which elastomeric material:
        - 4.1.1. Durometer value
        - 4.1.2. Rubber type
    - 4.2. Thickness of elastomeric layer

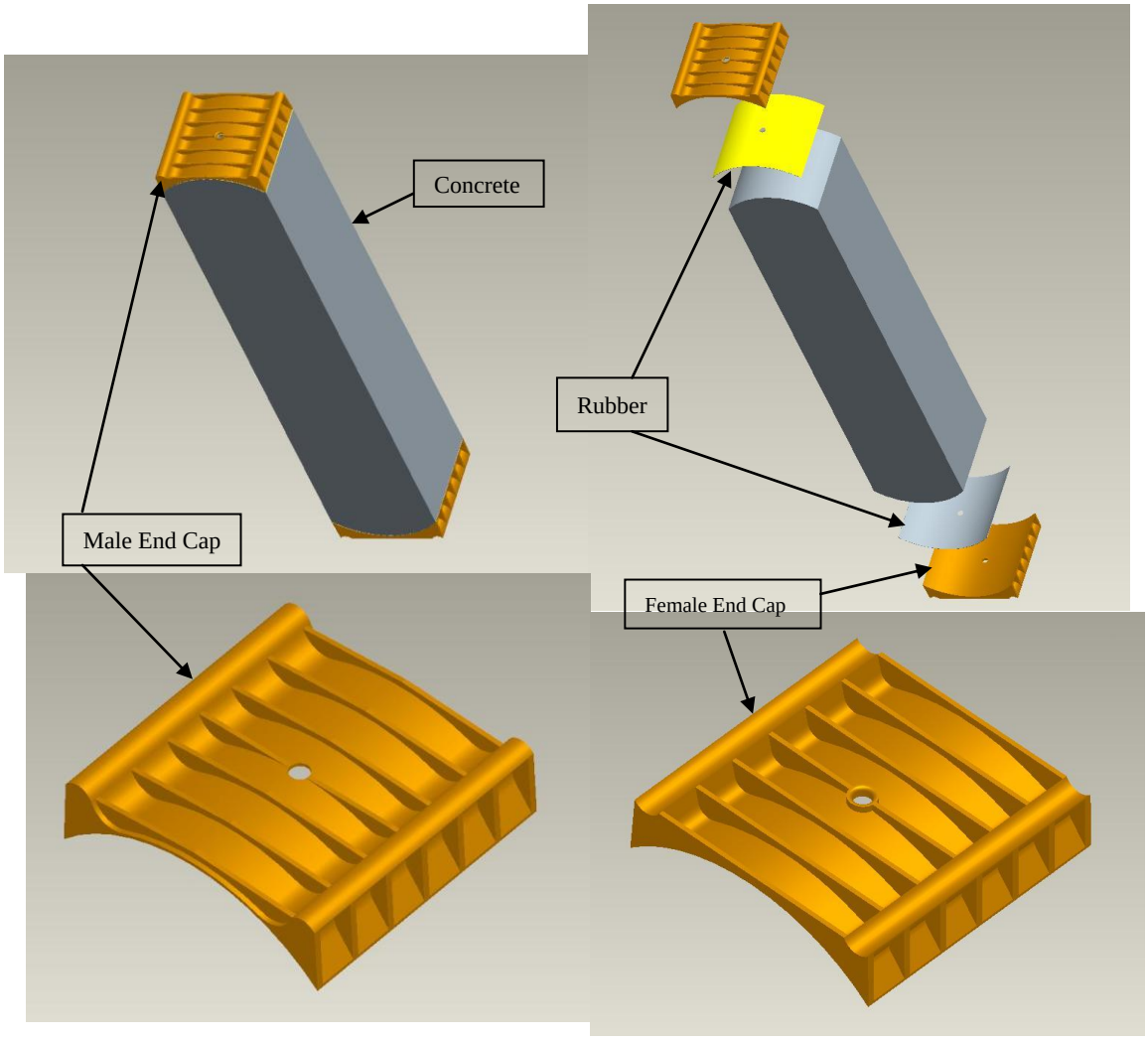

Figure 17. Final MS Joint Segment Design

This is the list of design parameters which may be varied in seeking an optimized EB joint post design (in the context of this study):

1. Number and lengths of segments
2. Sheet metal thickness
3. Rubber thickness
4. Rubber durometer
5. Rubber Type
6. Rubber bonding scheme: semi-bonded, partially bonded, etc.

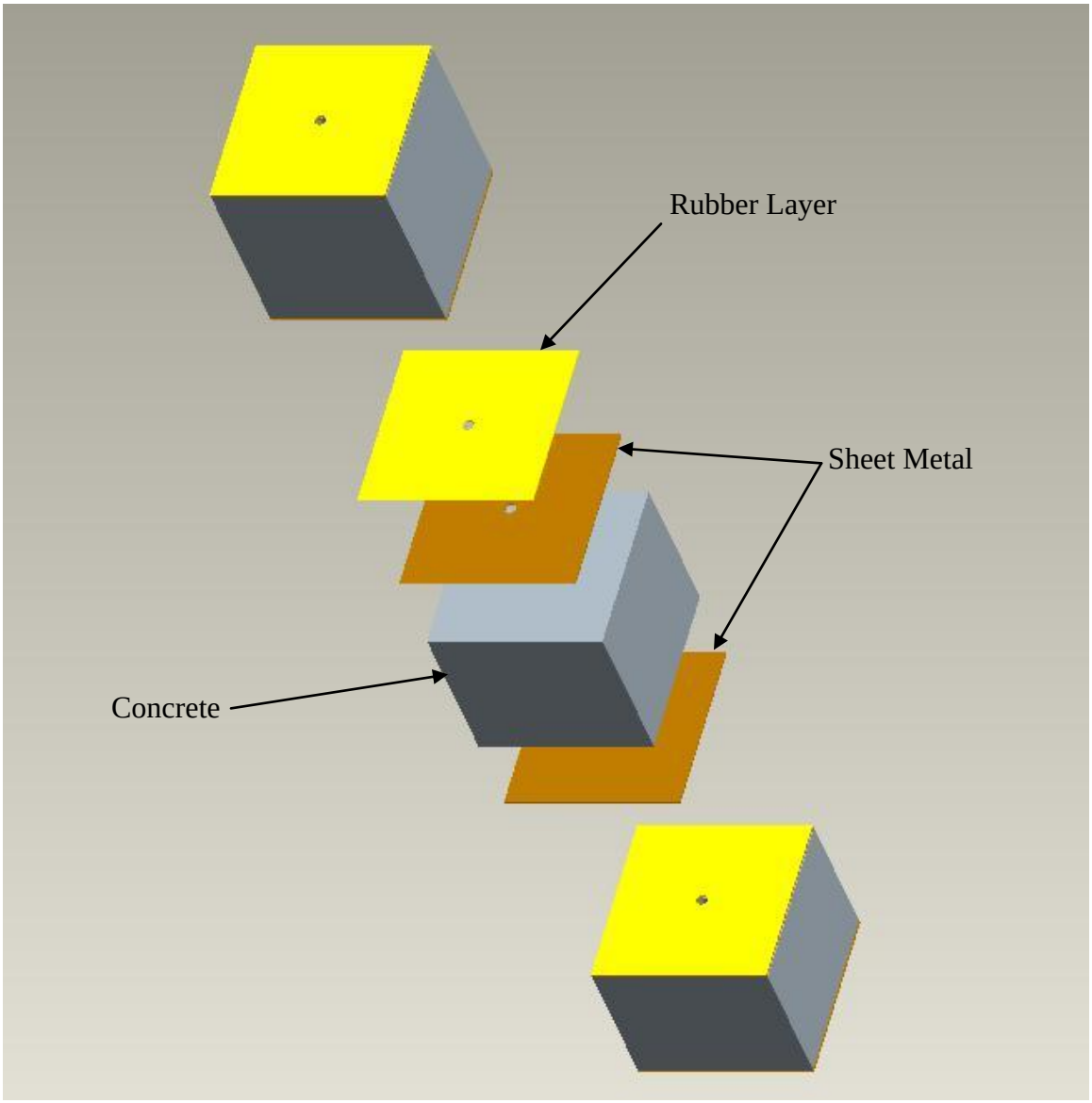

Figure 18. EB Joint System

The optimal segment lengths are the final consideration. Initially a uniform length was chosen which was fairly arbitrary. The aspect ratio was taken from a common Acme brick. Then through successive iterations the optimal lengths were determined. Actually there is room for further optimization work here when considering multivariant interactions. In the process of this length optimization, or segmentation process, a number

of phenomena were discovered (these results were found through hundreds of manual FEA iterations):

1. A graduated segmentation pattern is optimal: shortest segments at bottom to tallest at top, for a cantilever pole; in terms of minimal cost and minimal stress.
2. The optimal segmentation varied as loading varied: preload and shear loading. Also there was variance with varying end cap geometry.
3. For the EB joints, the shorter the initial (bottom) segment the lower the stresses at the lowest segment and all higher segments.
4. For the MS joints, for a given set of boundary conditions, the bottom segment has an optimal length such that if made shorter the stress will increase, converging toward the stress levels for a single joint at the base with no segmentation.

For the EB joint the segmentation process was stopped at five segments for the sign post portion between the ground level to the centroid of the stop sign. Further segmentation would further lower maximum stress levels and consequently increase the M_R. But at five segments the goal of the study was far surpassed, and a further optimization maybe done in subsequent studies.

Throughout this study the Rankine stress criteria was used for the concrete and the rubber. That is for brittle substances, or substances that fail under normal stresses, only the principle stresses are considered: maximum principle and minimum principle stresses, comparing to the tensile and compressive yield stress levels. For elastomers strain energy levels are better indicators of yield conditions but because the rubber always remained well under yield levels for the Rankine criteria, the Rankine criteria was considered sufficient.

3.4 Relaxation Behavior of Elastomeric Layer

The relaxation behavior (or strain creep) of the elastomeric layer becomes an important factor in any designs which utilize the proposed joint structures. This is because the proposed joint system's elastomeric layers act as integral components of the stress transmission through the structures. The compressive segments are the major structural components; volumetrically. If these segments are connected through EB or MS joints then the rubber layers will be under constant prestressing pressures. These constant pressures will cause some degree of permanent compression set. However with the proper maximum stress levels, shape factors, durometer and operating conditions the compression set will not pose any serious problems[5, 6, 7, 8, 9]. If the compression set is too large joint surface separation may occur under certain loading conditions. Another potential problem posed to the overall structures is stress relaxation, a product of the strain creep, thereby reducing the nominal stresses. The steel tendons will also creep. These various creeps will cause an overall reduction of prestressing stresses. If the creep is kept under a critical level then the structures will not be significantly affected.

Among the various design parameters two are most important in regards to controlling the rubber resiliency: the durometer and shape factor. The harder the durometer, the less creep and compression set, but also there will be less compliance which is important for the joint stress reduction function and to absorb thermal expansion strains. For bridge bearing pads the durometer is usually 50 to 70 Shore A[6].

The shape factor describes the role of the shape in determining how a part with parallel load faces will behave under compressive forces. The concept of shape factor is useful in design engineering. If the elastomeric part does not deflect enough to do its job, the designer can reduce the shape factor by increasing the thickness, or increase the peripheral area, of the pad. Essentially he increases the area free to expand under load. If the pad deflects too much, he may decrease the free area. Bridge bearings are designed to

have large shape factors. This is accomplished by laminating stacks of alternating sheet metal and rubber layers. The sheet metal surfaces in contact with the rubber contribute to the numerator of the shape factor. The free peripheral area of the rubber is the denominator. The shape factor is a ratio of restrained surface area to the unrestrained areas. It is calculated by dividing the plan area by the free area in a layer. As an example of the shape factor (SF) calculation, a 0.5 inch by 10 inch by 10 inch pad has a SF of 5. For reinforced pads, such as used in bridge bearings, each individual layer of rubber would have a SF associated with it. For a bridge bearing pad with 10 layers of rubber each with dimensions of 0.5 inch by 10 inch by 10 inch the bearing pad would still have a SF of 5. For multiple layered bearings the shape factor of the thickest layer would be the bearings overall (controlling) shape factor.

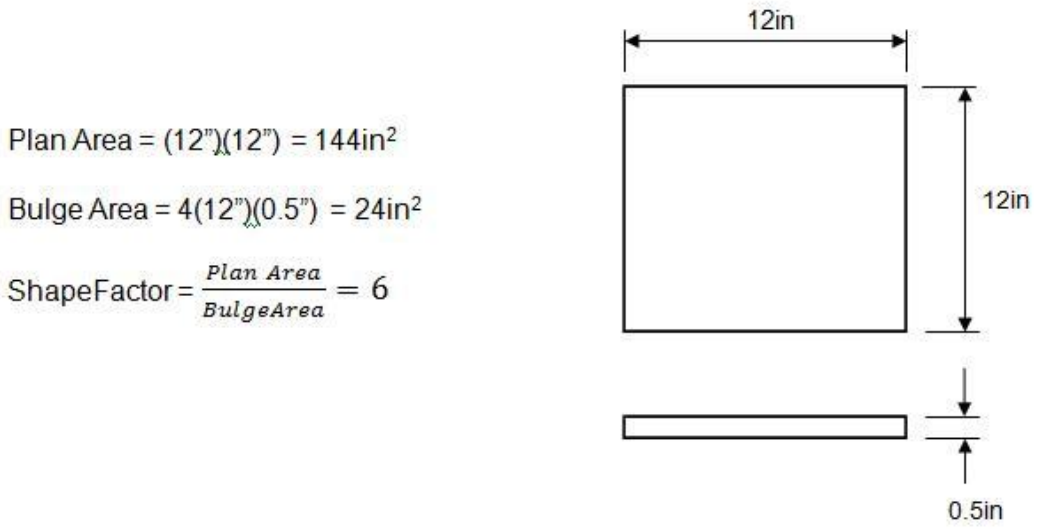

Figure 19. Shape Factor Calculation Example

Another important parameter is the maximum shear strain, measured by the ratio of the shear displacement to the rubber thickness. From various resources a rule of thumb has evolved which is a 50% shear strain limit[6]. Throughout the various studies presented here, for the new joint concepts, the resultant values are well under this limit.

Searching through the relevant literature there is data related to long term compression set behavior in the various engineering elastomers[5, 6, 7, 8, 9]. The compression set is highly dependent upon stress, time, temperature and shape factor. In order to get a quick measure related to long term compression set there are elevated temperature testing methods. One common test is ASTM standard D 395, "Method B: Compressive Set 22 hrs at 212 F (100 C), Max %". From a survey of elastomer references it was found that the maximum imposed compressive stresses, within a reasonable maximum service temperature (< 100 C), should not exceed 1,600psi. And that the maximum compressive set under these conditions would be 35%. These values pertain to the rubber used in construction bearing pads such as Neoprene and EPDM with their corollary durometer values [5, 6, 7, 8, 9].

3.5 M_R Comparison

Throughout the development of the EB and MS joint systems M_R comparisons were conducted as the primary performance check between successive iterations of design, and also between the conventional post and the proposed joints. Simultaneously the stress levels were checked to verify they did not exceed either the maximum principle stress or the minimum principle stress levels for the material in question (Rankine criteria); primarily in regards to the concrete. Three methods of determining the maximum M_R were utilized.

The first method for M_R determination is applicable to the conventionally constructed concrete pole. It is an empirical calculation that comes from a number of

idealizations, but has proven to correlate well with field data over the years. The second method is applicable to only the MS joints after the joint opens. This method is from classical static equilibrium. Because the reactive lever arm is relatively constant in the MS joint after opening, the M_R is easy to calculate: basically it is the preload force multiplied by the lever arm. The third method is through FEA analysis and is applicable to the conventional pole, the EB joint, and the MS joint. Basically it consists of modeling the sign post with the proposed design parameters, simulating the preloading and shear loading, and then varying the shear load until a stress limit is reached.

The empirical calculations for the conventionally constructed concrete pole are based upon an idealized crack at the base of the pole; or beam. This crack is represented as a plane cutting thru the pole perpendicular to the longitudinal axis of the pole. After sufficient loading is applied a portion of material in this crack plane remains uncracked. For this portion there is a compressive stress distribution, which is idealized as rectangular (see figure 6) with a width $d_{nu} = 0.75/2 \times D$; D = the width of the post[10]. However because it really is not a symmetric distribution, the centroid of the stresses is skewed such that the reactive lever arm is defined as: $D/2 - 0.4 \times d_{nu}$ (see Eq. 3.3).

Below are the standard/classical equations used in the empirical Maximum Resistive Moment analysis:

$$q" = \frac{A_S}{\frac{D^2}{2}} \frac{f_{pu}}{f'_c} \tag{3.1}$$

$q" = 0.4$ Steel Index (balance/ratio of steel and concrete strength)

$f_{pu} = 270000psi$ Tendon steel yield (ASTM A 416 properties)

$f'_c = 4000psi$ Concrete compression strength (28 days)

$D = 4in$ Width of pole cross section

A_S Tendon Cross sectional area

$$A_S = \frac{f'_c}{f_{pu}} \frac{D^2}{2} q" \quad (3.2)$$

$$A_S = 0.047in^2$$

$$M_{Rc} = q" f'_c D d_{nu} \left(\frac{D}{2} - 0.4 d_{nu}\right) \quad (3.3)$$

$$d_{nu} = 0.75 \frac{D}{2} \quad (3.4)$$

$$M_{Rc} = 1.344 \times 10^4 lbf \cdot in$$

An assumption of the above analysis method is that the concrete pole fails under compressive stress; however as can be seen from figure 3 the tensile stresses are well over the yield level at the crack terminus. This stress state existed at an M_{Rc} level a bit lower than the calculated level from equation 3.3 ($1.344 \times 10^4 lbf \cdot in$), however the maximum compressive, or minimum principle, stress was well below yield at that point (17Mpa). So it is postulated that the section still connected, that is not cut by the idealized planar crack, actual starts to fail from spider cracks spreading from the crack terminus, which further reduces the effective connected, or solid portion. This occurs because of

the fact that the tensile stresses at the crack terminus are products of shear and bending. Tensile stresses normal to the crack surface do not exist because of the unbonded contact at the crack.

The second type of M_R analysis was used for the initial development of the end cap and elastomeric layer. Illustrated in figure 16, a simplified assembly was used to simulate an approximation to the conditions present when an MS joint just becomes open, i.e. contact with only one lobe and minimal angled opening. The M_R is simply calculated as: $M_R = L_{arm} \times P$. This assembly proved useful in executing a large number of simulations for investigating proposed geometry, material properties and assembly configuration, quickly. Later with the full sign post assembly simulations it was verified how good these initial simulations were. Subsequently there was a good match which would indicate that the simplified initial FEA simulations were valid for the purposes of design guidance.

As can be seen below the M_R from the second type of analysis, for the proposed MS joint system, is 38% greater than the conventional concrete post calculation M_{Rc} (Eq. 3.3 ($1.344 \times 10^4 lbf \cdot in$)). Both the MS joint and conventional structure were under 80% tendon preload (K=0.8).

Calculations for the maximum resistive moment of the 4" square post, for the proposed MS joint design:

Using the equivalent tendon cross sectional area: $A_S = 0.047in^2$

Lever arm developed from FEA model (figure 16): $L_{arm} = 46mm$

Tendon preload (fraction of tensile strength): $K = 0.8$

$$P = Kf_{pu}A_S \tag{3.5}$$

$$P = 4.555 \times 10^4 N$$

$$M_R = L_{arm}P \tag{3.6}$$

$$M_R = 1.854 \times 10^4 lbf \cdot in$$

$$\frac{M_R}{M_{Rc}} = 1.38 \tag{3.7}$$

The third type of M_R analysis was utilized for all three construction types (conventional, EB and MS joints) for final verification simulations. And also for the segmentation refinement work for the EB and MS joint posts. From these final simulations it was found that all three construction types fail under tensile stress (maximum principle stress) in the concrete; except for the 100% preload condition for the MS jointed pole. The steel and rubber remained comfortably distant from their respective yield levels in all simulations.

The setup of the conventional pole FEA model in Abaqus consisted of the following:

1) 2D plane strain, with quad dominated FEA elements; fine mesh quad elements local to crack.
2) Pole modeled as a monolithic prism: 4” × 4” × 99”; from planar crack up to the centroid of the sign.
3) No reinforcement steel modeled; initial tendon pre-load force imposed normal to top of prism, with an equivalent pressure loading, = 45,550N (10,200lbf); 80% preload.

4) Fully constrained at base; buried base section approximated with short block (50mm tall) below planar crack; constraint applied to horizontal bottom surface.

5) Planar crack modeled as contact analysis between top prism and bottom block; friction factor set at 2.

6) Shear load, or wind load, at top of prism. The maximum loading was determined for various scenarios:

    a) At 80% preloading

    b) At 100% preloading

    c) Per the classical Maximum Resistive Moment calculations; for the conventional post

    d) For the conventional post, through a number of iterations: by determining the maximum moment which the pole could withstand (1.66E06Nmm, for 100% tendon preload); which was limited by the maximum principle stress of 3.66MPa. The maximum shear load was 660N.

Through Finite Element Analysis (FEA) the maximum principle stresses were determined for an imposed shear loading, or M_R for the MS and EB joint designs. The various design parameters were evolved in order to keep the maximum principle stresses below yield and to simultaneously minimize the costs (i.e. minimize material).

The initial studies were carried out with an 80% of tensile strength on the tendon, or preload. This degree of loading is a common one for tendon preloading and is a good representation of an approximate tension in the tendon within the domain simulated for ungrouted poles. That is, for ungrouted structures there is a larger amount of strain available because the total tendon length can stretch during shear loading and the initial preload will be close to the final loading. However for a structure with grouted tendons a better approximate tendon loading is 100% of the tendon tensile strength, or preload. This

is because local to a crack, or joint opening, the strain is very high. The grout does not allow much, if any strain to be distributed from the total tendon length. Besides the 80% and 100% tendon preloading being simulated, a lower loading was found for the two proposed systems in order to simulate a minimal or reduced tendon diameter.

The reduced tendon simulations were meant to explore a cost reduced proposal which simulated sign posts with the new joint systems, but at the same maximum shear or moment loading as the conventional post. Simulations were carried out to find the lowest tendon loading which still maintained allowable stresses using the Rankine criteria. In essence these reduced tendon scenarios represented the lowest feasible steel indexes that could produce an M_R equivalent to the convention pole's M_{Rc}.

Along with the reduced tendon study, the 100% preload, at 0.4 steel index, represents an over-strength condition in that, in comparison to the conventional pole, the proposed poles could handle much higher loading. This represents structures which may handle more load per given material used; saving tendon costs. Potentially there can be designs with relatively smaller, or variable, cross sections thereby saving on concrete costs as well.

The setup of the FEA models for the new proposed poles, in Abaqus, consisted of the same setup for the conventional pole (above) except for the various material sections and the contacts. The contacts between lobes in the MS joints were modeled with a coefficient of friction of zero. The contacts between the top surface of the rubber layers and the steel in the EB joints were set to a coefficient of friction of 2.

For the MS joint pole a minimum joint pole was developed (3 elements) to study and compare to the conventional construction pole. For the EB joint pole the segmentation was carried out for 4 segments up from the bottom, or ground level. The segments are progressive in length from bottom to top. 3D models represent pole sections from ground level to the sign centroid; illustrated below:

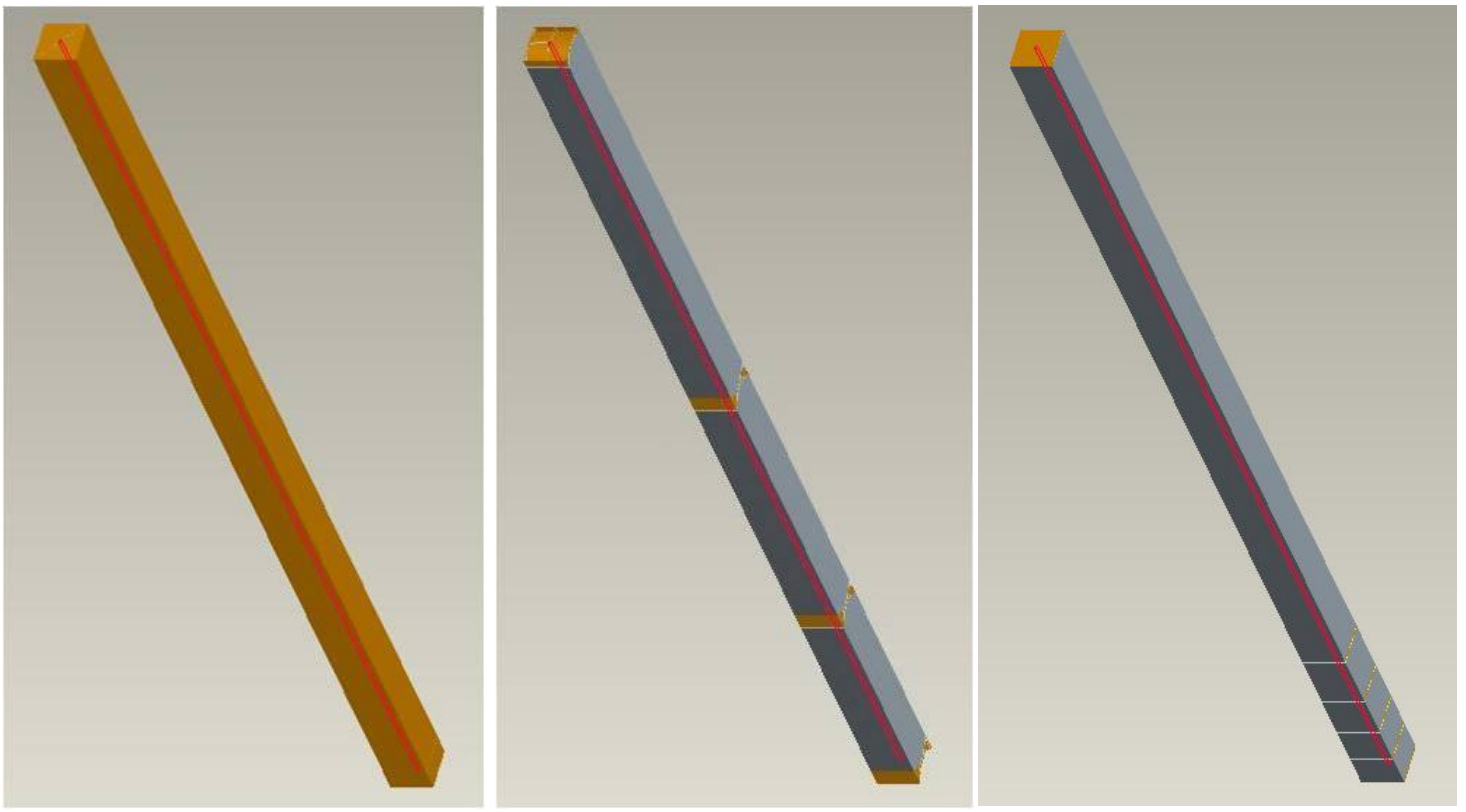

Conventional MS Joint EB Joint

Figure 20. Segmentation Setup of Three Post Alternatives

Chapter 4: Sign Post Study

4.1 Assumptions

This comparison study focuses on the highest performing designs and their maximum M_R's and the corollary stress fields. To capture accurate stress fields the proper FEA methodology is important. Abaqus was used for the FEA simulation code because it is very well developed and capable software. For the most part the simulation defaults were utilized because they tend to be optimal for achieving the most accurate results[11]. Abaqus also allows a very large range of material properties to be represented.

Table 1. The various material properties involved

Material	**Young's Modulus**	**Compressive Yield**	**Tensile Yield**	**Von Mises Yield**	**Poisson's Ratio**
Concrete	30,000 MPa	27.5 MPa	3.66 MPa	-	0.2
Mild Steel	200,000 MPa	-	-	170 MPa	0.3
Tendon Steel	210,000 MPa	-	-	1,864 MPa	0.3
Rubber (EPDM)	-	11 MPa (Compression Set Limit)	17 MPa	-	0.4942

The following rule of thumb was used to determine the maximum principle stress for concrete[12] which is approximately 13% of the compressive yield:

$$f_r = 7.5\sqrt{f'_c}\ {}^{lbf}/_{in^2}\ USCS\ units \quad (4.1)$$

$$f_r = 0.7\sqrt{f'_c}\ MPa\ in\ SI\ units \quad (4.2)$$

The Neoprene or EPDM rubber was modeled as a hyper-elastic material using the Mooney-Rivlin material model[31]. The Abaqus input constants were (see Appendix C for more details):

Table 2. The rubber hyper-elastic coefficients

Mooney-Rivlin Constants	Shore 35	Shore 52	Shore 70
C_{10}	0.162	0.333	0.736
C_{01}	0.041	0.083	0.184
D_1	0.057	0.028	0.013

For this study the tendon steel properties were not important in terms of the FEA simulation because the tendon load was simply applied to the top of the posts. The tendon was not modeled. However for future studies involving large MS joint deformations the tendons will need to be modeled.

As stated previously the steel index was set as 0.4 because this value represents a balance between the steel strength and the concrete such that either one may fail at a maximum load level. Equation 3.1 calculates the value for the steel index. Its use is empirical in that it relates the behavior of prestressed members to experimental observations.

In general, typical tendon preloads are between 70% and 80% tendon tensile strength. Initially an 80% tendon preload was used. Otherwise 100% tendon preloading was used.

In order to evaluate the hypothesis of this dissertation the total costs of the 3 different pole constructions must be evaluated, therefore costs of the various components were determined. The cost study doesn't include assembly costs of the posts. Also the fabrication costs of some components are yet to be determined, such as the end caps.

Table 3. Material costs

Item/Material	Cost	Unit	Comment/Source
Concrete	120	$/yd^3	By cement truck, 10 cu yards
Mild Steel (Hot rolled)	0.68	$/Kg	From: http://www.thesteelindex.com/
Tendon (ASTM A 416)	0.27	$/ft	Based on 1/2" 7-Wire Strand, local supplier
Rubber Pad (1.14mm thick)	0.44	$/ft^2	Neoprene/EPDM sheeting, Firestone PondGard

These costs were taken at the time of publication from various sources with phone calls; for U.S. Sources; for low minimum order quantities.

Any conventional reinforced concrete construction includes reinforcement that is not composed of prestressing tendons, such as rebar. This requirement was taken into account for the conventional sign post in this study. Although the sign post is too small for standard rebar, steel reinforcement throughout the post body needs to be included in the design. This reinforcement steel would be low carbon steel wire. The reinforcement, or stirrup steel, is only in the conventional pole.

Total stirrup steel for pole = 105,885 mm^3. This total volume is based upon 12 inch long square loops, ½ inch deep, running around the periphery of the post cross

section, spaced 1 inch apart running up the length of the pole. See section 4.3.2 for calculations and results of the cost analysis[13].

4.2 Development Status

The process of developing the new joint systems was iterative. And after a large number of exploratory simulations the various geometric, material and boundary conditions were evolved. For purposes of this study these investigative simulations were not exhaustive but were conducted to the point of finding values sufficient to prove or disprove the study's hypotheses. The following are the current design parameters.

For the EB joint:

1) Segmentation → Segment lengths: 1st Segment = 81mm, 2nd = 90mm, 3rd = 105mm, 4th = 133mm, and 5th =2106mm
2) Sheet metal thickness = 1.2mm
3) Rubber thickness = 1mm
4) Tendon, ¼" diameter solid wire - equivalent cross sectional area

For the MS joint:

1. Segmentation → 1st Segment = 600mm, 2nd = 800mm, 3rd = 1144mm
2. End Cap lever arm → below is the results of a process of searching for a maximum resistive moment. In this case it was for 100% preload and 0.5mm thick rubber.

Table 4. MS Joint lever arm study

Lever Arm (mm)	Tendon Load (N)	Resistive Moment (N-mm)
49.5	35997	1781852
48.16	41453	1996376
47	44379	2085813
46	47244	2173224
45	49530	2228850
44	50091	2204032

The 45mm lever arm was chosen for the 1mm thick rubber structure.

3. Outer Webbing on End Cap → 7 × 2.47mm web thickness, 17% webbing density
4. Inner Webbing on End Cap → 7 × 1.74mm web thickness, 12% webbing density
5. Tendon, ¼“ diameter solid wire - equivalent cross sectional area
6. Concrete end profile 90° circular arc

The following are the design parameters which may be optimized further, thereby improving the proposed joint structures performance beyond that presented in this study:

➔ Find interactions between design parameters and variables: Durometer versus rubber-thickness verses deflection levels…segmentation verses all other parameters verses M_R levels verses Steel Index verses preload verses various bonding methods/materials…etc.

➔ Best rubber material type

- ➔ Assembly issues: rubber adhesive/bonding, Partial bonding options for EB, corrosion protection for mild steel and tendon steel
- ➔ Best end cap fabrication method/(s)
- ➔ Leash configurations
- ➔ 4-way MS joint end cap details & verification/optimization (figure 38)
- ➔ Various concrete end profiles: mirrored exponential curves show promise; with a brief effort, an exponential profile was found which had only about 10% higher stress levels than the circular arc profile.
- ➔ The reduction of concrete use. The removal of concrete through the central axis is a good candidate for reduction. However the reduction of concrete though the annular axis could raise the tensile stress levels. Also of course tapering of the pole from the ground level to the top could be applied to all three poles, which would reduce the amounts of concrete required.

The initial MS end cap designs were without webbing, solid with pivot lobes. Using the model in figure 16 many various shapes were tried. The initial solid depth design performed best in comparison to subsequent end cap profiles, but in an effort to reduce the amount of steel required for the end caps more complex profiles were tried which used less steel. This approach was guided by the margin between maximum stress levels and the yield stresses of the concrete, which initially were fairly large. Next the pivot lobe was connected to a uniform thickness steel arc through a finger structure. This reduced the amount of material considerably but also increased the stress levels in the concrete a great deal. Next webbing was modeled into the end cap structure surrounding the fingers. This was done by varying the elastic modulus of each web section, in direct proportion to the percent of material through the end cap depth (webbing density). This process was done until an optimal design was reach; at least in regard to the hypothesis goals.

The process of segmentation, as described in section 3.3, was also iterative. And although sufficient configurations of segments were reached, the future optimization of this aspect of the proposed joint systems are possible and important. There remains a great potential for strength improvement as well as the development of details which may guide future EB and MS joint structural designs.

4.3 Results

4.3.1 M_R and FEA Results

Results for the sign post comparison study reveal that the EB and MS joints performed much better than the conventional post structure in terms of strength, or maximum shear loading. Both of the new joint systems reduced stress concentration within and near the joints. Also at outside surfaces of the concrete segments which see the greatest bending stresses. As it turns out the tensile stresses are the primary mode of failure in all cases except for the MS joint at 100% tendon preloading, see figure 28. Not all simulation results are presented below, just the ones most pertinent to the hypothesis.

The following figures present the results for all three sign posts under 100% tendon preloading, which for the two proposed joint systems represents the Over Strength design studies. The 100% tendon preload is represented by a force of 56,940 N. Additionally for the conventional sign post an 80% tendon preloading is shown. The Reduced Tendon studies for the EB and MS joint post are also shown.

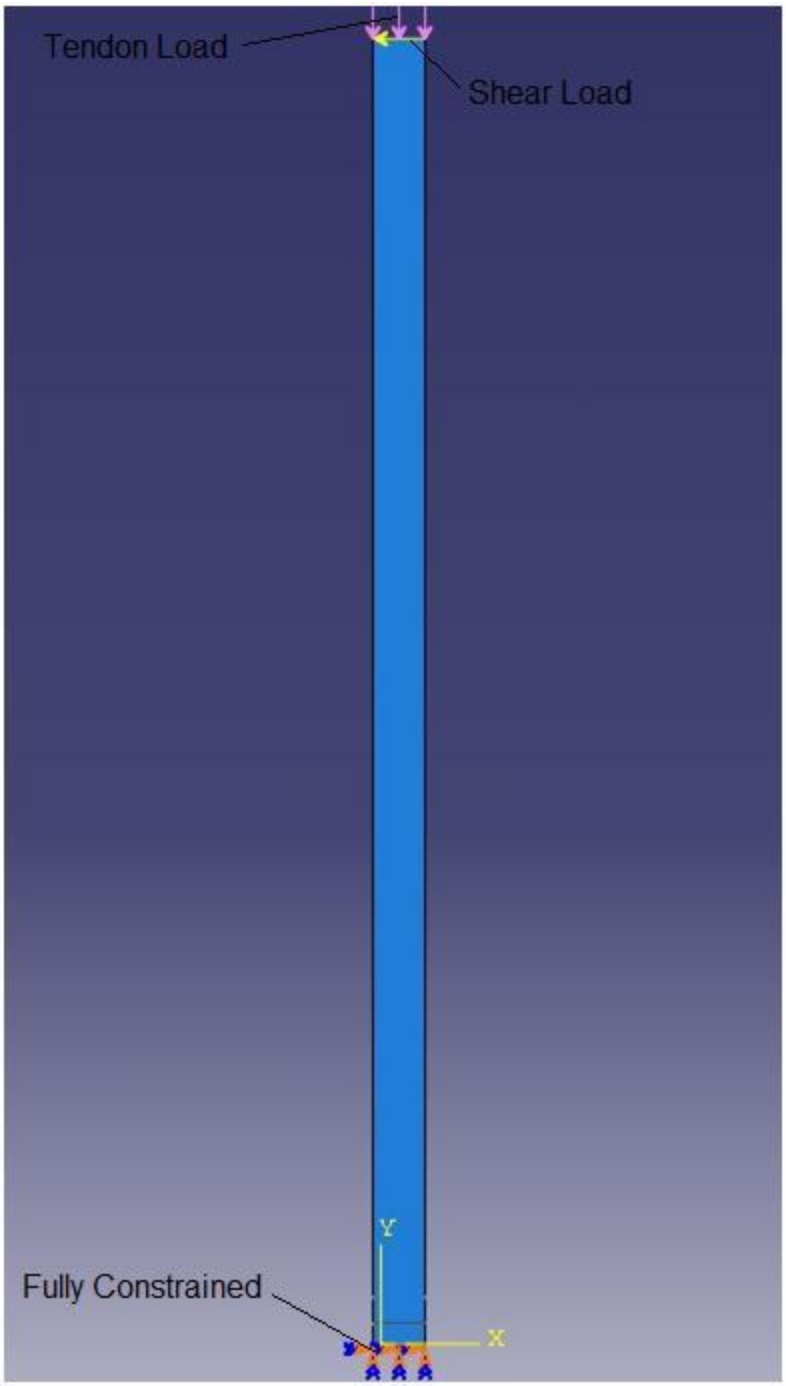

Figure 21. Conventional Post FEA Setup

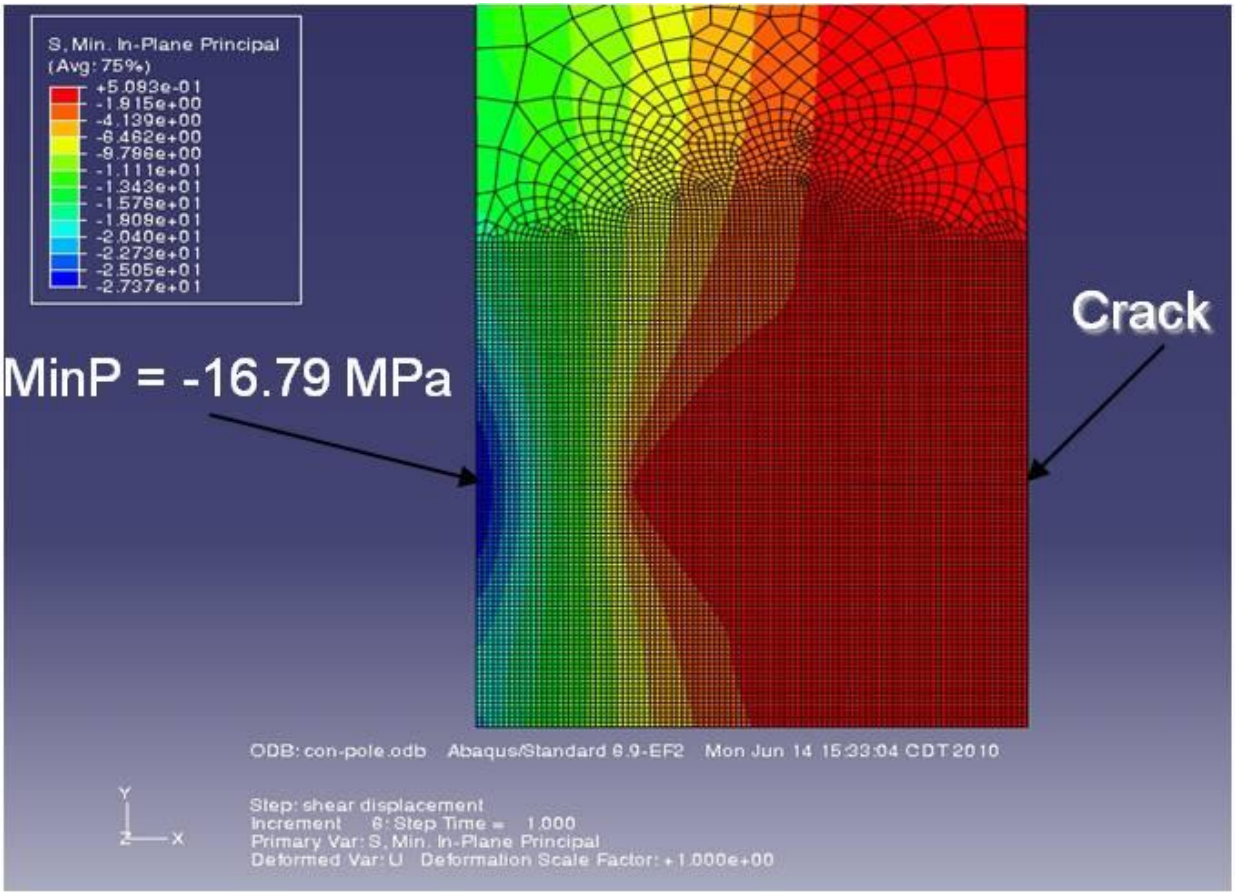

Figure 22. Conventional Pole with 80% Tendon Preload, Min Principle
Resistive Moment = 1.52E06N-mm

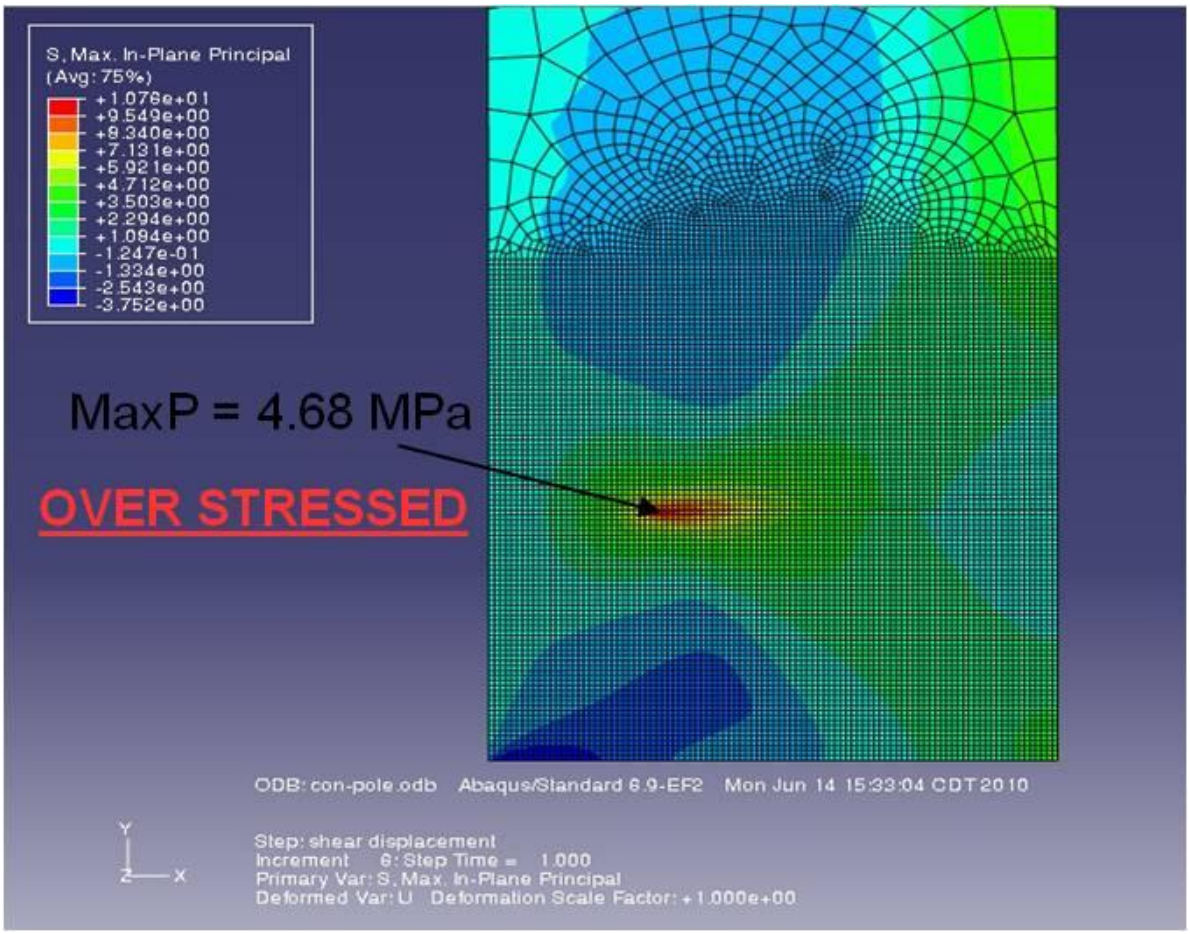

Figure 23. Conventional Pole with 80% Tendon Preload, Max Principle
Resistive Moment = 1.52E06N-mm

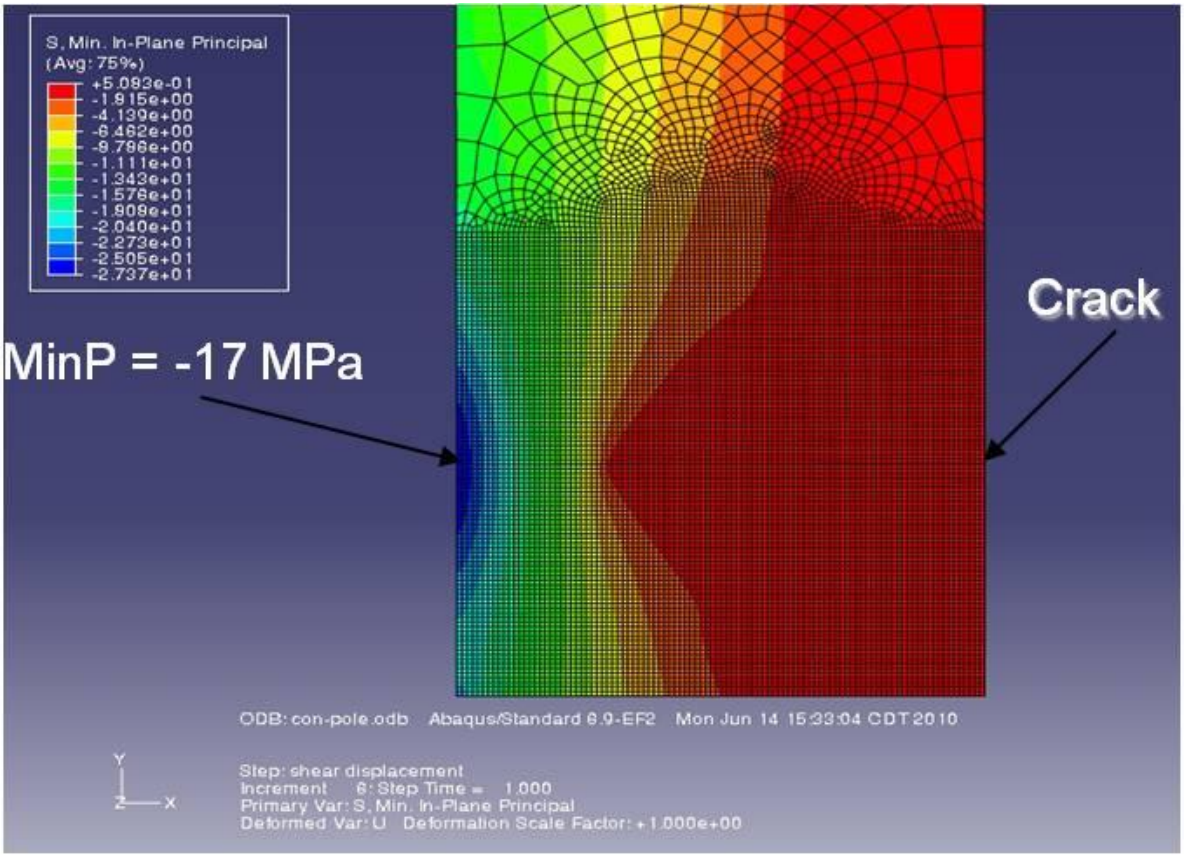

Figure 24. Conventional Pole with 100% Tendon Preload, Min Principle
Resistive Moment = 1.66E06N-mm

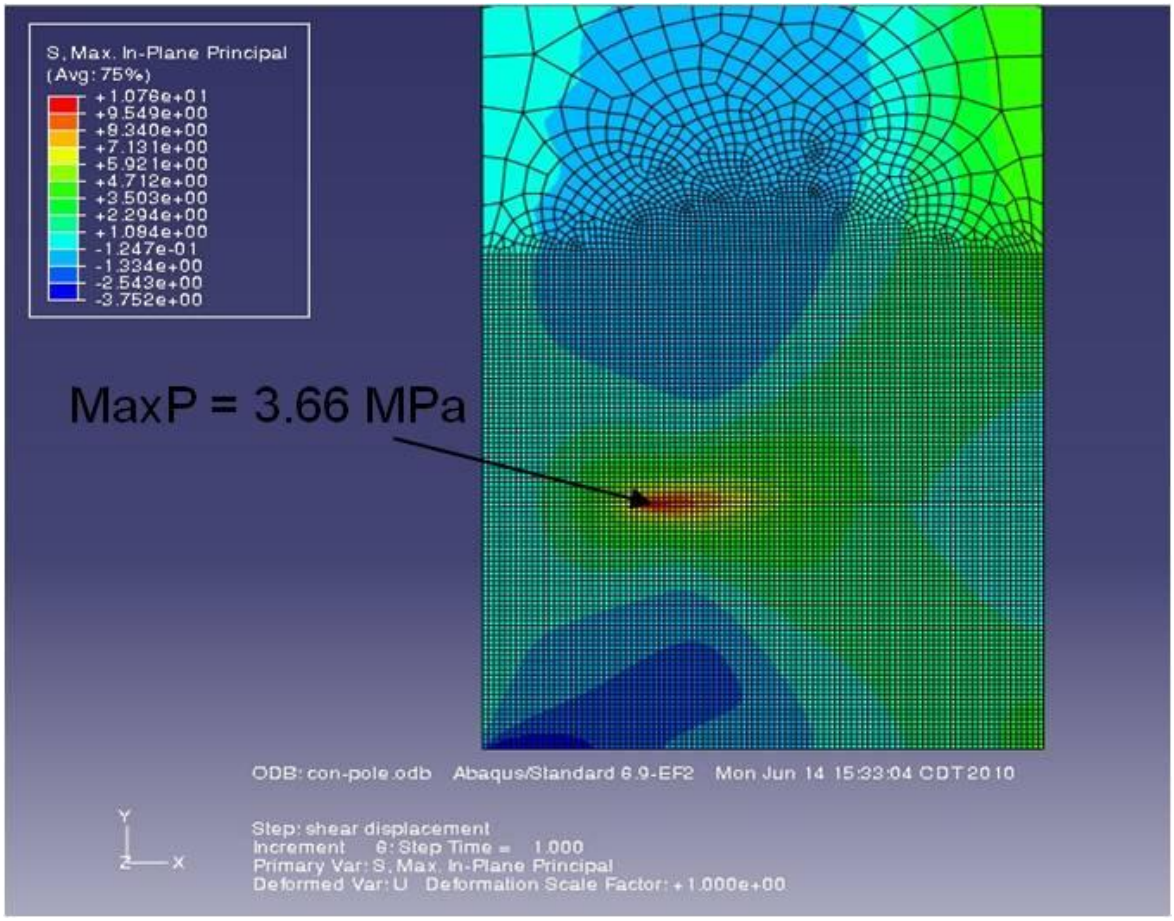

Figure 25. Conventional Pole with 100% Tendon Preload, Max Principle Resistive Moment = 1.66E06N-mm

The above FEA results confirms that the classical Maximum Resistive Moment calculation, per equation 3.3, were fairly accurate. If the 80% tendon preloading is used the FEA results show that equation 3.3 is too aggressive, that is the post will fail at loading below the maximum predicted by the equation - 1.52E06 N-mm. But at 100% preloading the FEA shows that the equation is conservative because the post will reach a

higher M_R (1.66E06 N-mm) before tensile failure occurs. The 100% preloading should be considered more realistic; as discussed above, because of tendon grouting.

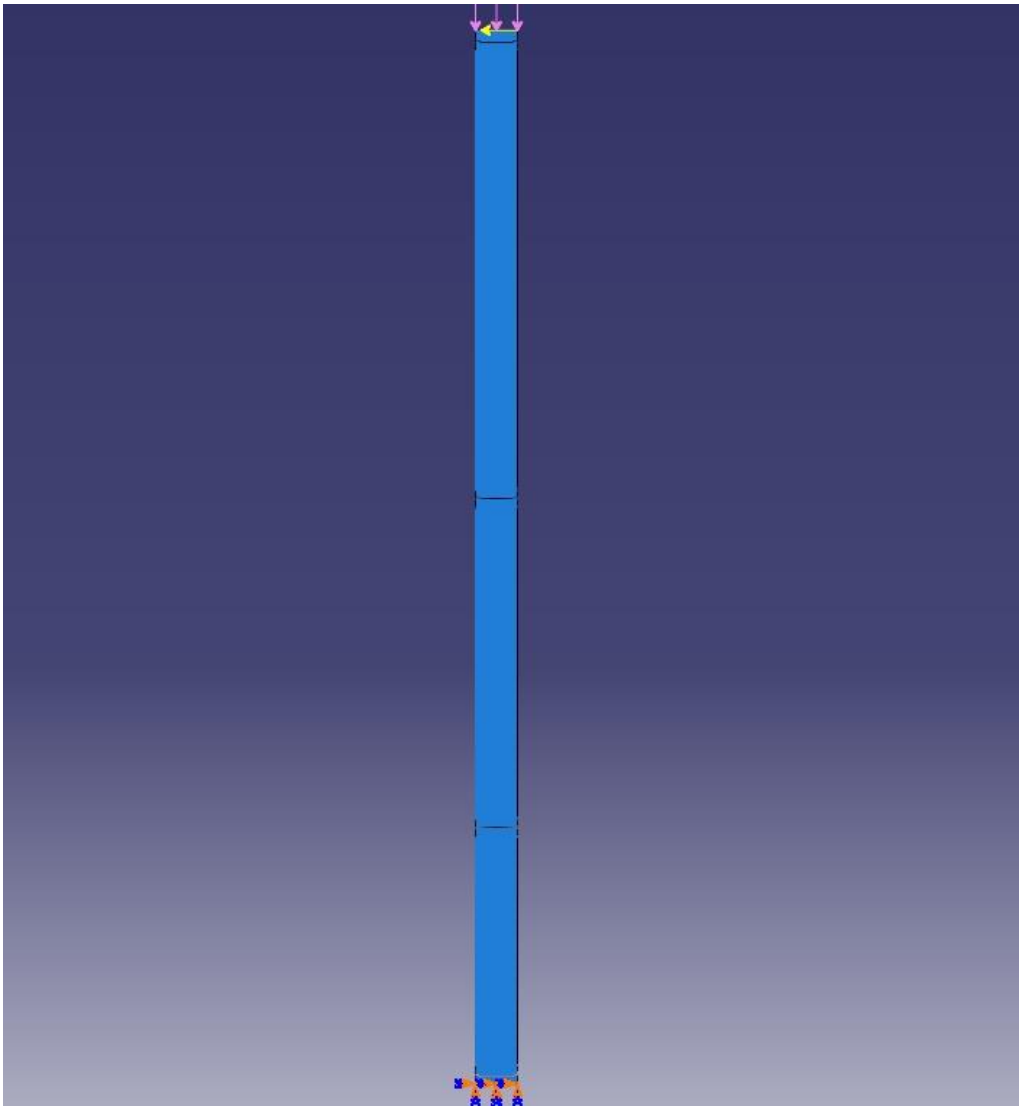

Figure 26. MS Joint Post FEA Setup

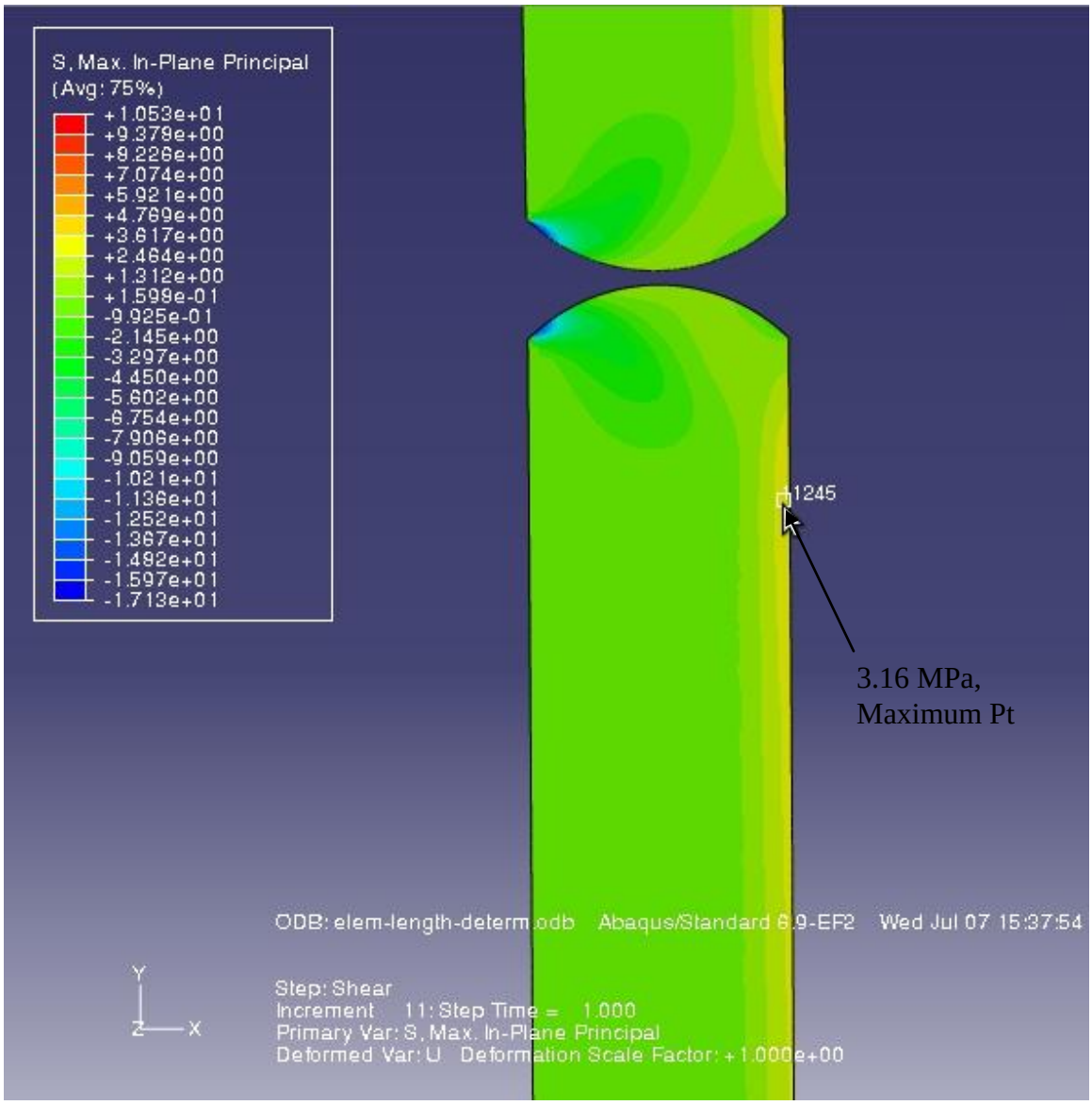

Figure 27. Maximum Principle Stress, Over Strength design for the MS Joint, at M_R = 2.88E06Nmm

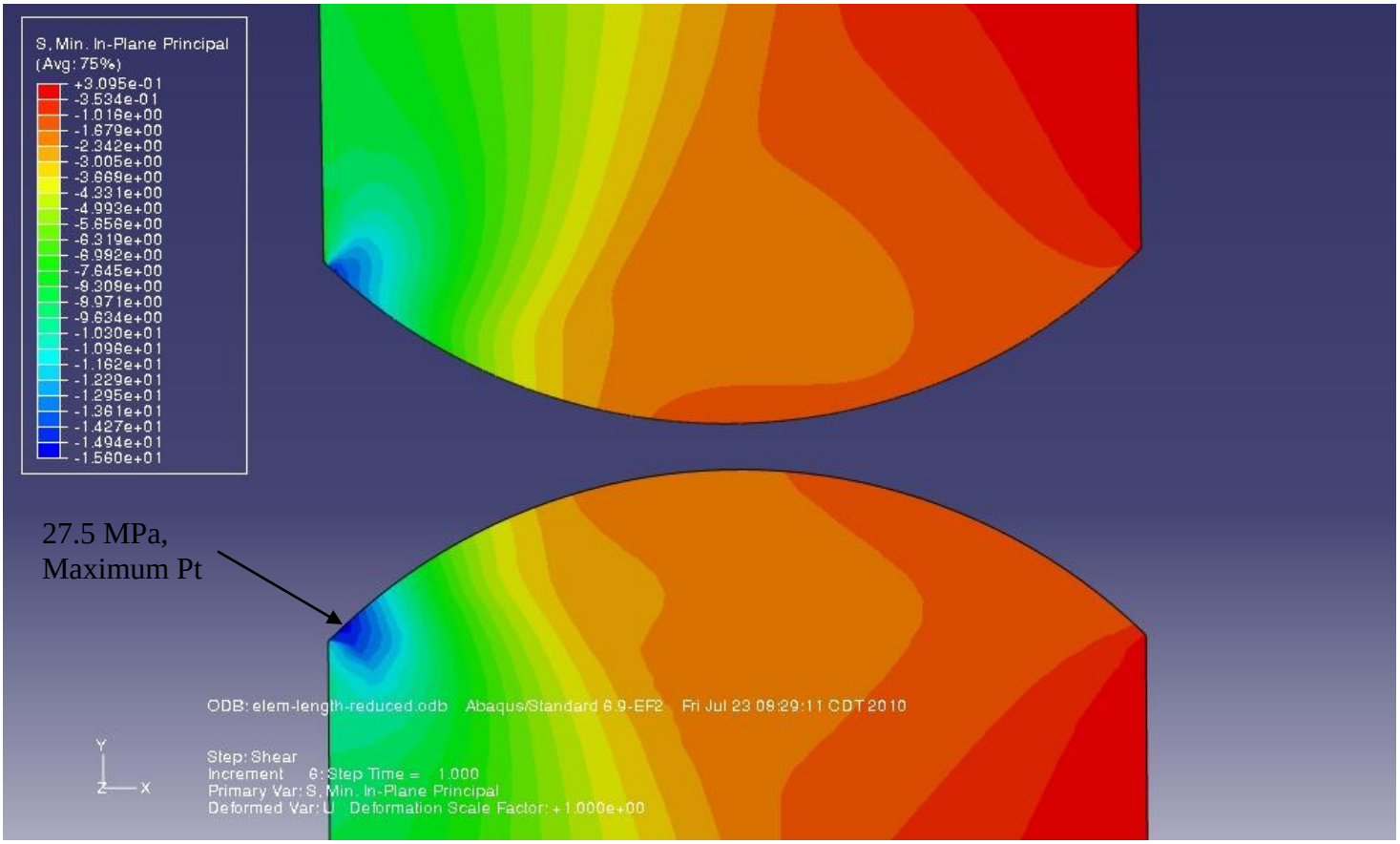

Figure 28. Minimum Principle Stress, Over Strength design for the MS Joint, at M_R = 2.88E06Nmm

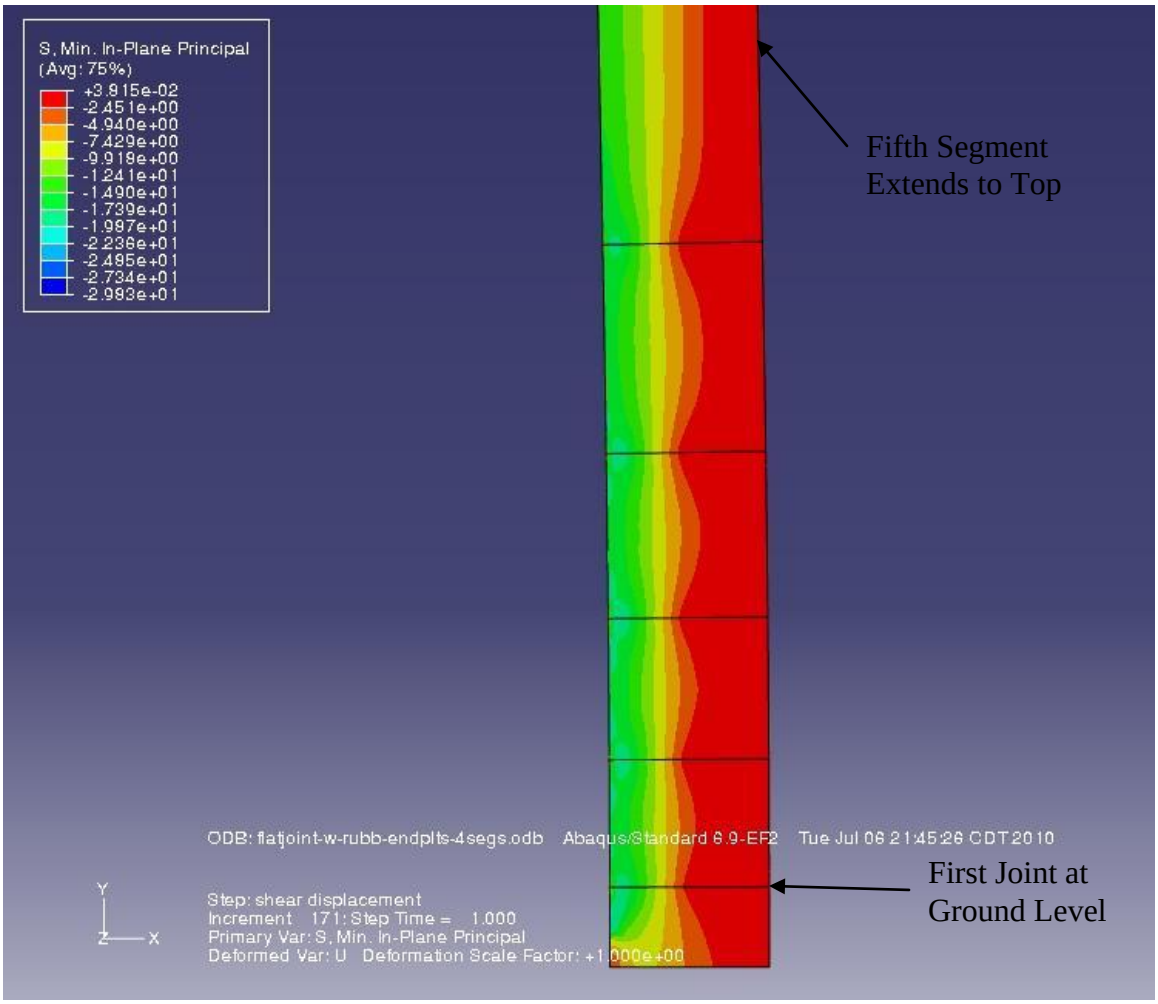

Figure 29. EB Joint Segments; Over Strength, Minimum Principle Stress, at M_R = 2.55E06Nmm

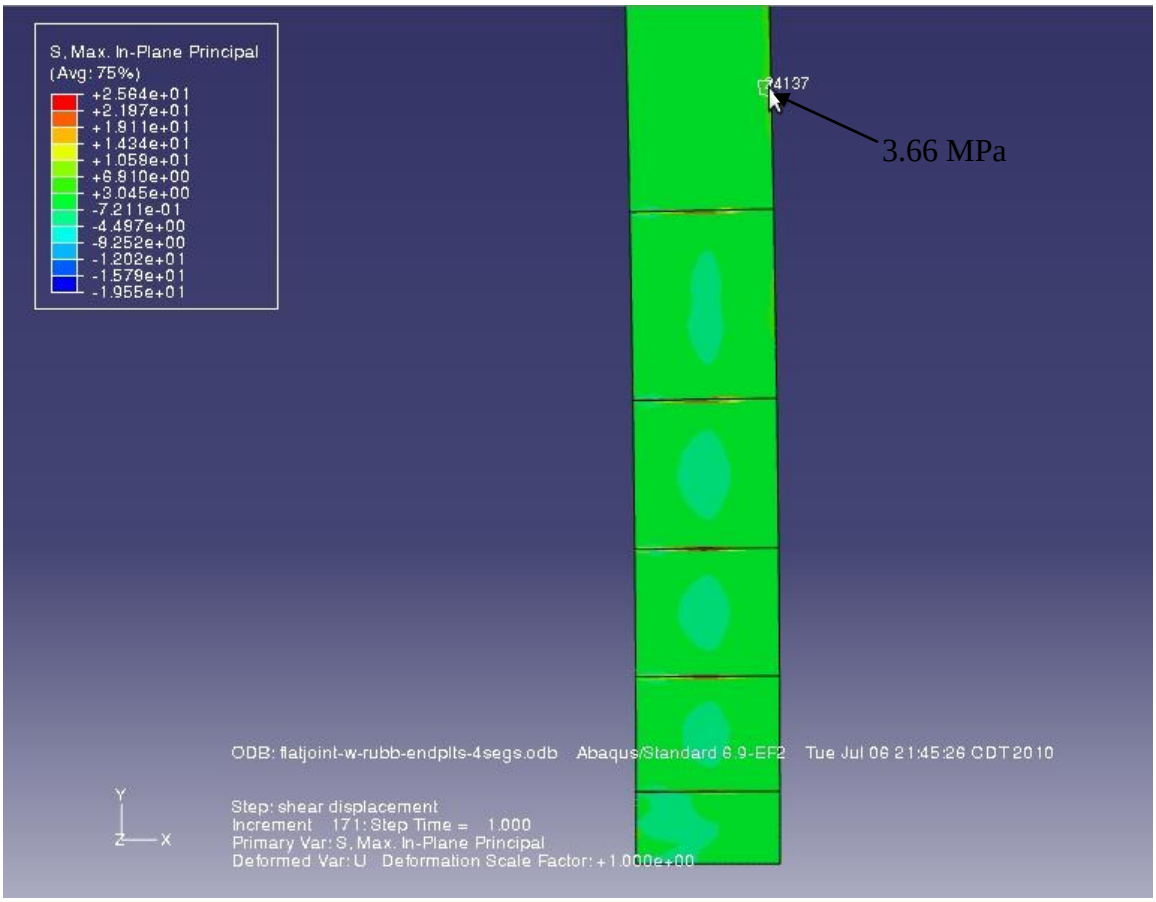

Figure 30. EB Joint Segments; Over Strength, Maximum Principle Stress

M_R = 2.55E06Nmm

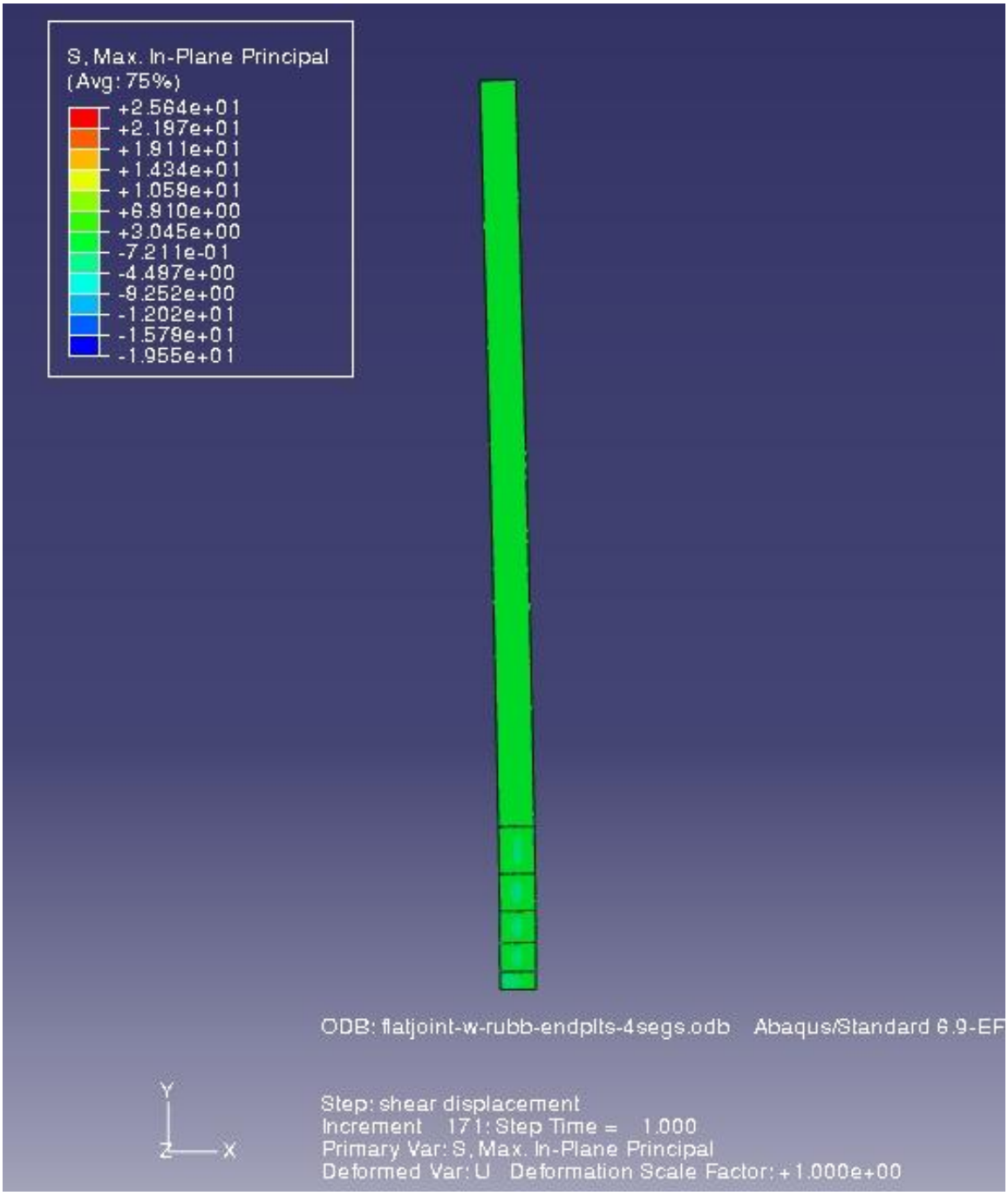

Figure 31. Complete EB Joint Post FEA, Under Load

For the reduced tendon study the maximum tendon forces were 31,900N for the EB joint and 27,500N for the MS joint. The maximum deflections were: -90.37 mm for the EB joint and -46.78 mm for the MS joint.

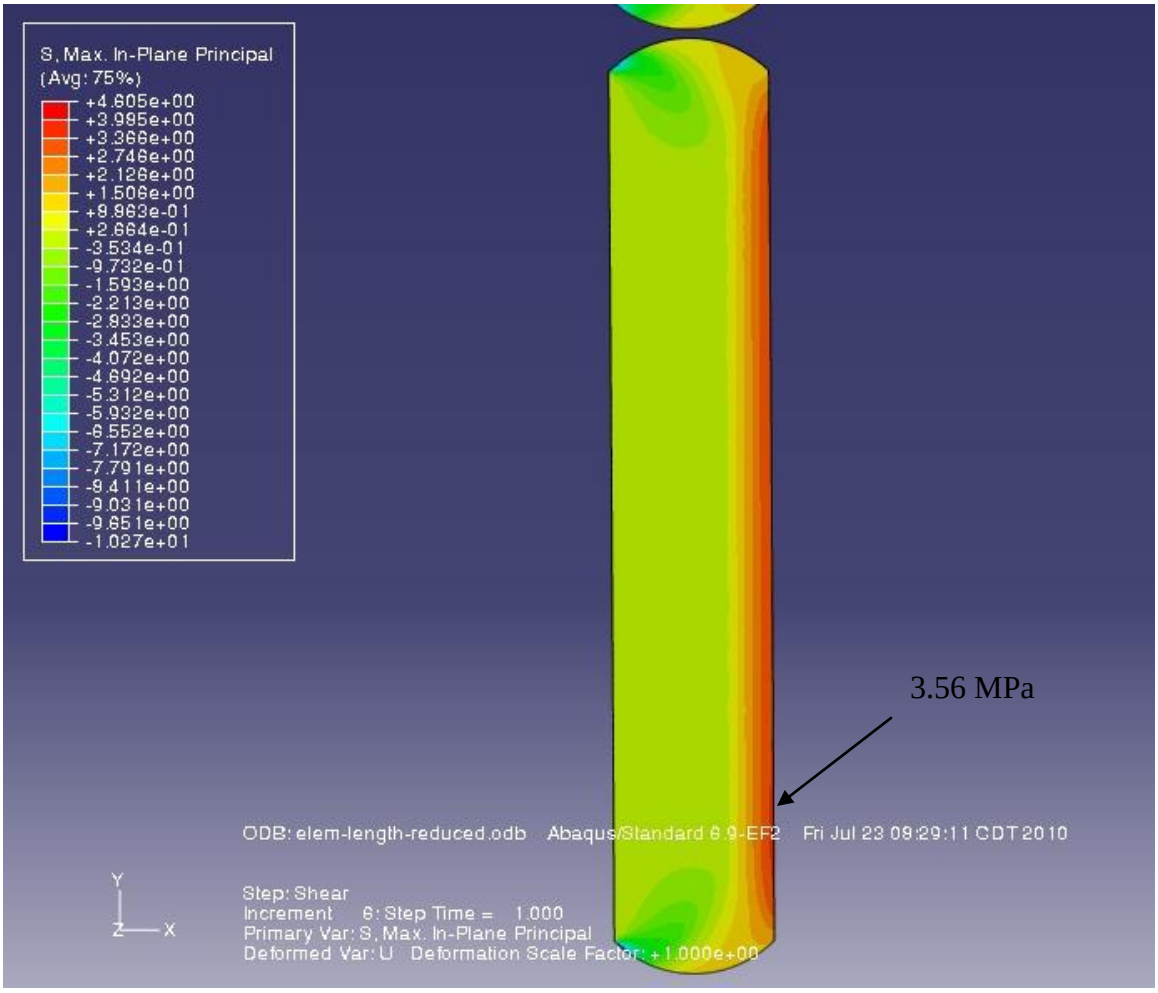

Figure 32. Max Principle Stress, Reduced Tendon Steel for the MS Joint at M_R = 1.66E06Nmm

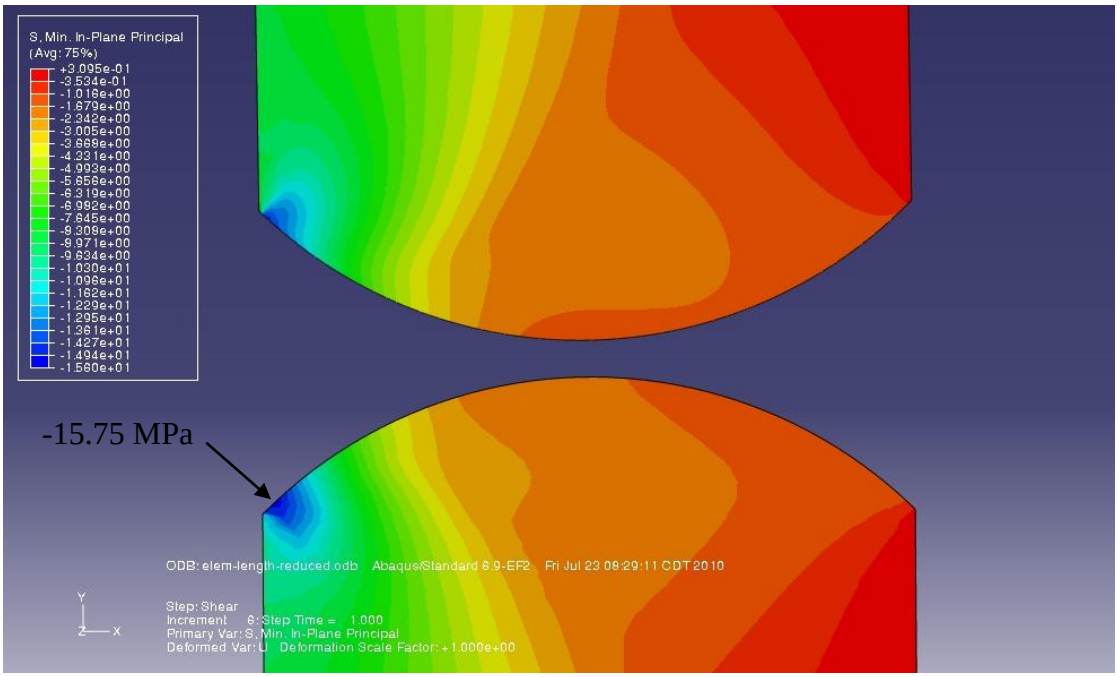

Figure 33. Minimum Principle Stress, Reduced Tendon Steel for the MS Joint at M_R = 1.66E06Nmm

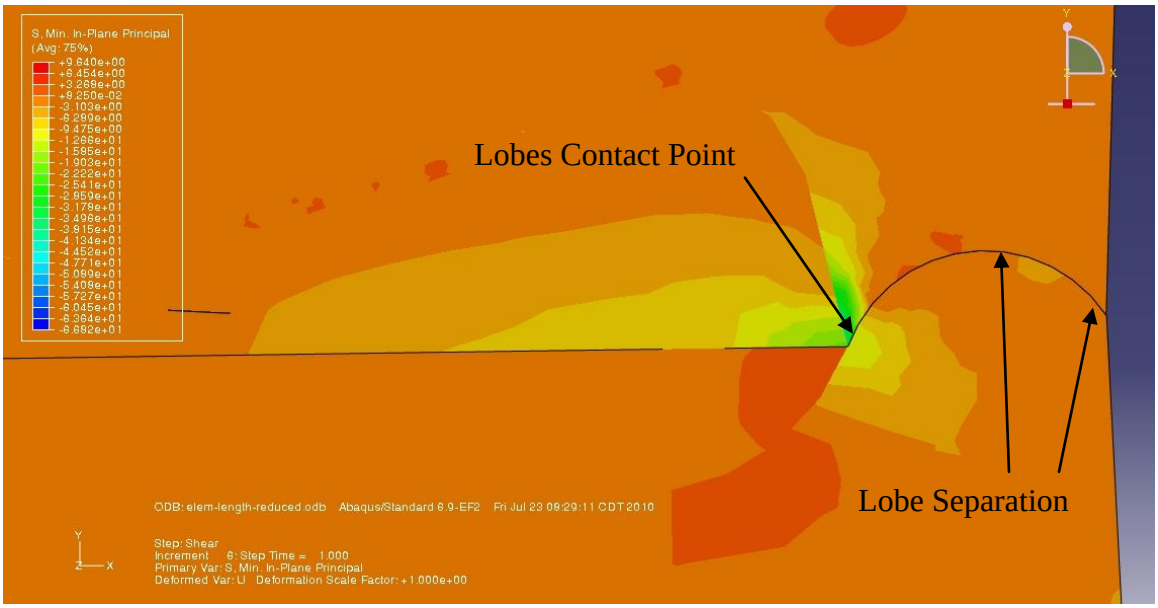

Figure 34. Joint Opening at Minimum Principle Stress, Reduced Tendon Steel Study for the MS Joint, Bottom Joint

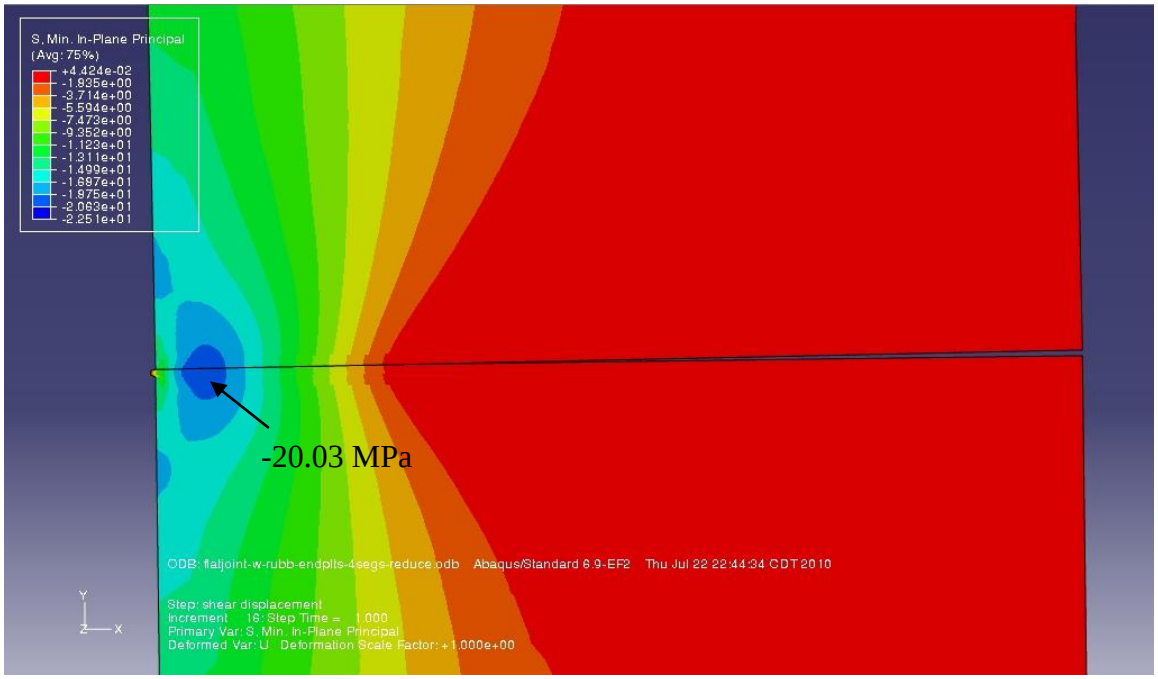

Figure 35. Minimum Principle Stress, Reduced Tendon Steel for the EB Joint, 3rd Joint, M_R = 1.66E06Nmm

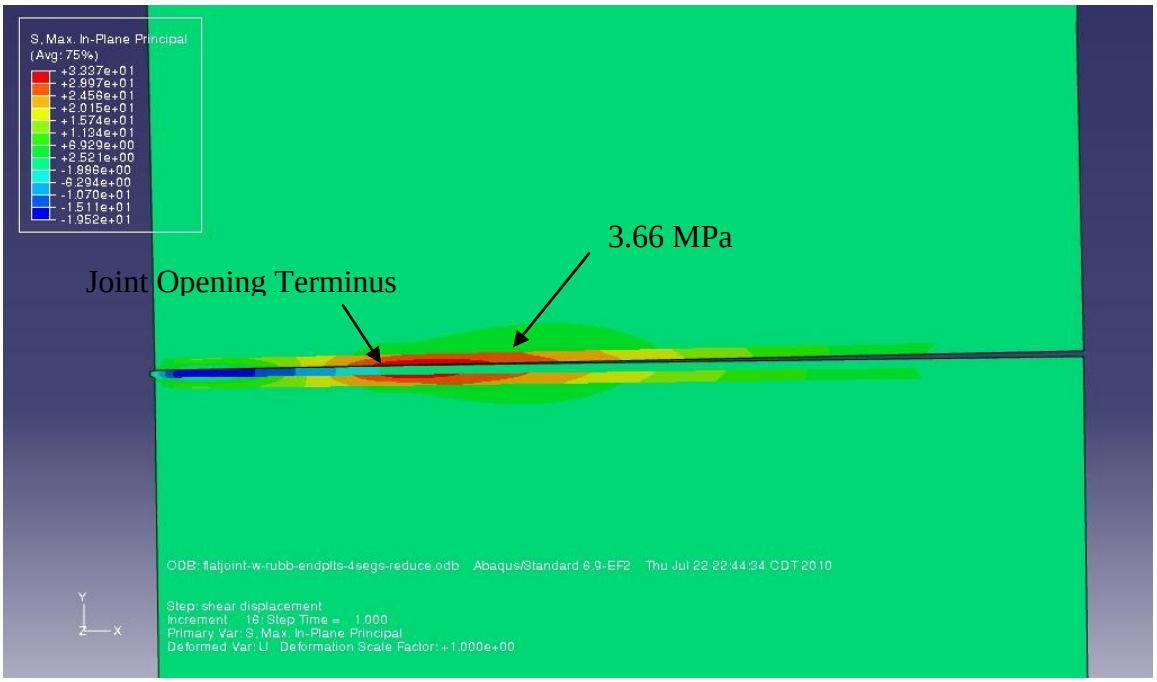

Figure 36. Maximum Principle Stress, Reduced Tendon Steel for the EB Joint, 3rd Joint M_R = 1.66E06Nmm

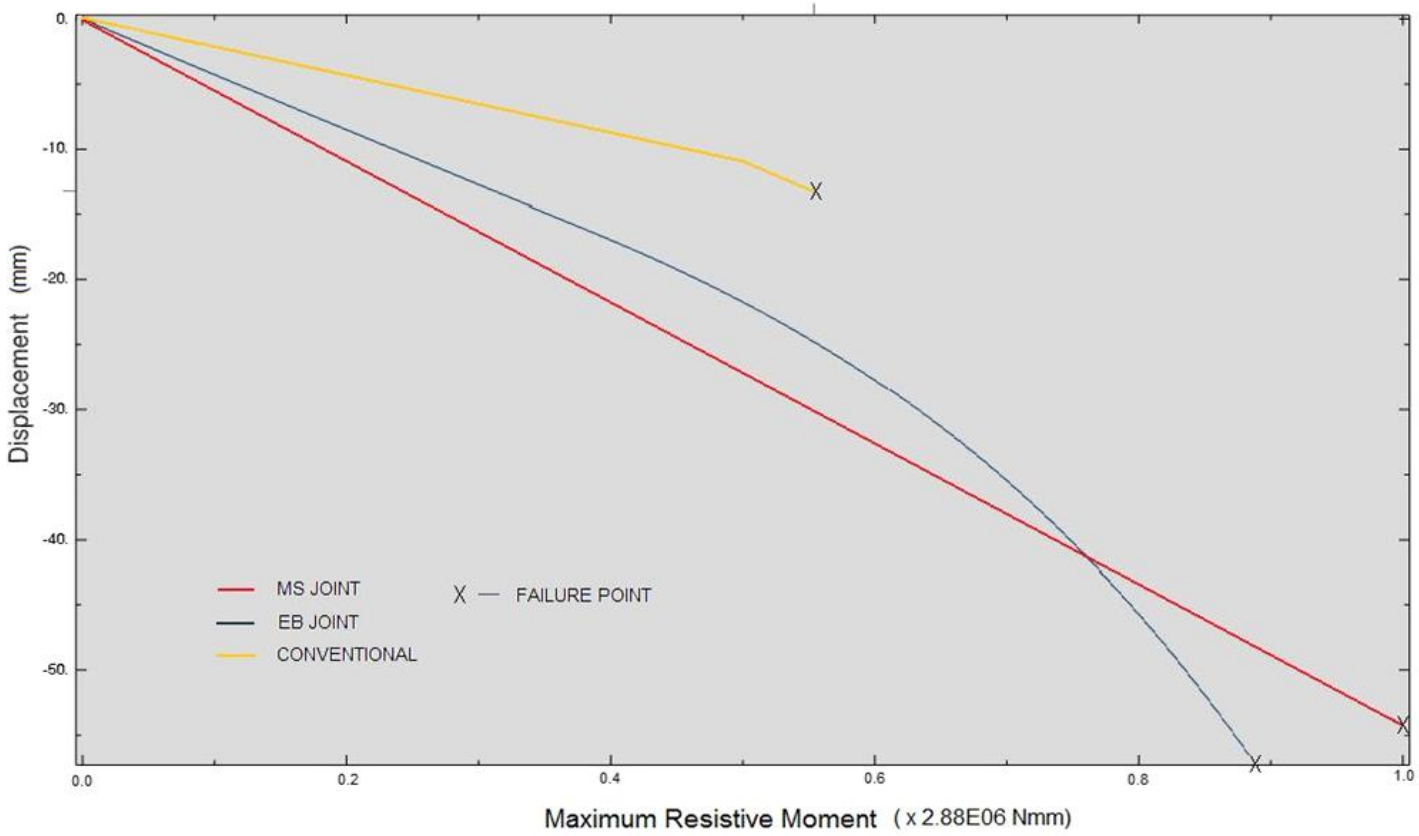

Figure 37. Deflection Comparison Between All Three Sign Posts at 100% Preload

The deflections in figure 37 show the maximum deflections for each sign post model. The limit of each curve represents the points of failure of each post, that is, the maximum resistive moments. For the MS joint the maximum deflection was -53.68 mm. For the EB joint maximum deflection was -57.02 mm. For the conventional post the maximum deflection was -13.25 mm. As can be seen from figure 37 the conventional post is much stiffer than the proposed joint structures however much weaker in terms of the maximum shear load which it can withstand before complete failure. For sign posts the stiffness is not extremely important. Although for many other structural applications

stiffness is more important. These deflections were at 100% tendon preloading. For the reduced tendon study the maximum deflections were much higher:

The Over Strength comparison showed that the EB jointed pole had a strength increase of 54% over the conventional pole. And for the MS jointed pole a 73% strength improvement. These percent figures can be thought of as correction factors, a strength value in relation to a given amount of structural material. These factors represent the degree of improvement in structural efficiency over the conventional pole structure. For the Reduced Tendon comparisons the correction factors were 44% for the EB joint pole and 52% for the MS joint.

There appears to be a large potential for further improvements for the proposed joint systems, especially the EB joints. As can be seen from figure 30 the maximum principle stress occurred at about 100mm above the fifth joint. This indicates that further segmentation would drastically reduce stresses at this point, and at successive high stress points above the highest segments. However further segmentation was not carried out because the hypothesis was easily proven with 5 segments. But it is important to note the potential for much more improvement for future studies.

4.3.2 Cost Study Results

Below are the cost calculations for the three different sign posts. For the conventional pole there is only one case, its cost is: $9.72. For the MS and EB joint poles there are two cases each: the reduced tendon and the over strength. For the over strength designs the total pole costs (adjusted) are: for the MS joint $8.60; for the EB joint $8.50. For the reduced tendon designs the total pole costs (adjusted) are: for the MS joint $9.33; for the EB joint $8.82 (calculations shown below).

In all cases the new proposals are lower in cost when adjusted for strength improvement or material (tendon) savings. The adjustments in cost were related to the tendon savings, either achieving more structural strength with a given tendon size or a reduction in the necessary amount of tendon. Concrete was not reduced or optimized in regard to material usage. There are definitely opportunities to develop cost reduced designs by reducing the amount of concrete as well.

Total cost of concrete: 4" × 4" × 144" × \$120/yd^3 × yd^3/46656 in^3 = **\$5.96/Sign-Post**

The same for <u>all 3 types of posts</u>

Total cost of stirrup steel (<u>conventional post</u>): 105,885 mm^3 × 0.298 \$/lbm × 0.284lbm/in^3 × in^3/16387.064 mm^3 = **\$0.547/Sign-Post**

Total tendon cost:

<u>For conventional post:</u>

12' × \$0.21/ft = **\$3.21**

<u>For Over Strength Posts:</u>

The EB joint tendon cost is reduced by 0.54 (correction factor from previous section) = \$3.21- 0.54 × \$3.21 = **\$1.48**

The MS joint tendon cost is reduced by 0.73 (correction factor from previous section)

= \$3.21- 0.73 × \$3.21 = **\$0.87**

<u>For Reduced Tendon Posts:</u>

The EB joint tendon cost is reduced by 0.44 (correction factor from previous section) = \$3.21- 0.44 × \$3.21 = **\$1.80**

The MS joint tendon cost is reduced by 0.52 (correction factor from previous section)

= \$3.21- 0.52 × \$3.21 = **\$1.54**

Total rubber cost (<u>for EB joint</u>):

1/3' × 1/3' × \$0.44/ft^2 × 5 = **\$0.24**

Total rubber cost (<u>for MS joint</u>):

1/3' × 0.37' × \$0.44/ft^2 × 6 = **\$0.33**

Volume of sheet metal plate: 12,387 mm^3

Total mild steel cost (<u>for EB joint</u>): 12,387 mm^3× 0.298 \$/lbm × 0.284lbm/in^3 × in^3/16387.064 mm^3 × 12 plates/sign-post = **\$0.768/Sign-Post**

Volume of male MS joint: 49,837 mm^3, Volume of female MS joint: 47,083mm^3

Total mild steel cost (<u>for MS joint</u>): (49,837 mm^3 + 47,083 mm^3)3 × 0.298 \$/lbm × 0.284lbm/in^3 × in^3/16387.064 mm^3 = **\$1.50/Sign-Post**

Total Conventional Post Cost: \$5.96 + \$0.547 + \$3.21 = **\$9.72**

Total EB Joint Post Cost:

<u>With Over Strength correction factor</u>: \$5.96 + \$0.24 + \$0.768 + \$1.48 = **<u>\$8.45</u>**

Total MS Joint Post Cost:

<u>With Over Strength correction factor</u>: \$5.96 + \$0.33 + \$1.50 + \$0.87 = **<u>\$8.66</u>**

Total EB Joint Post Cost:

With Reduced Tendon factor: \$5.96 + \$0.24 + \$0.768 + \$1.80 = **\$8.77**

Total MS Joint Post Cost:

With Reduced Tendon factor: \$5.96 + \$0.33 + \$1.50 + \$1.54 = **\$9.33**

2" Schedule 40, Steel Conduit – 12' long -> \$14.65 (typical steel stop sign post)

The above cost results coupled with the FEA-M_R results, show that the hypotheses were proven. That is, that both the EB and MS joint structures are stronger than the conventional sign post and for less cost.

Chapter 5: Mechanistic Mode, Additional Considerations

Depending upon the structural system the tendons can be tied together in series of networks so that strain energy can flow from an entire complex structure into an area where concentrated loading or deflection is occurring. This could allow very large deformations at certain locations, and subsequently the structure could regain its original shape (option 6 below). Otherwise for the mechanistic mode to exist means must be installed for allowing extreme strain in the tendon while maintaining tendon stress levels below yield.

Means of limiting tendon stress and allowing massive strains (for this study 15 °of rotation at each joint was considered a maximum) could be achieved a number of ways:

1) Simply trade off a large amount of static structural strength, i.e. greatly reduce the M_R and utilize the available strain to achieve more strain for the dynamic domain…this may not achieve a great deal of additional strain however.
2) Design the internal tendon channels such that the MS joint can act as a break-over mechanism. The annular tendon channels can be made wide enough to allow large lateral movements of the tendon. Allowing a variable eccentricity of the tendon axis. When the tendon moves to the pivot point of the MS joints the M_R of the joint will drop to zero. A few problems here are: a) Rehabilitating the static state, b) Mechanisms at each joint would have to be employed to center the tendons until a certain degree of opening, or loading, occurred.
3) Have a deformable link coupled between the tendon and the rest of the structure such that upon reaching stresses just below yield the link would plastically yield and allow massive deformations. The link would have to be replaced and the structure re-preloaded to rehabilitate it.

4) The tendon can be designed to deform upon extreme overloading. And subsequently the tendon would need replacement for structural rehabilitation, as well as re-preloading: basically under-reinforce the structure and design the tendon with large amounts of available malleability.

5) An elastic spring could be coupled between the tendon end and an anchor. The spring could be nonlinear in order to reduce the size, for the force and displacements required. A nonlinear spring could lead to the structure acting more as a break-over mechanism.

6) The best way, if possible, is to tie tendons together in large networks thereby increasing the strain available for each tendon. This can be done if a large complex structure is involved, such as a building. The tendon strains would be shared or distributed throughout the structure ideally allowing relatively constant stress levels in all the tendons. Also this would allow high levels of stress to be maintained throughout the dynamic range of motion, at least at one or more locations in the structure. The goal being increased load capacity and increased resiliency. However compression element stresses could become excessive under such extreme overloading conditions.

If option 6 were pursued in a complex structure then detailed simulations would need to be done in order to evolve and verify the structure's design. Details such as leash slack, strength and anchoring method, for each element. These would all affect the structures behavior and maximum stress levels for the various loading requirements. Segmentation as well as other design parameters could be changed between successive simulation runs in order to develop an optimal design. Depending upon the type of loading, dynamic FEA simulation may be required as well. The following is a list of design parameters that should be considered in developing a structure design with a mechanistic mode:

a) Leash details: slack, strength and anchoring

b) Segmentation: element length, also cross section and taper

c) Steel Index, for each tendon section

d) Concrete strength, including special localized reinforcements

e) Rubber thickness and hardness

f) Internal lubrication: type and degree

g) Additional dampening devices

h) Overall structure geometry, such as truss density or type

The simulated loading can be any number of overload scenarios: earthquakes, wind storms, impacts, explosions, traffic overloading, tsunamis and partial structure loss. The final goal of the structure behavior could be structure survival, controlled collapse, or protection of occupants.

The leashes can act as additional reinforcement if extended into the body of the compression element, such as depicted in figure 7. Leashes may also be an integral part of any variable eccentricity and tendon centering device that would be part of a joint break-over function (option 2 above).

Another interesting possibility is the development of self erecting structures. This may be accomplished through the process of post tensioning. A structure that is in a collapsed state but completely linked together with tendons could be pulled into an erect state as the tendons are tensioned. One example is a tower or pole that would lie on the ground initially untensioned; it could also be in a coiled state. Then after the base is secured to the ground a hydraulic ram would start to tighten the segments together. This ram could act through a window in the tower base. And as the tendon tension increased the tower would slowly pull itself into a standing position one segment at a time. Similar to the growth of a fern as the fronds uncurl upward. At the full prestressed state the

tendons would be anchored. This kind of erecting process could save money by eliminating the need for cranes.

In the previous chapters the discussions have been relative to a single plane of rotation in the MS joint structure. Basically only 2D motions were discussed and developed. However the MS concept can easily be extended to multiple planes of rotation; either two planes (as depicted in figure 38), or any number of planes with addition of pivots.

So far only bending rotations have been discussed. But torsional rotation may also be important in certain applications. For multi-axis MS joints, such as in figure 38, with joint pivots in a single plane perpendicular to the element's axis, there is an inherent mechanistic torsional deflection response. This function manifests itself when a length of elements becomes loaded torsionally. The series of elements can react with the sequential opening of the joints. However instead of the joints opening in a single plane as when under pure bending, the joint openings will alternate opening from one plane to the perpendicular plane. This will create a spiral deflection pattern which includes an element of torsional deflection (see figure 39). The figure only shows the mechanistic deflection of 4 degrees. There would also be the material torsional deflection which would add to the mechanistic deflection under actual loading. If the plane that the joint pivots lie in were not perpendicular to the element axis then the torsion deflection could be increased dramatically, depending upon the joint plane angles.

Practically any number of structural geometries can be built with this basic concept of multidirectional mechanistic-static joints held together with networks of tension elements. Elongated beam or prismatic members but also plates and complex frames maybe developed. In figure 40 a plate structure is illustrated.

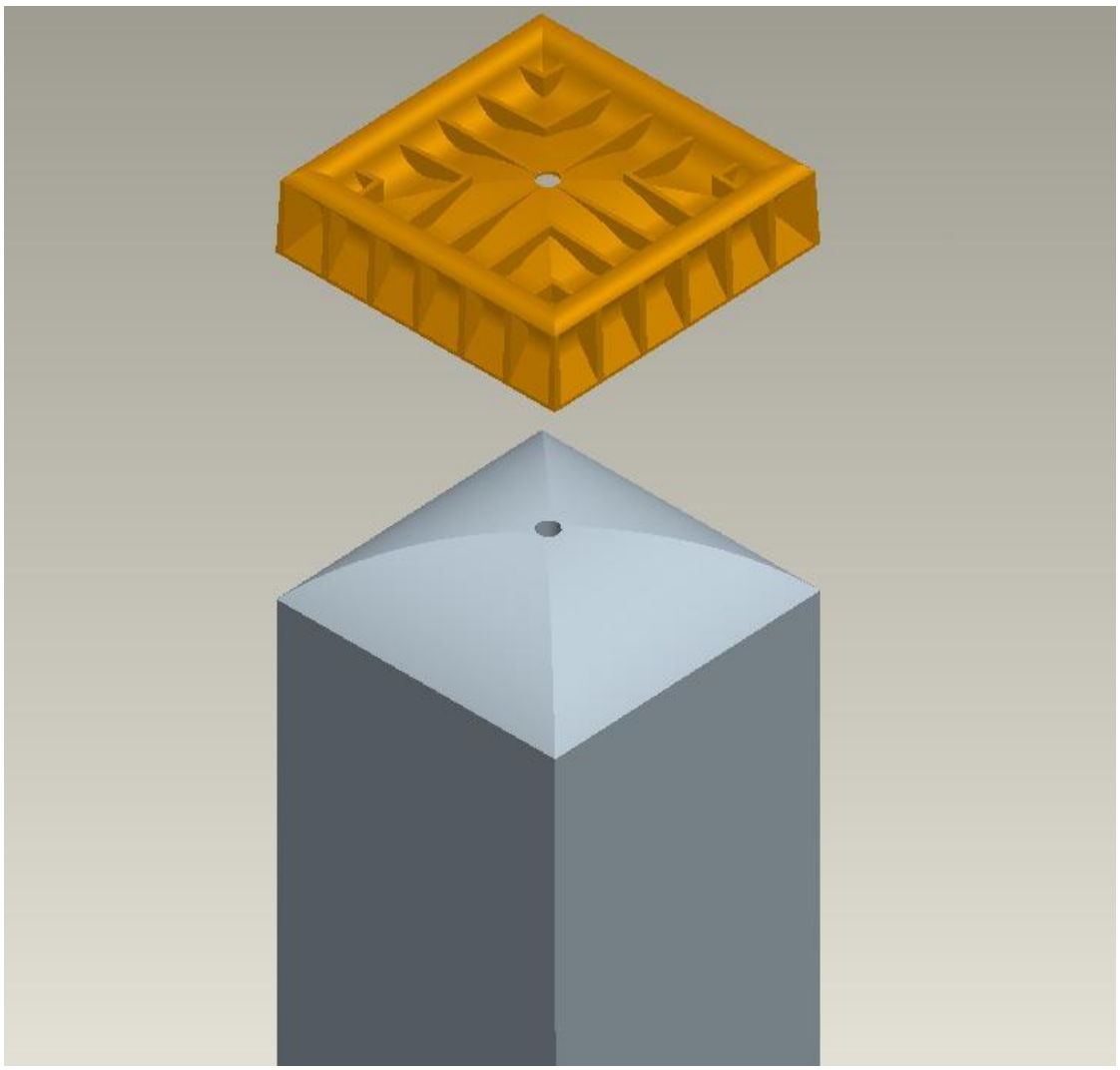

Figure 38. Two Plane of Rotation MS Joint

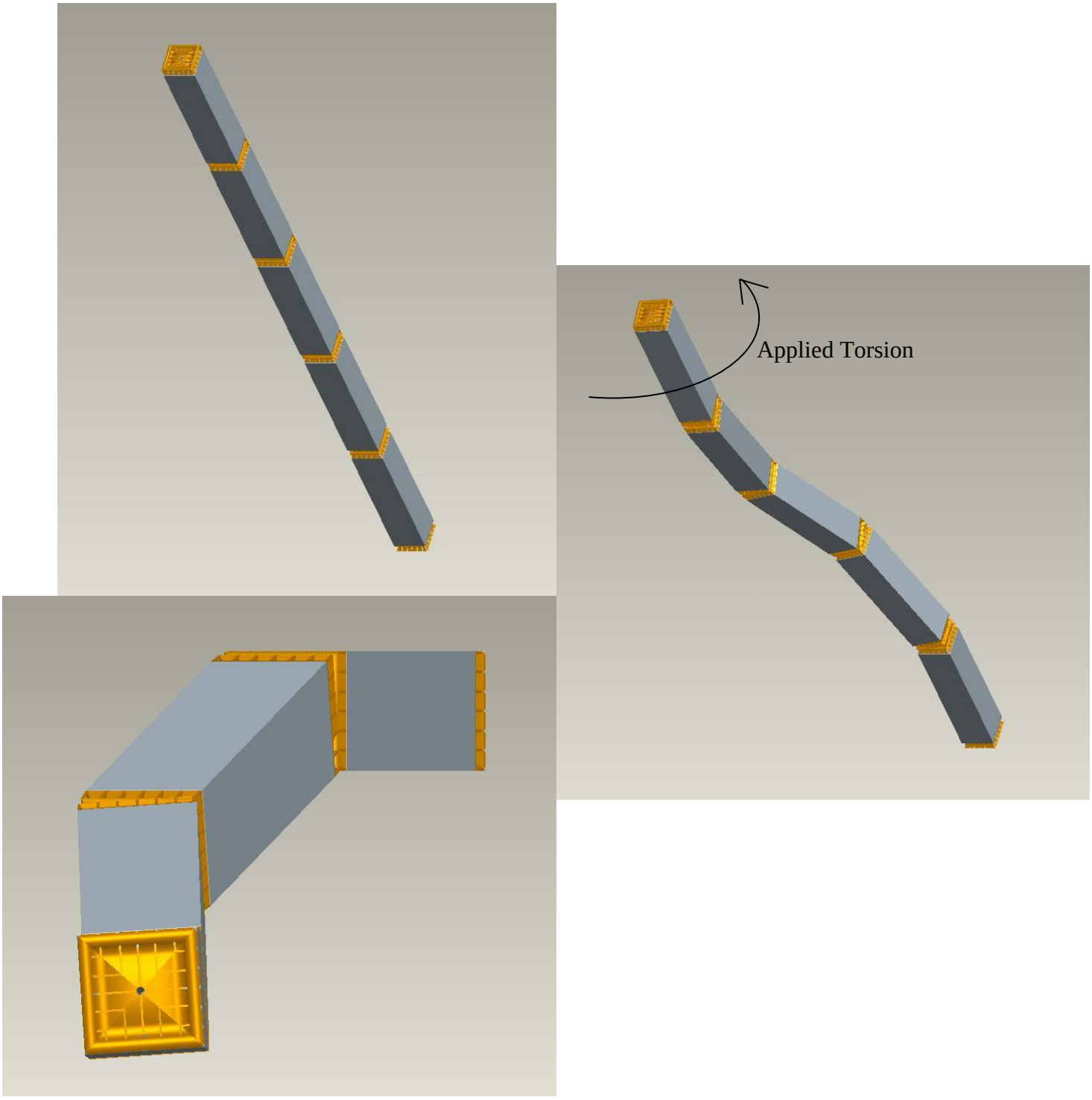

Figure 39. Torsional Mechanistic Deflection (4°)

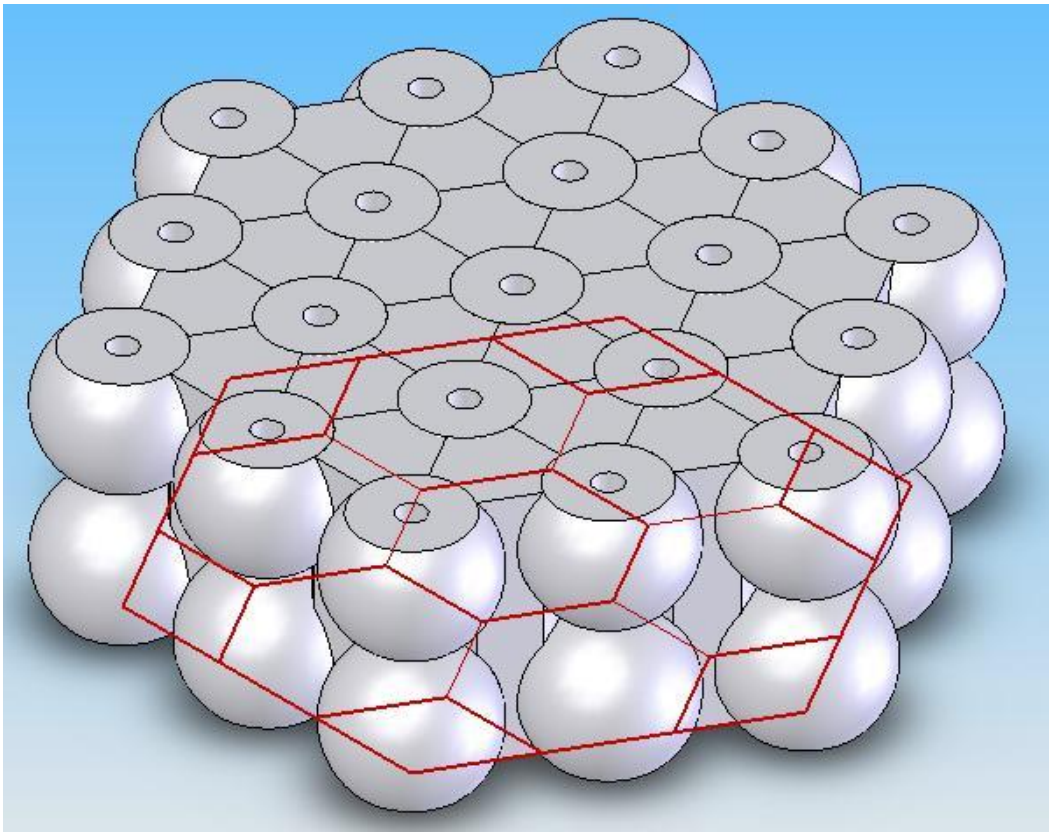

Figure 40. Proposed Hexagonal Plate Structure, Tensile Elements Shown in Red

Chapter 6: Segmental Pavement

6.1 Background

Segmental Paving dates back as far as the Roman Empire, in the form of paving stones. Paving stone roads are very durable in fact many Roman stone roads are still in service. In large part this can be attributed to the simplicity of repair. In figure 41 is a Roman road in Southeast Italy that is still in service after 2,300 years. Later in the late 1940's concrete pavers were developed in the Netherlands as a replacement for clay brick streets.

Concrete block pavements offer many advantages: ease of maintenance, access to utilities, and low maintenance costs. Additionally, they offer superior resistance to freeze-thaw and de-icing salts. Heavy use pavements constructed of concrete pavers have found widespread use in docks and airports in present day construction. Aside from pavers there are a number of other forms of segmental pavement.

Figure 41. Via Appia, Roman Road Built in 312 B.C.[34]

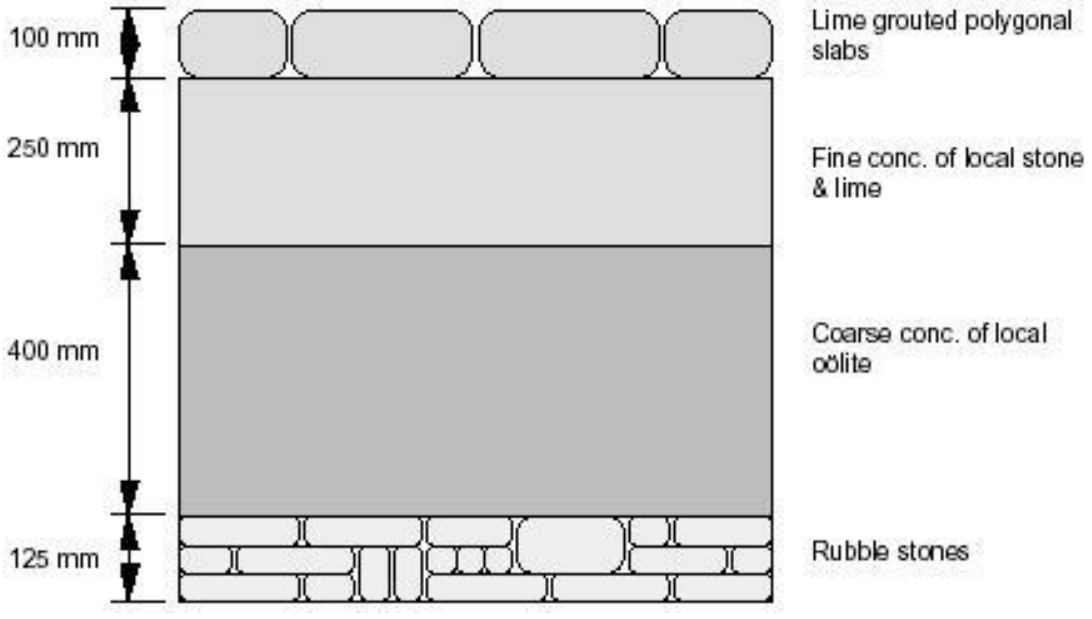

Figure 42. Typical Roman Road Construction[34]

The various forms of segmental pavement include:

- ➔ Jointed plain (JPCP)
- ➔ Jointed reinforced (JRCP)
- ➔ Prestressed concrete pavement (PCP)
- ➔ Continuously reinforced concrete pavement; soon after construction (CRCP)

JCP is more of a general designation which subsumes JPCP and JRCP. JPCP is unreinforced concrete that is usually broken up into slabs through saw cut induced crack joints. JRCP is similar to JPCP, often with saw cut joints, except that steel reinforcement runs through the concrete, typically rebar. The JRCP can also be precast and then brought together to form an extended pavement. PCP sometimes has well defined joint boundaries where the precast slabs come together in sections of pavement and are prestressed. In some cases PCP is post-tensioned and in others prestressed internally.

Continuously reinforced concrete pavement (CRCP) may in a sense be thought of as jointed concrete, in that CRCP will form joints through random cracking. And when these cracks cut through the concrete there are various shaped segments created. However these random segments are not optimal as they can lead to severe flaws such as spalling and punch-outs that occur later in the CRCP life cycle.

Methods of design and construction for segmental paving have changed significantly throughout the ages, and currently there are many different systems available. Some that are germane to this study are[14]:

- ➔ Pavers
- ➔ Raft Units
- ➔ Precast Bridge Deck Panels
- ➔ Segmental Bridge Joints
- ➔ Precast Panels for Pavement Repair

Pavers as discussed above are very old technology with many advantages. However the speed of construction and overall costs concerns tend to make it unattractive for most large roadway pavement projects.

Raft units are precast concrete panels used primarily for temporary roads, or rapid highway repairs. Raft units are usually square, though hexagonal units have been used. Generally, raft units are usually 2m x 2m (6.6ft x 6.6ft) and between 75 and 220mm (3-9 in.) thick, but have been constructed as large as 2.29m x 10.0m (7.5ft x 32.8ft). Angle steel is sometimes used around the top edges of raft units and welded to the upper reinforcing layer to minimize damage from impact loading. When angle steel is not used, the edges are typically detailed with an inverted V-shape; this is done to reduce spalling at the joint[22, 14].

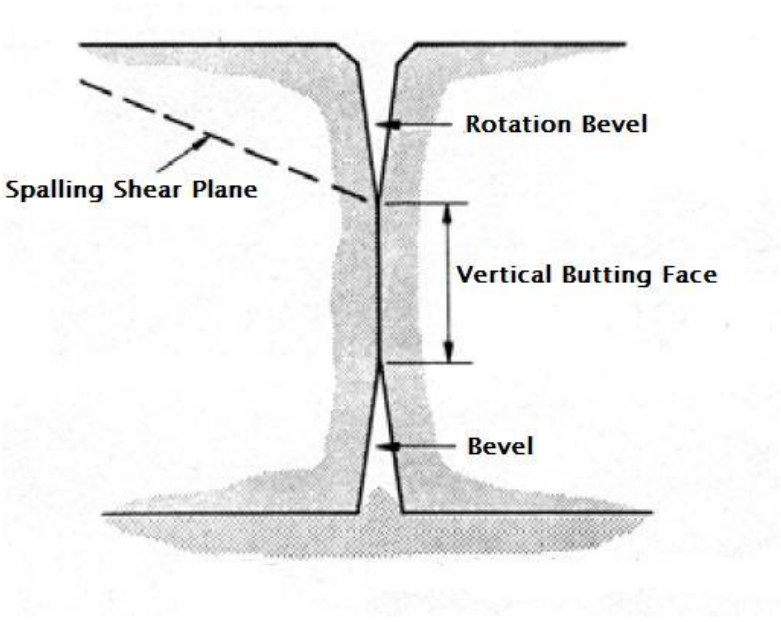

Figure 43. Raft Unit Joint[14]

Bridge deck panels are often precast but also can be cast in place using a technique called match-casting, wherein adjacent panels are cast next to each other. This method could potentially be applied to the fabrication of pavement slabs. This technique uses a bond-breaker along the adjoining edge of the panel to keep it from bonding to the adjacent panel. The adjacent panel is then cast using the edge face of the previous panel as one side of the casting form. This technique assures a tight, uniform joint between adjacent panels and could provide a means of adjusting to roadway transitions such as turns, banks and dips; however it is very slow as construction has to wait for the curing of each slab in sequence. Concrete bridge deck panels are usually prestressed during fabrication and/or placement. Some of the considerations for prestressing include prestress methods, levels of prestress and stressing timeframe. Prestressing methods include pretensioning, post tensioning, or a combination of both. In common practice, panels are usually pretensioned in one direction (i.e., longitudinally) during fabrication and post-tensioned in the other direction (i.e., transversely), after they are set in place, through post tensioning ducts cast into the panels. Levels of prestress for bridge deck slabs vary, depending on the application of the project, the concrete strength, and the prestressing method. Literature on bridge deck panels reveals that prestressing levels vary from 200 to 450 psi, on average, to as much as 1,000 psi[14].

Segmental bridge construction was discussed in previous chapters. The similarities and differences were explored in reference to the joint concepts presented in this dissertation. However the discussion focused more on the bulk structure and not so much in relation to a pavement structure. Critical to the joint performance in current segmental bridge joints is the epoxy grout. This fact points to a need for more compliant joint interfaces as opposed to dry joints, in order to improve performance of any post-tensioned segmental structures.

Recently many proposals have been developed which focus on precast panels for rapid pavement repair as well as longer life pavements. One method will be primarily

discussed in comparison to the proposals of this dissertation: the "Neil Cable" system[14] a post-tensioned precast pavement which is most comparable to the joining systems presented here. However there are a number of important differences the main one being the joint structure. The Neil Cable concept uses epoxied key joints very similarly to segmental bridge systems. The Neil Cable system is basically a combination of conventional prestressing methods (post-tensioned and pretensioned) applied to precast panels or slabs, although with many specific caveats such as: relatively low prestress levels (to reduce tendon costs), centralized post tensioning, interspersed expansion joints and both tendon and surface grouting.

This dissertation focuses primarily on the joint design and the application of the proposed joining systems (EB and MS joints). The precast concrete segments are also an integral part of the joining systems. But cast in place methods are applicable as well. As in match-casting, cast in place processes can produce segmental pavement, with the use of casting boundaries which act as the joint interface surfaces after the concrete cures. These casting boundaries could be composed of the EB or MS joint structures. Also precast slabs may facilitate the production of specific slab geometry such as hollowed out or cored sections. The following proposal includes both precast and cast in place slabs.

6.2 A Proposal for Pavement Construction

6.2.1 Definition

It is hypothesized that for the following pavement proposals either the MS or EB joint concepts should work well. However because of the lower cost of the EB joint system and considering the generally low level of deformation that pavements see, the EB joints are the focus of the proposals.

For bridges or for roads on unstable ground: flood zone, silty-sandy bases, peat soils, cavernous sub-strata or earthquake zones or basically surfaces which may see a large degree of deflection the MS joint would be most applicable. For pontoon bridges this would definitely be the case, as vehicle and wave loading can cause large repetitive deflections of segments.

A proposed configuration and assembly method was developed in order to construct an FEA model to study the feasibility. The objective being to take advantage of all the EB joint functions applicable to pavement structures:

- ➔ The relative compliancy of the rubber layers offers a means of helping to absorb thermal expansion, as expansion joints; while maintaining load transfer across joints.
- ➔ The compression set of the rubber layer offers a means of mechanically interlocking with the sheet metal. The sheet metal can have various non planar surfaces such as a hole pattern or embossed pattern, that the rubber would partially conform to. Or a toothed rubber pattern could fit into a pattern in the steel plate.
- ➔ The rubber and sheet metal layers offer a relatively compliant interface which also spreads and cushions the contact stresses between the slabs. This is turn allows a tilt-up (wedging) prestressing assembly method; described below.

➔ As with the sign post structure an EB jointed pavement should allow much more loading and maximum deflection in comparison to other joining methods. In turn this will allow a reduction in required material such as the thickness of the pavement, which will reduce the concrete costs.

The relaxation behavior of the elastomeric layer becomes an important factor in pavement designs which utilize the proposed joint structures. This is because the proposed joint system's elastomeric layers act as primary components of stress transmission through the structures. For pavements connected through EB or MS joints that are precast and post-tensioned, the rubber layers will be under constant prestressing pressures as well as additional pressures generated from thermal expansion. Therefore some compression set will be seen in the rubber layers. The percentage of set was set at 0.35, or 35% (see section 3.4). This is a rough initial estimate of worst case that would need to be verified with experimental trials. Additionally it would be advisable to check compression set properties of production samples to verify that rubber properties met specification tolerances prior to and during a construction project.

For purposes of the pavement proposal a typical precast slab utilizing the EB joint system consisted of: a precast slab with bonded sheet metal on all peripheral side surfaces, with a bonded rubber layer on one of the transverse sides and one of the longitudinal sides.

The tilt-up wedging is a proposed method of prestressing which may reduce the amount of steel required in pavement, and represents a convenient alternative to the common methods of post tensioning (figures 45 through 47). This method tilts pairs of slabs together during the pavement assembly process. As the slabs are flattened into place the ground level ends of the slabs press against tendon anchors or end restraint structures.

There are two general cases being considered: post-tensioned and post-compressed. Post-compressed, in the following context, refers to a tendonless method of

prestressing concrete pavement. This method applies external compressive pressures to peripheral surfaces of a series of concrete slabs and then locks the slabs in place. The locking is accomplished with retention structures which dam the slabs against any movement that would diminish the prestressing pressures. Dependant on the retention dam structure costs this method may present large savings compared to post-tension prestressing because of the savings in tendon costs. This post-compression approach is a novel method of pavement construction. The only prior literature that documents this idea is a patent issued in 2002, U.S. patent number 6,409,423. Patent 6,409,423 is an extensive body of various configuration options concerning post-compressing techniques. In figure 44 is illustrated an option using a flexible rubber bladder to provide the compression forces (the bladder is labeled 60a).

The tilt-up method can be applied to pavement in either the longitudinal or transverse directions. Although they are very similar processes they differ in certain aspects.

The transverse tilt-up prestressing is for the transverse joints. For 12 foot slabs there would have to be at least two lanes for this to work as it takes a minimum of two adjacent slabs tilted up against each other (see figure 45). Tendons which are preset with anchored ends to the precise length for the desired preload are attached to the exterior slab faces. There are clearance grooves in the bottom of the slabs for the tendons. These grooves can be filled with grout after the slabs are flattened. Also the grooves can be filled with performed concrete wedges, placed between the ground and tendons. These wedges can be adhered to the slab grooves with epoxy, or with grout during the tendon grouting process.

Also the tendons can be highly eccentric toward the bottom of the slabs in order to reduce the intrusion of the grooves into the slab. Additionally this would generally increase the loading capacity, or downward resistive moment, of the pavement. However in order to prevent the slabs from popping up at the center joint it may be necessary to

fasten the tendons into the bottom of the slabs. This could be done after the slabs are pressed into their flat position, with anchor bolts or anchor rivets inserted from the top; before grouting.

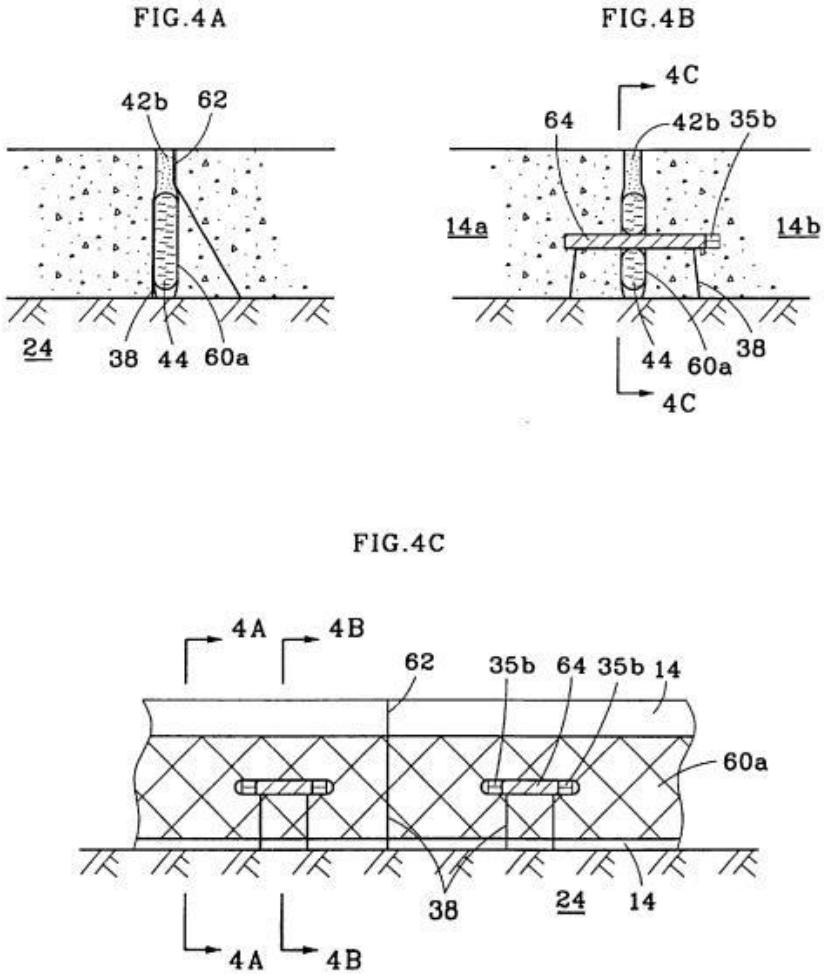

Figure 44. "Prestressed Pavement System", a Post-Compressed or Tendonless Prestressing Method[37]

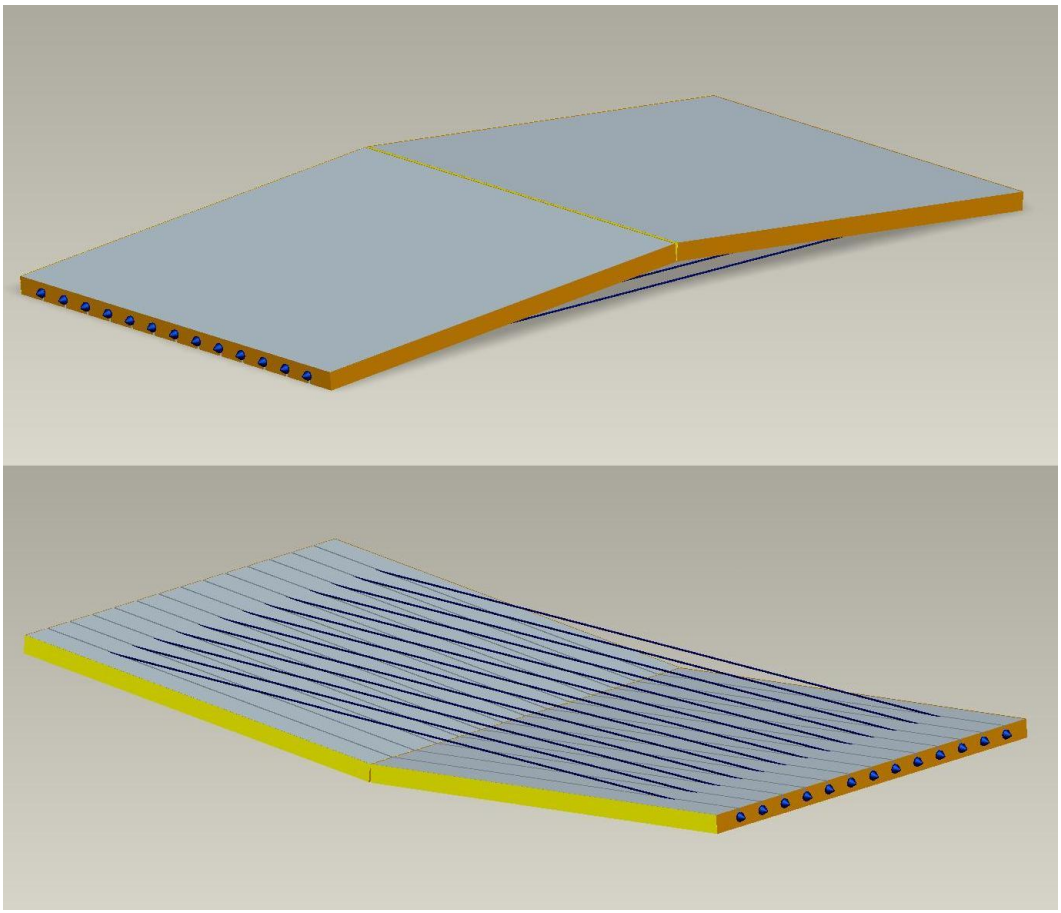

Figure 45. Transverse Tilt-up Wedging at Initial Positions, Top and Bottom Views, Using Tendons

The longitudinal tilt-up wedging prestresses the longitudinal joints. In the longitudinal direction tendons may be completely eliminated. This can be done with the use of retention dam structures. These dam structures would be placed at the opposite ends of a length of roadway in order to fully constrain the pavement slabs to a fixed constrained length. The precast slabs would be placed between two retention dams until there is only enough space to fit a number of final slabs pairs into the remaining space, but in the tilted up positions. Ideally the tilt-up slabs pairs would be evenly distributed within the length of pavement between the dams. It might be necessary to place at least one adjustment shim within the length of slabs so that the prestressing load is correct after the tilt-up slabs are lowered into the final flat positions (see figures 46 and 47). In order to determine the correct prestressing load, along with the tilt-up angle, all the various design parameters need to be determined. Below is illustrated the process for an initial optimization of the slab parameters.

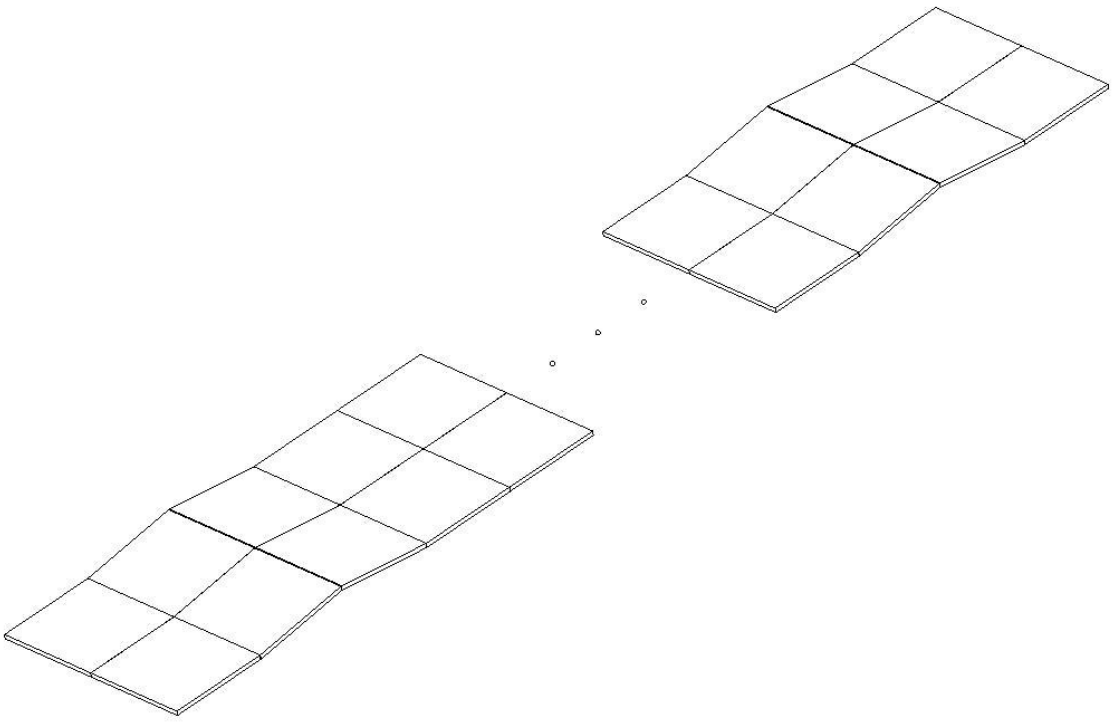

Figure 46. Longitudinal Tilt-up Wedging for Two Lane Pavement

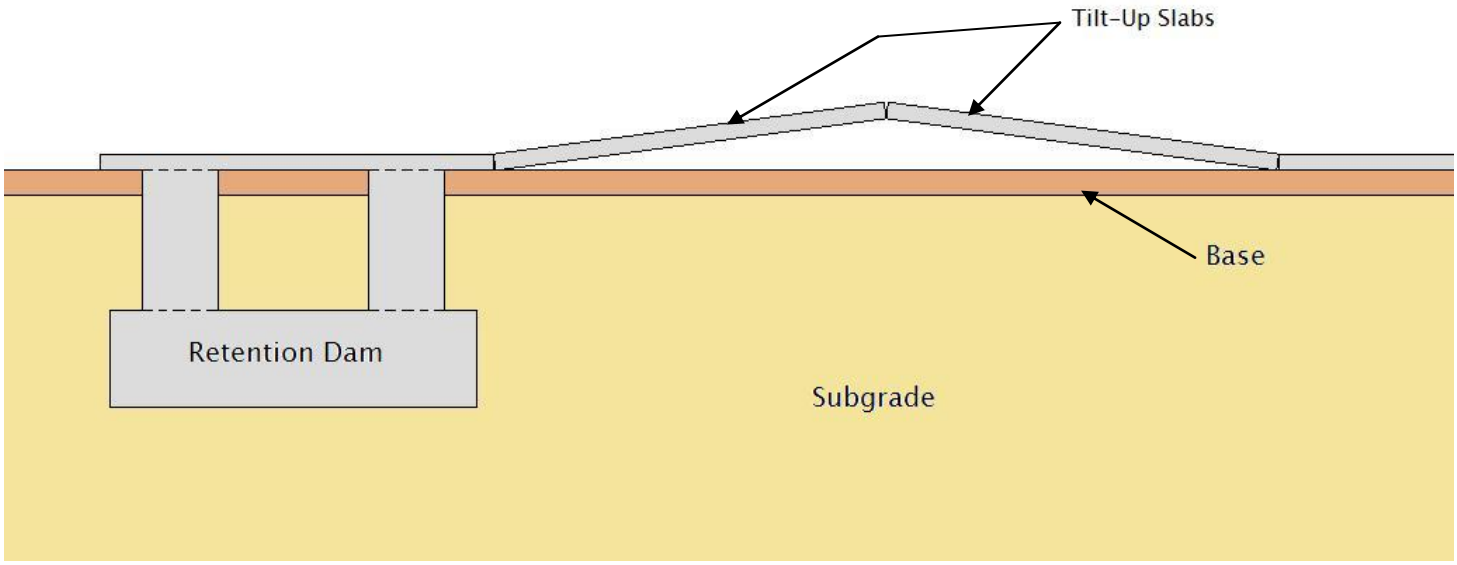

Figure 47. Longitudinal Tilt-up Wedging Pavement Cross Section

Of paramount concern is the integrity of the joints throughout the pavement life. That is, the joints should not experience excessive stresses or too low stress levels (compressive), especially zero stress, which would allow the joints to disengage. For the highest stress level 1,600 psi was chosen as this is the generally accepted high service limit for elastomeric bearings[6]. For the lowest stress level 6 psi was chosen. The two operating variables which affect the joint stresses the most are thermal expansion/contraction and rubber creep, or compression set. Other factors are important, such as tendon creep and concrete shrinkage but they are neglected for this initial optimization study because they are a lesser affect.

6.2.2 Optimization

Assumptions and simplifications for the pavement-state governing equations:

1) That the system can be simplified to a one dimensional problem.
2) That the concrete and steel layers are combined, sharing the properties of concrete; the steel layer effects being negligible.
3) Slab width and length = 12ft (square). This is from standard lane width. And for length, the handling considerations with a safety factor of 1.4; considering simply supported slabs.
4) Slab thickness set at 6 inches, based upon minimal slab thicknesses in current use (generally); this is only used in the FEA verification.
5) The sheet metal layer set at 1.2mm thick; used in the FEA verification.
6) Rubber is linearly elastic using an approximation found from the previous FEA results: the elastic modulus: E_R = 100 MPa based on rubber durometer of 70 Shore A and the approximate shape factor.
7) The elastomer set is modeled at 35% - reduction in elastic strain, reflected in equation 6.10, 6.13 and 6.16 (below).

The design variables which can be optimized in order to insure the proper joint stresses are: slab length, slab thickness, rubber thickness, rubber durometer, and initial prestress. These variables both affect and are affected by the various stress states that the pavement experiences during the life of the pavement. Five states are illustrated in figure 48 below. The first is state (zero) is the initial state with no applied stresses. State 1 is immediately after the prestressing load is applied at nominal temperature and with no rubber compression set. Nominal temperature is assumed as the mean temperature between high and low extremes (not used in the calculations). State 2 is at nominal temperature but after maximum compression set. State 3 is at minimal service

temperature after compression set. State 4 is at maximum service temperature after compression set.

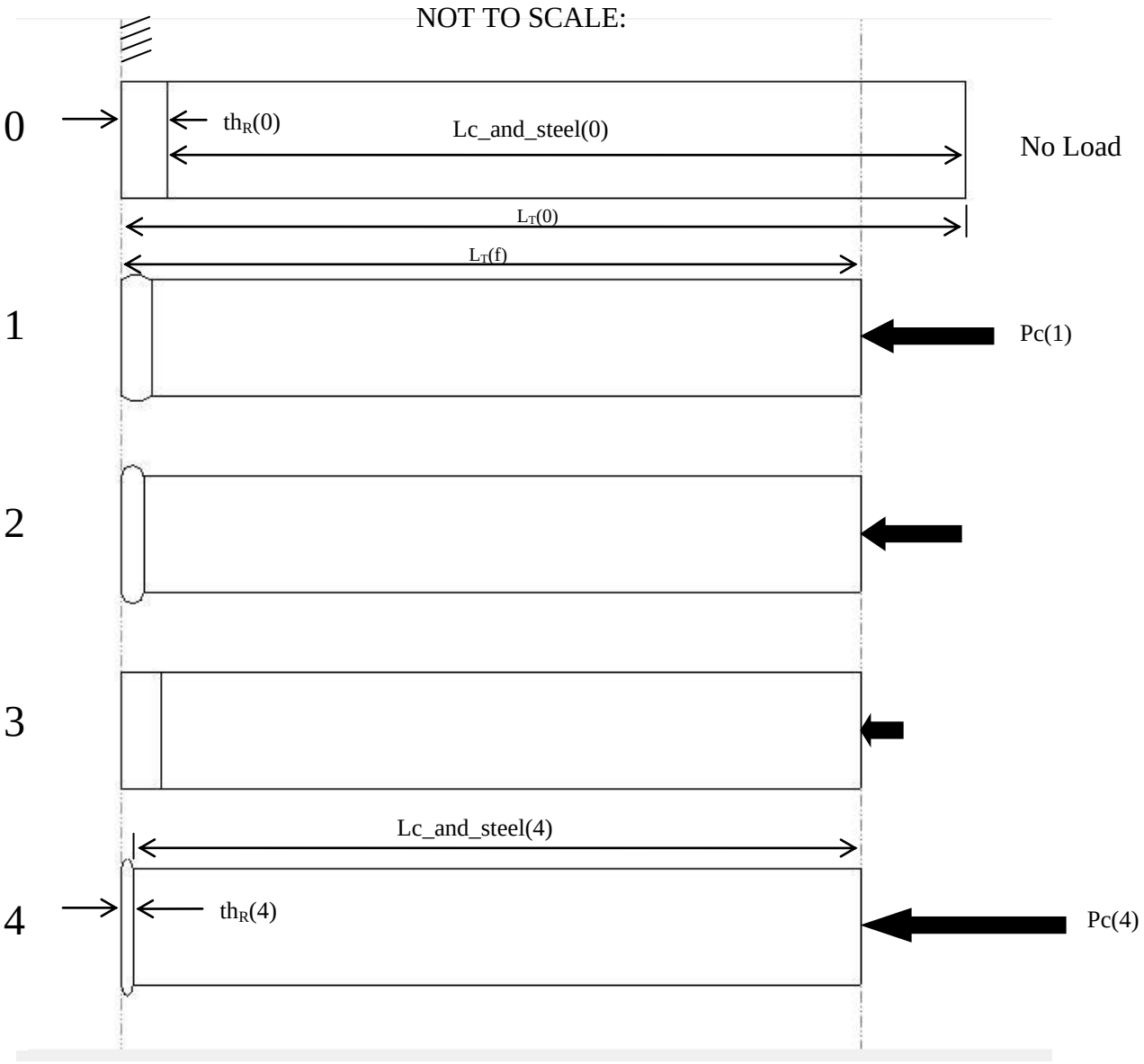

Figure 48. Pavement Stress States

In order to determine the optimal design the governing equations were developed with the extreme variable conditions and ranges. Then an algorithm was applied which finds approximate solutions to systems of nonlinear equations. The algorithm used was MathCad's Minerr function (see Appendix B), which utilized the nonlinear Quasi-Newton method[15].

The following equations are the governing equation for the 5 states. The variables $th_R(0)$ through $th_R(4)$ denote the rubber thickness in each state. The variables $L_{c\ and\ steel}(1)$ through $L_{c\ and\ steel}(4)$ are the slab lengths excluding the rubber. $L_T(0)$ and $L_T(f)$ are the overall slab lengths including the rubber. $P_C(1)$ thru $P_C(4)$ are the internal compressive loading (pressure). The constants used in the equations are:

$L_{c\ and\ steel}(0) = 12$ ft — Unloaded slab length

$E_R = 100$ MPa — Elastic Modulus of rubber

$\alpha_C = 12 \times 10^{-6}\ °C^{-1}$ — Concrete coefficient of thermal expansion

$\Delta T = 25°C$ — Temperature swing, above and below nominal

$E_C = 2.99922 \times 10^{10}$Pa — Elastic Modulus of concrete

Boundary Inequalities:

$$th_R(0) < 10mm, \tag{6.1}$$

$$P_C(4) < 1600psi, \tag{6.2}$$

$$P_C(3) > 6psi, \tag{6.3}$$

Initial Step (0):

$$th_R\,(0) + L_{c\_and\_steel}(0) = L_T(0), \tag{6.4}$$

Step (1):

$$th_R\,(1) + L_{c\_and\_steel}(1) = L_T(f), \tag{6.5}$$

$$P_C(1) = \frac{L_{c\_and\_steel}(0) - L_{c\_and\_steel}(1)}{L_{c\_and\_steel}(0)} E_C, \tag{6.6}$$

$$P_C(1) = \frac{th_R\,(0) - th_R\,(1)}{th_R\,(0)} E_R, \tag{6.7}$$

Step (2):

$$th_R\,(2) + L_{c\_and\_steel}(2) = L_T(f), \tag{6.8}$$

$$P_C(2) = \frac{L_{c\_and\_steel}(0) - L_{c\_and\_steel}(2)}{L_{c\_and\_steel}(0)} E_C, \tag{6.9}$$

$$P_C(2) = 0.65 \times \frac{th_R\,(0) - th_R\,(2)}{th_R\,(0)} E_R, \tag{6.10}$$

Step (3):

$$th_R\,(3) + L_{c\_and\_steel}(3) = L_T(f), \tag{6.11}$$

$$P_C(3) = P_C(2) - \alpha_C \Delta T E_C, \tag{6.12}$$

$$P_C(3) = 0.65 \frac{th_R(0) - th_R(3)}{th_R(0)} E_R, \tag{6.13}$$

Step (4):

$$th_R(4) + L_{c\_and\_steel}(4) = L_T(f), \tag{6.14}$$

$$P_C(4) = P_C(2) + \alpha_C \Delta T E_C, \tag{6.15}$$

$$P_C(4) = 0.65 \frac{th_R(0) - th_R(4)}{th_R(0)} E_R, \tag{6.16}$$

The optimal solution of the equations:

$$th_R(0) = 3.25mm$$

$$th_R(1) = 3.02mm$$

$$th_R(2) = 2.93mm$$

$$th_R(3) = 3.18mm$$

$$th_R(4) = 2.63mm$$

$$L_{c\_and\_steel}(1) = 3.65672m$$

$$L_{c\_and\_steel}(2) = 3.65681m$$

$$L_{c\_and\_steel}(3) = 3.65655m$$

$$L_{c\_and\_steel}(4) = 3.65712m$$

$$P_C(1) = 7.2346 \times 10^6 Pa$$

$$P_C(2) = 6.4981 \times 10^6 Pa$$

$$P_C(3) = 1.2575 \times 10^6 Pa$$

$$P_C(4) = 1.2486 \times 10^7 Pa$$

$$L_T(0) = 3660.85mm$$

$$L_T(f) = 3659.73mm$$

This optimization method had good results in general. Two key design variables from the above results are the rubber thickness and the initial preload, $th_R\,(0)$ and $P_C(1)$. Both are within the boundary inequalities prescribed ranges: 3.25mm and 1049psi respectively; from inequalities 6.1, 6.2, and 6.3. However $P_C(4)$ exceeded the boundary requirement, inequality 6.2, by 13%; its value being 1811psi. This is not a strong concern because this would only occur at extreme temperature conditions. A pavement structure based upon these results was constructed for FEA studies.

6.2.3 Results

Figure 49 illustrates the net moment on the left tilt-up slab: the moment from the horizontal preload force, generated from the slab interferences minus the moment generated from the slab's weight. The prestressing load is for the initial longitudinal (State 1). The chart was developed considering the slabs as rigid objects. It shows that a flattening downward force needs to be applied to the slabs for the domain between 5.2 to 2.3 degrees. This is because there is a net positive moment that rotates the slabs upward, or open, in this domain of slab rotation. The maximum flattening force would occur at 3.95 degrees and would have to counteract a 4.942336×10^5Nm moment (the maximum moment).

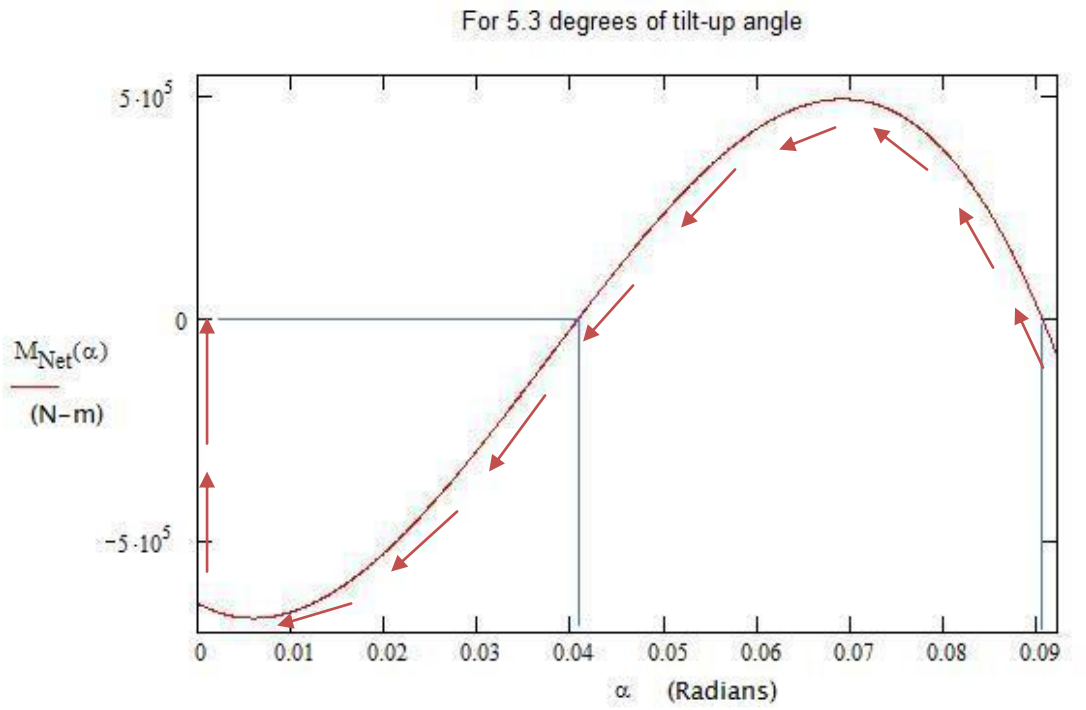

Figure 49. Initial Tilt-Up Angle (5.3°), Slab Resistive Moment Vs Rotation Angle for Longitudinal Prestressing

For the tilt-up FEA study the slabs were tilted up at 5.3 degree angles. The prestress loading at the final flat position was set at the $P_C(1)$ level. The flattening force was not included in the FEA study, although at the 5.3 or 0.0 degree positions the flattening force is zero.

The following FEA results are of the EB joint pavement proposal under maximum tire loading. And also results of the tilt-up prestressing process. Both are done as 2D plane strain models.

FEA model parameters (aside from the optimized design parameters above):

1) The roadbed was modeled as linearly elastic with a 9 inch base layer above a 3 meter subgrade. The base having an elastic modulus of 410MPa and the subgrade at 83MPa[16].
2) The tire load was modeled as a 229mm long contact, at 120psi[17].

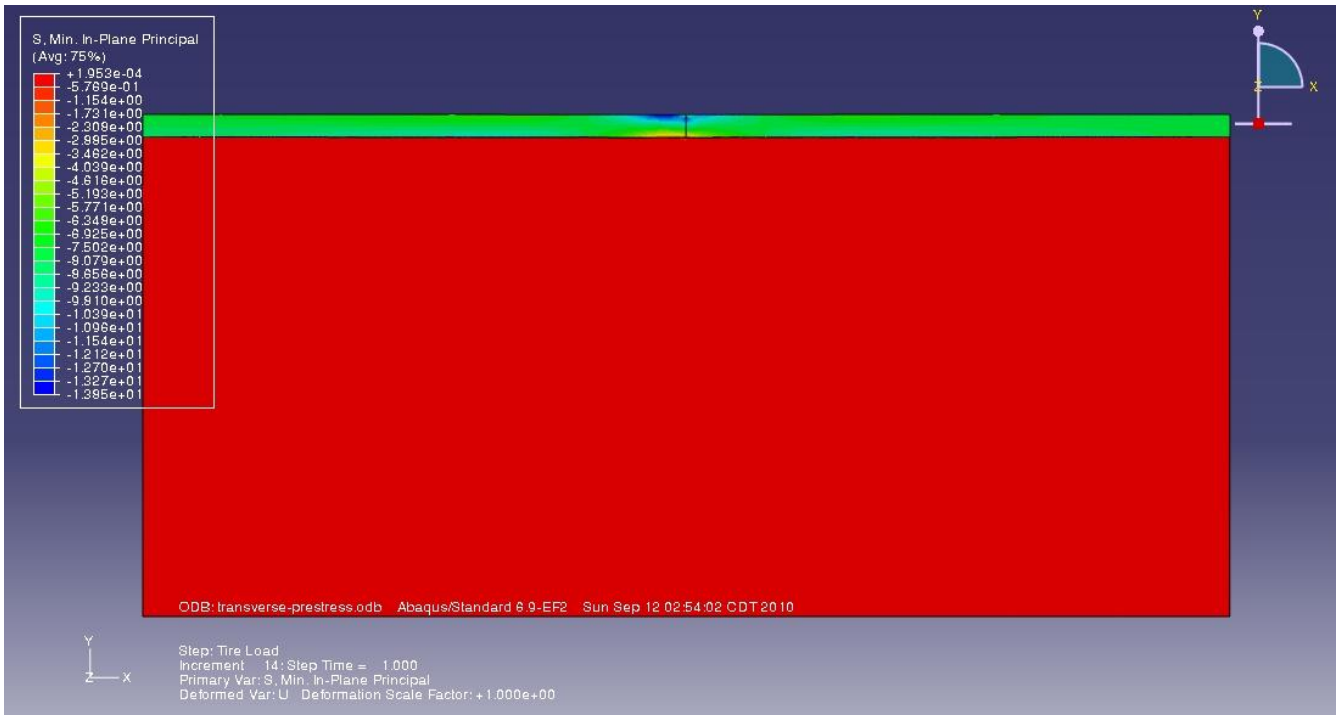

Figure 50. Longitudinal Section of Pavement at Initial Preload (1049psi), and Maximum Tire Load.

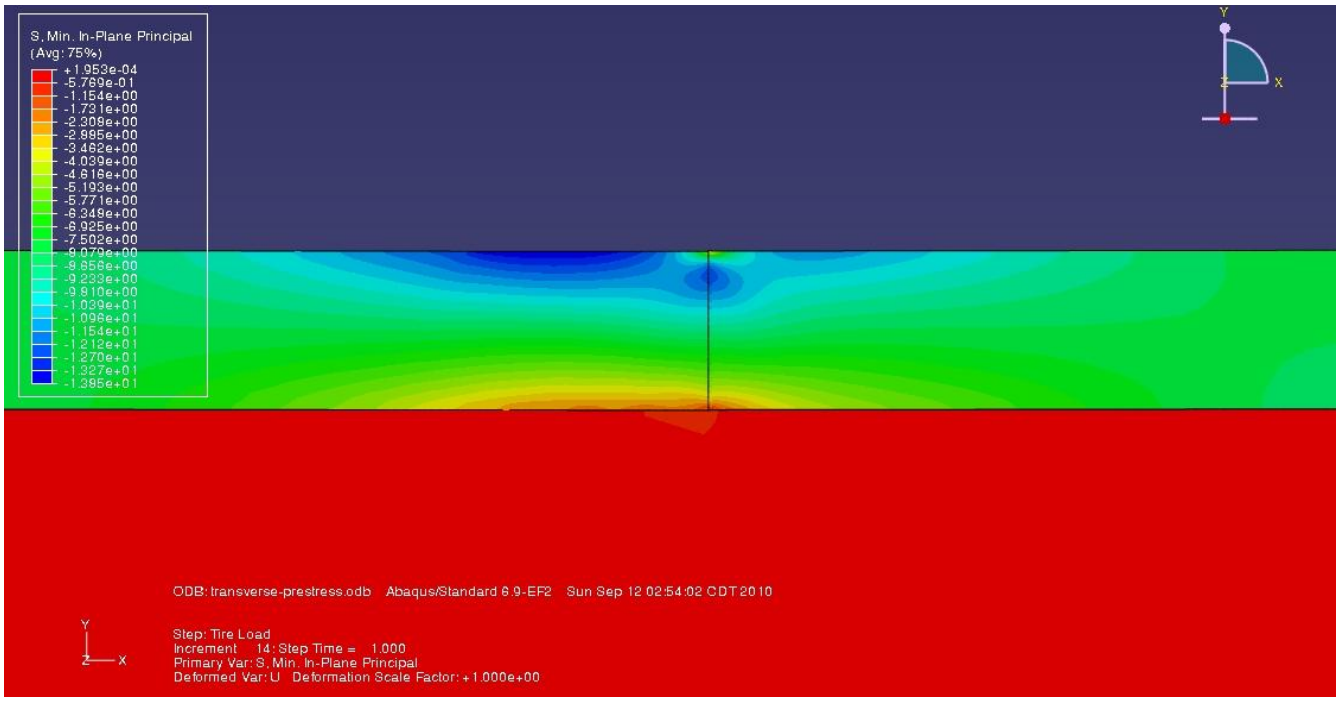

Figure 51. Longitudinal Section of Pavement at Initial Preload (1049psi), and Maximum Tire Load, Near Joint.

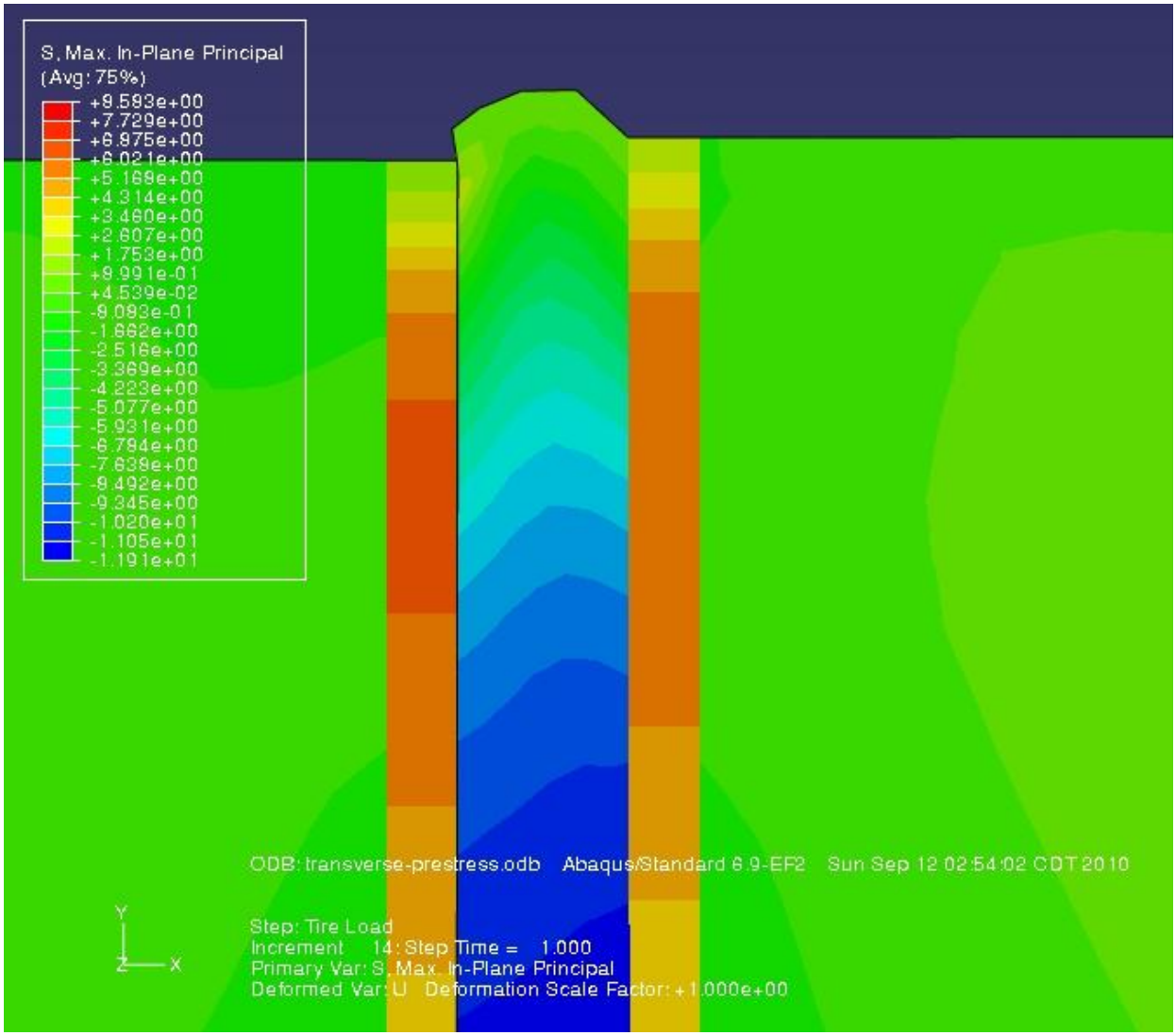

Figure 52. Longitudinal Section at Initial Preload (1049psi), and Maximum Tire Load. Step at Rubber: 0.383mm.

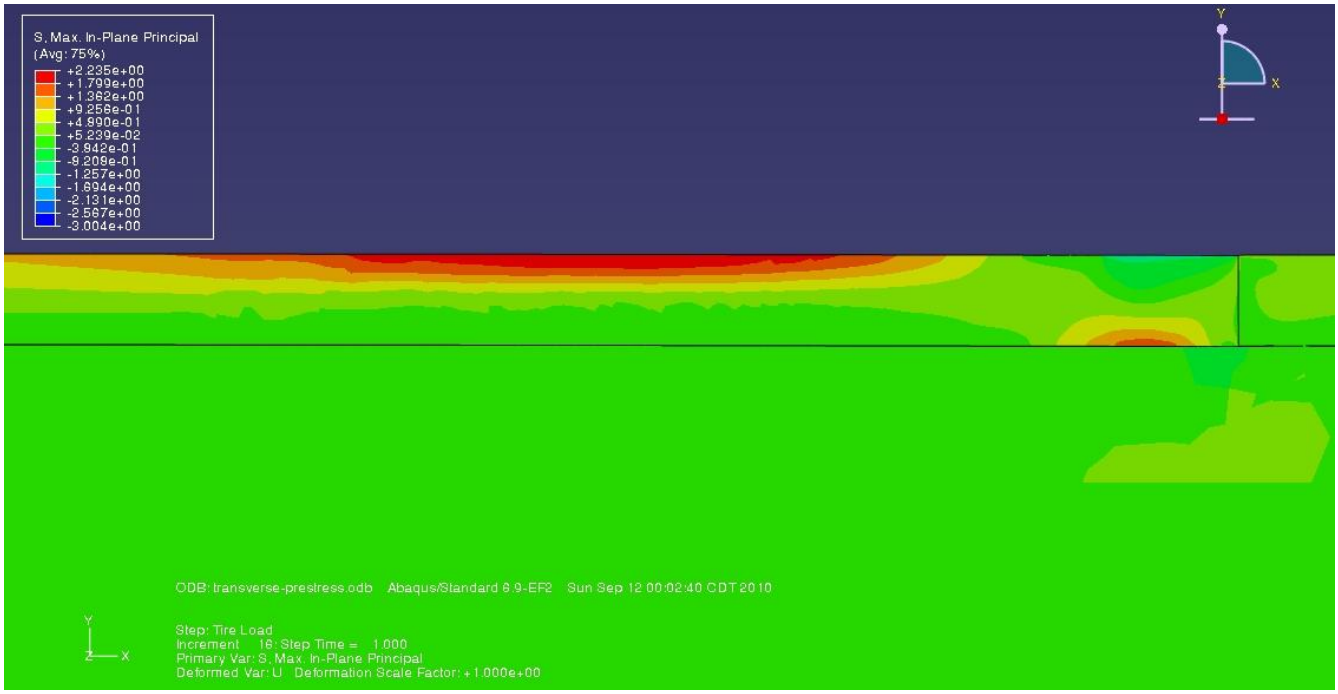

Figure 53. Longitudinal Section at Minimum Preload (6psi), and Maximum Tire Load (MaxP).

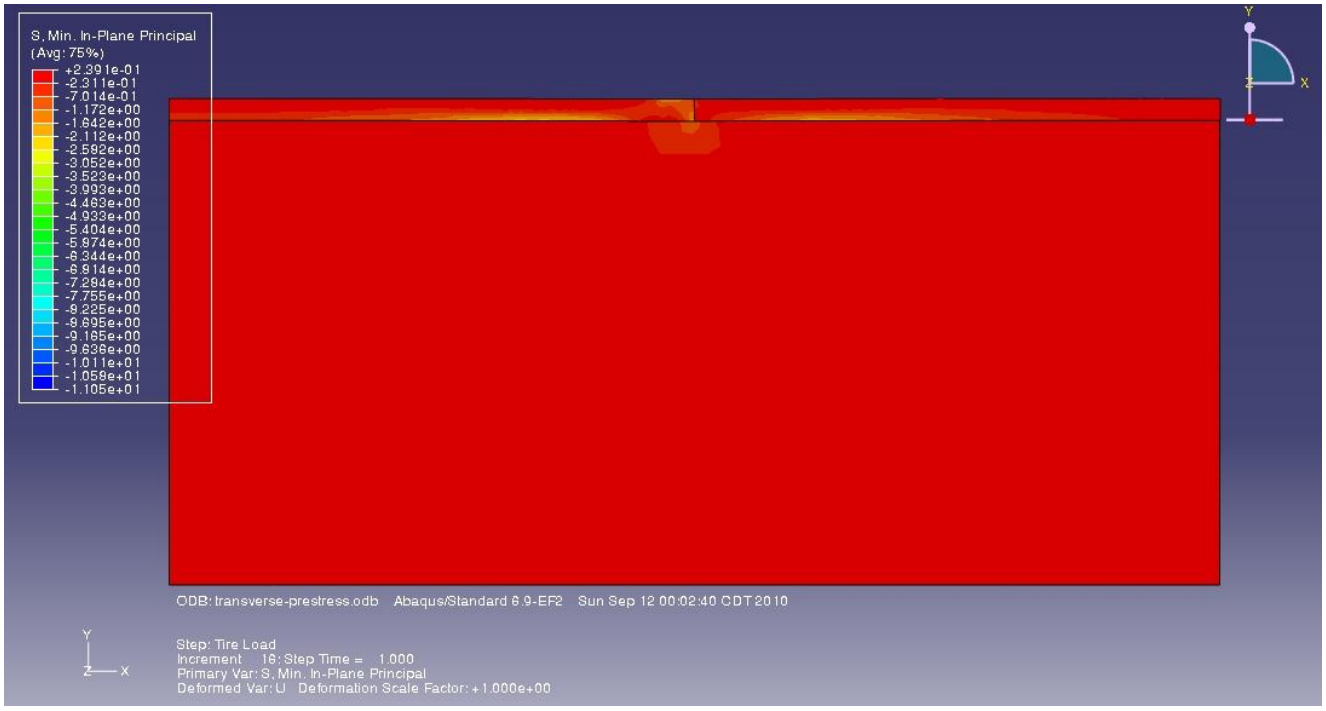

Figure 54. Longitudinal Section at Minimum Preload (6psi), and Maximum Tire Load (MinP).

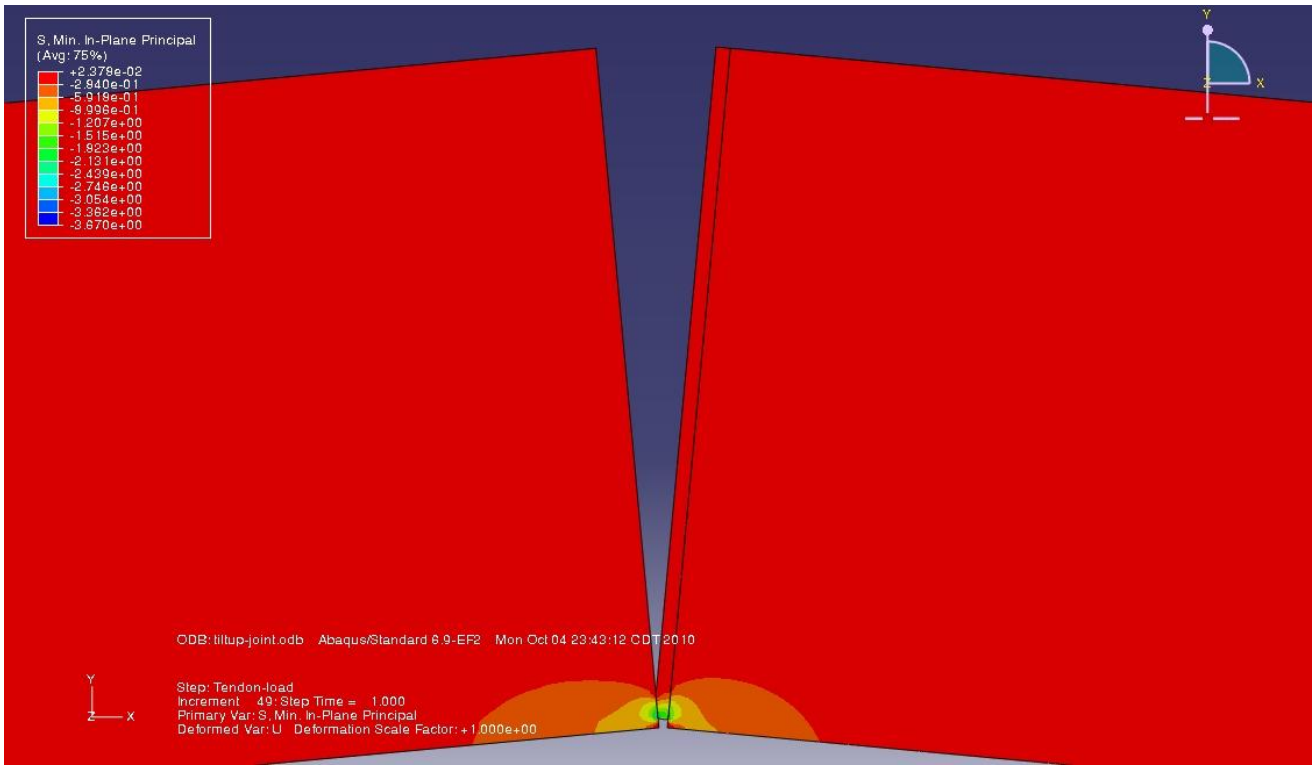

Figure 55. Tilt-Up Prestressing at 5.3 degrees (at Top Start Point), 6psi Preload.

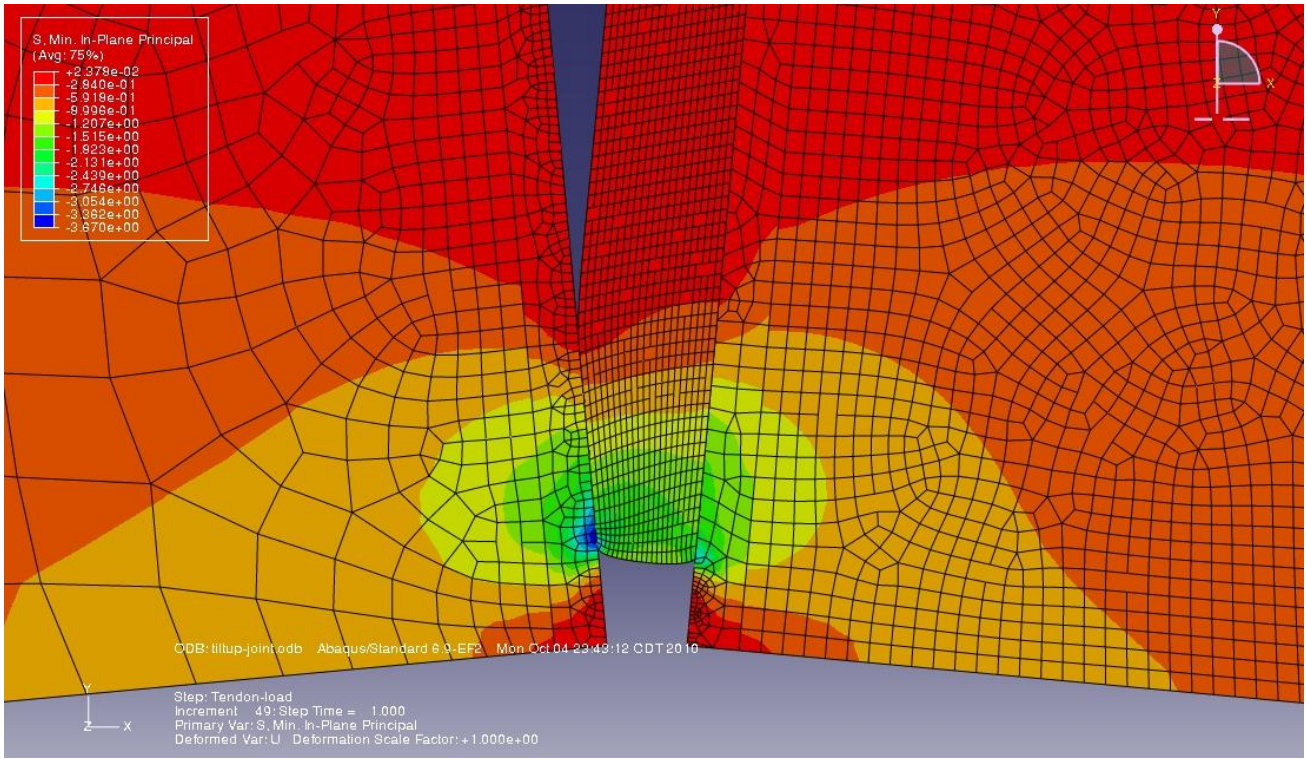

Figure 56. Tilt-Up Prestressing at 5.3 degrees (at Top Start Point), 6psi Preload. Close Up at Initial Contact Point.

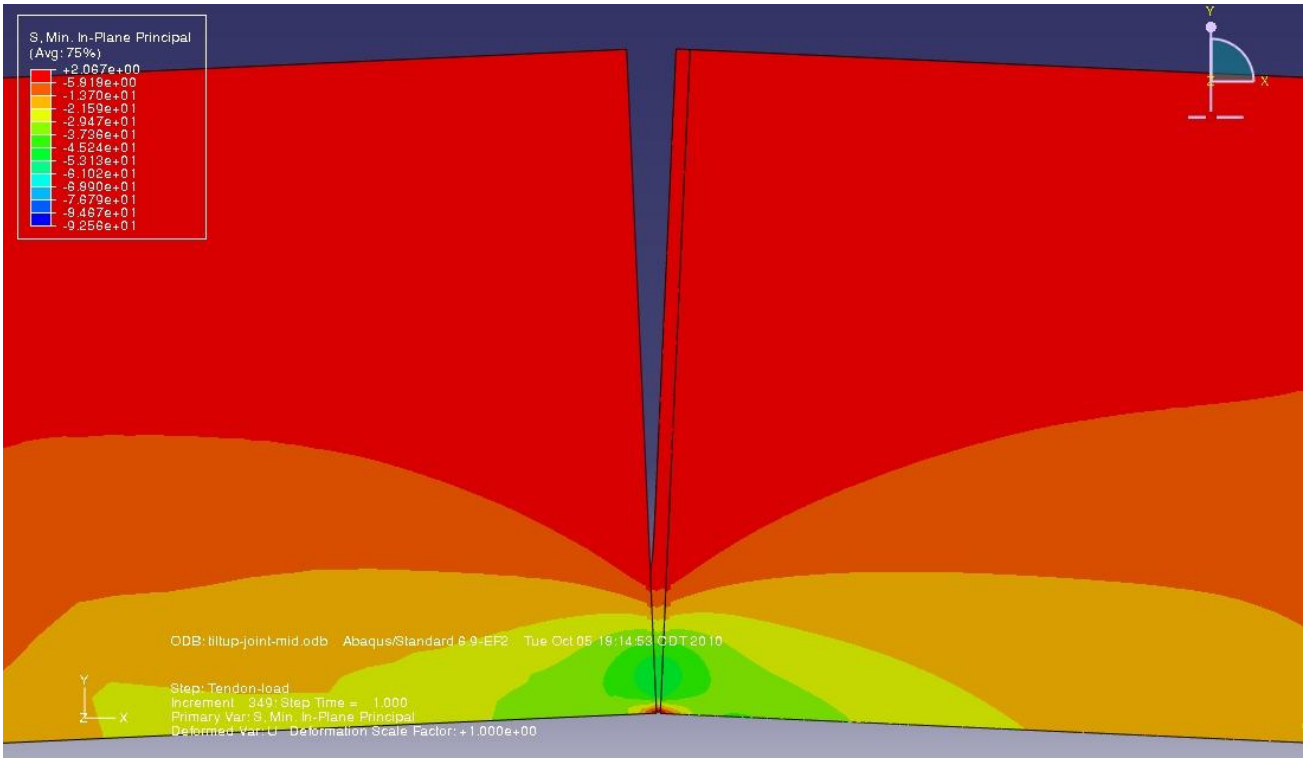

Figure 57. Tilt-Up Prestressing at 2.65 degrees (at Mid Rotation Point), at 868psi Prestressing Pressure.

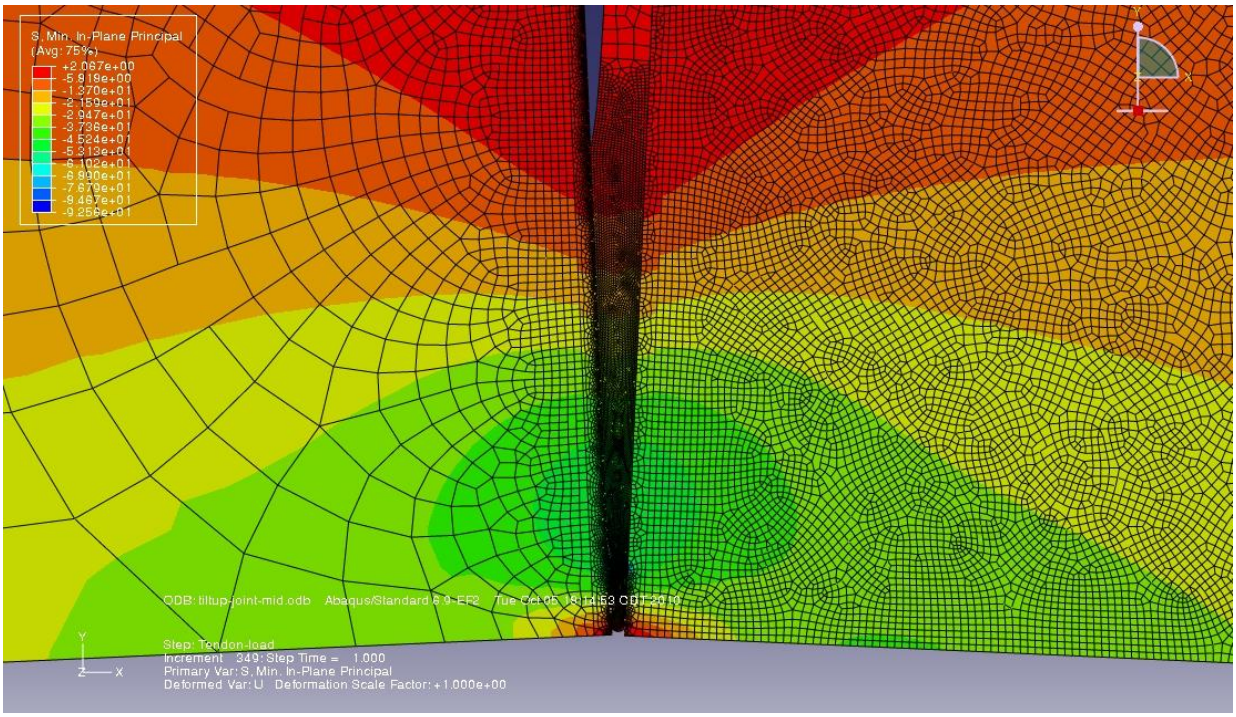

Figure 58. Tilt-Up Prestressing at 2.65 degrees (at Mid Rotation Point), 868psi Prestressing, Close Up.

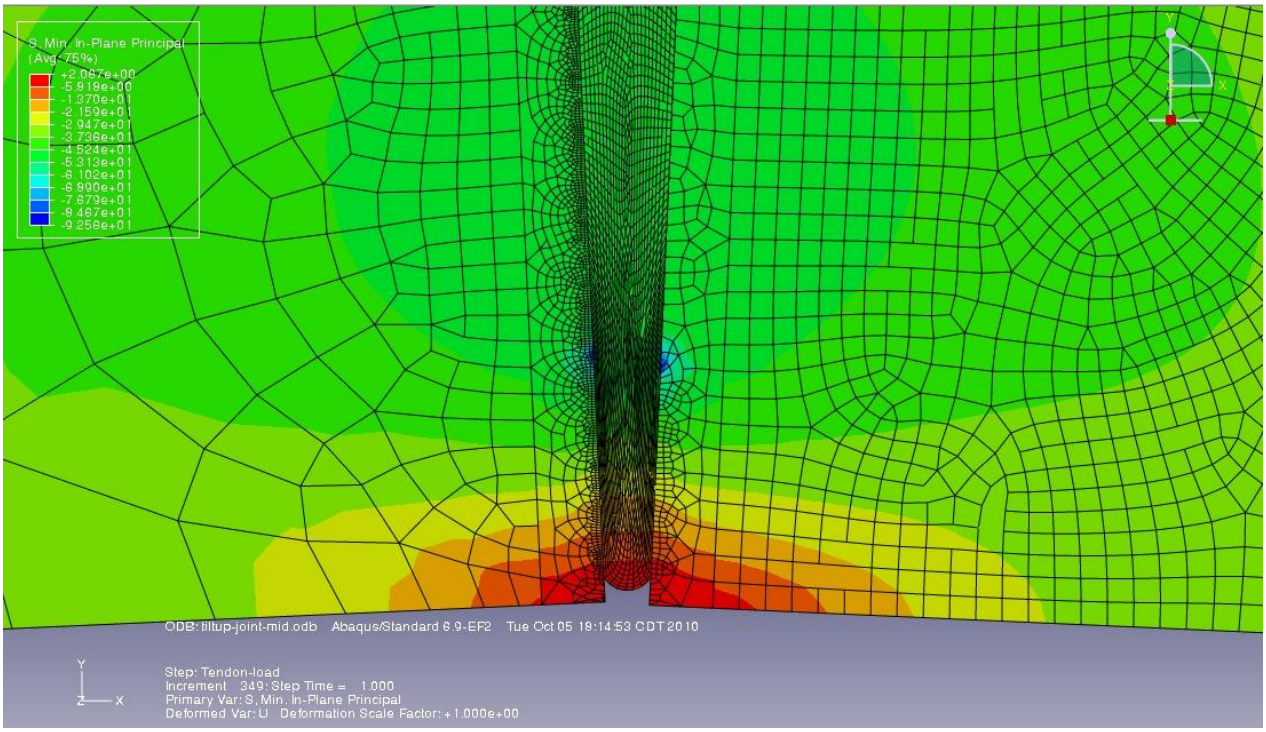

Figure 59. Tilt-Up Prestressing at 2.65 degrees (at Mid Rotation Point), 868psi Prestressing, Close Up at Rubber Clearance Groove.

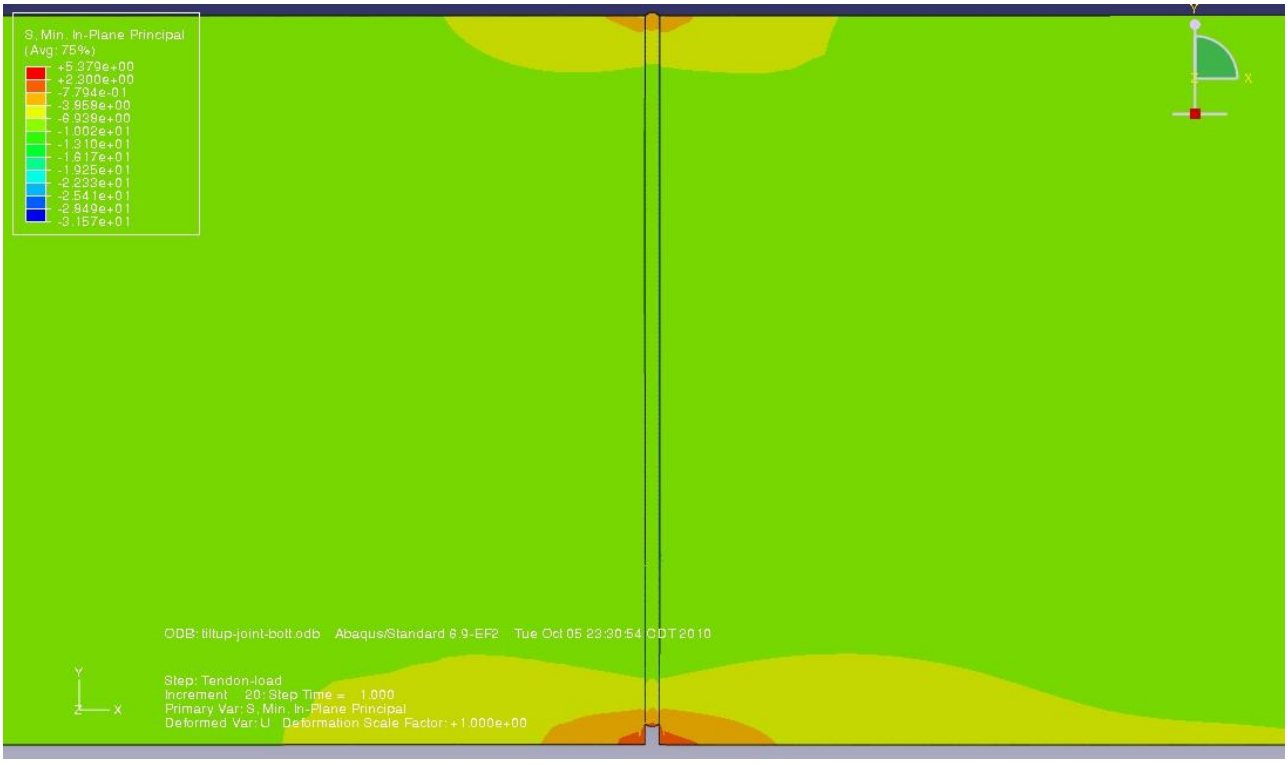

Figure 60. Tilt-Up Prestressing at 0 degrees (at Bottom of Rotation), 1049psi Prestressing Pressure.

For the pavement under tire load results, the stress levels for the concrete are well under yield. This is the case for either maximum principle or minimum principle stresses. The results can be considered conservative in that the 2D model does not include the transverse concrete support that a tire would see. This would lower the stresses and deflections at the tire contact. The 2D model reflects the loading of a 120psi roller along the full transverse width of the slab, an extreme worst case.

From the prior literature on doweled joints, the maximum deflection shown in figure 52 is within a range seen in thicker, non-prestressed, pavement such as doweled CRCP[18]. The deflection load transfer efficiency is 0.87. While the stress load transfer efficiency is at 0.78 for the initial preloaded state (figure 51). For this initial study a comparison between the proposed joint and doweled, or free joints, was not done. This type of comparison will require extensive 3D FEA models and analysis. The joint stiffness and behavior under load for the EB joint in comparison to a jointed or free joint, is likely to be quite a bit different because of the prestressing as well as the joint structure. The level of preload, or prestressing, will affect the load transfer properties of the joint. The steel end plates can abruptly change the stress fields as seen in the above figures. And the rubber provides a continuous connection from slab to slab which is quite different than the discrete dowel connections seen in current joint technology.

As per the optimized design from section 6.2.2, the joint under all conditions (considered) should remain coupled together. If the joint remains coupled then the slabs will consistently stay in registration to each other after repeated deflections. And the rubber layer will provide a seal for the joint preventing the damaging effects of fluid-silt pumping.

If the stress variability is too high such as when pavement temperatures become too low the slabs could become uncoupled. This could entail pavement rehabilitation later, however a series of incidental key joint devices are presented in section 6.2.4 which could help assure adjacent slabs recouple, or reregister, after partially uncoupling under

such conditions. Unfortunately joint and pavement damage may occur under such temporary conditions if heavy loading is allowed during partial uncoupling. FEA analyses for these conditions would constitute a good future study.

From the tilt-up results it can be seen in figure 57 compressive stresses are beyond yield in the concrete, near the initial contact point, at mid rotation as the slabs rotate down to their flat positions. The maximum stress levels occurred near the mid rotation point. The stress level shown is for the longitudinal tilt-up prestress level. The transverse tilt-up prestress level would be 52% less than that in the longitudinal direction if a 500psi post tensioning load was chosen. So for the transverse joints, the over stressing during the tilt-up preloading process is much less acute. Moreover there are a number of alternative solutions for reducing the overstress levels in the joints during the flattening process.

A robust solution to the overstress conditions is to use MS joints for those joints that would see tilt-up stresses above yield. Or alternatively a combination joint: MS on the initial contact side and an EB joint on the opposite side. Because the stress levels of the proposed pavement structure are so much lower than that seen in the sign post designs the MS joint pivot journal may be much smaller in size relative to the overall joint size. This in turn would present a design which needs much less end cap steel relative to the sign post design, which means lower relative costs.

Another possible solution could be increasing the steel section thickness near the highest stress zones such that stresses can be absorbed, and spread out more. This approach is likely to be most effective when the concrete end profile is angled or curved away from the contact point; at the corner of the concrete, as was done in the MS joint designs.

Another approach could be to mimic the inverted V end profiles as is done in raft units (see fig. 43). In order to minimize the stresses through the tilt-up interaction the joint profiles could be optimized with curvilinear faces as opposed to the typical angular shown. However depending upon the end profile both the load transfer capability and the

M_R that the joint can generate, will be significantly degraded in comparison to the standard EB joint.

6.2.4 Further Configuration Options

Various options may be implemented concerning tilt-up prestressing. Not every slab within a pavement section needs to be tilted up to prestress a series of adjacent slabs. If every slab in a series is tilted up for prestressing, in pairs, then the required angle of tilt would be 5.3 degrees. If only one pair of slabs is tilted up for a series of ten slabs then the optimal initial tilt-up angle would be 7.56 degrees. Therefore eight out of ten slabs could remain flat for this prestressing configuration. The tilt-up slabs require a flattening force in order for them to reach their final flat positions. When they are initially tilted against each other there is a tiny rotation as they settle to a stable position/state. Then a force must be imposed to further rotate them down. As can be seen in figure 49 the resistive moment increases to a maximum value (from right to left on the graph). For the 5.3 degree initial tilt-up the maximum required force would be 2,500lbf/ft, along the upper slab edges, at 4 degrees rotation. For the 7.56 degrees of tilt-up the maximum downward loading (flattening load) would be a little over 2,800lbf/ft, at the 5.3 degrees rotation point. Then as the slabs continue to rotate downward the resistive moment, and flattening force, continue to decrease until they become zero, at the break-over point. Then the slabs will pop down into their final flat positions against the roadbed. The break-over point for the 5.3 degree tilt-up configuration is 2.3 degrees. Because of the fact that the total optimal prestressing force (initial) between the slabs is approximately 1,000,000 lbf the relatively even distribution of prestressing pressure, dependent upon the slabs sliding, is not a large concern. This is because the total weight for eight slabs is 86,000 lbf and given the friction factor between the roadbed and the slabs is 0.55[32] then the frictional force resisting sliding would be only 4.7% of the prestressing load, for these eight slabs.

For a longitudinal prestressing process covering an extended length of pavement it would be optimal to flatten the tilted slabs simultaneously. If the slabs were flattened in a serial manner then there would be an accumulation of displacement as the slabs would slide further and further from the starting retention dam. At the end of this serial process the final slabs may be tilted at an extreme angle and then the distribution of prestressing pressure could be quite uneven. However to flatten all the tilted slabs in parallel would take a number of flattening devices working in concert. These flattening devices could be specially built trucks which could straddle all the lanes of slabs, the slabs being previously prestressed transversely via the transverse tilt-up process. These flattening trucks would need to hold up large weights above the tilted slabs and precisely lower the weight onto the middle of the slabs. For a two lane road the weight that would have to be lowered onto the tilted slab edges would be in excess of 120,000 lbf. This is a massive weight in relation to the fact that generally 80,000 lbm is the maximum gross weight allowable per vehicle over public roads. So the flattening truck/devices would need to be assembled at the construction site. An interesting optimization problem is determining the optimal number of flattening trucks to use on a particular construction project. It would be a problem which required the consideration of construction logistics, various construction costs and the operating costs of the flattening trucks. The ratio of one tilted pair to 98 flat slabs (almost a quarter mile) would require 16.64 degrees of tilt-up. And the maximum variance in prestressing load through the 100 slab pavement section, due to friction, would be about 591,000 lbf maximum, a little over 1/2 of the total longitudinal prestressing load. For 30 longitudinal slab length less than 18% of the initial prestressing force would be lost due to friction.

For the transverse prestressing as in the longitudinal case many more than two slabs could be adjacent to each other, such as with a large multilane freeway. As in the above example ten lanes could be prestressed with a single pair of tilted up slabs, which may use tendons instead of retention dams. And the slabs that remain flat could simply

have the tendons running thru channels, as is the typical post tensioning configuration. While the tilted pair would require the bottom tendon grooves. However for the case where there is only one lane, such as on freeway ramps or rural low traffic roads, then a conventional, non-tilted, post tensioning configuration could be used.

For the example in figure 45, 500psi prestressing was chosen. In large part this was to have a comparable value to the Neil Cable transverse prestressing. The highest level used in the Neil Cable method was approximately 340psi. Choosing ½in, 7-strand, grade 270 tendons with 80% of yield prestressing, yielded 13 evenly spaced tendons for an initial proposal. However extensive simulation studies could point to more or less tendons as well as various configurations depending upon specific applications.

Another method for transverse prestressing can use retention dam structures. These dams could be combined with a curb, shoulder structure, roadside barriers, retention wall for a submerged roadway, or part of the bridge structure for an elevated roadway. However with this construction scheme the transverse prestressing would have to be done after the longitudinal prestressing as the transverse prestressing, or post compressing, would tend to lock the slabs in place as well as preventing the tilt-up and flattening process. The transverse retention dams (used in prestressing the sides of the pavement) could save costs in tendons, grouting and construction time but the slab locking could cause problems. Stress redistributions arising from initial stresses, thermal changes, concrete shrinkage and material creep would be retarded by side clamping. With the use of tendon prestressing, the pavement slabs need only overcome the frictional forces between the base and slab bottoms, this force would be less than 6,000lbf per slab. But the frictional side forces from the transverse dams could be in excess of 1,700,000lbf per slab, using a 500psi prestressing pressure. This side locking could be mitigated with self-lubricating, or solid lubricant, high load bearing layers between the retention dams and the slab sides[19]. Or the locking could be mitigated with thicker layers of rubber at the sides, allowing for higher shear strains. The use of transverse tendon prestressing allows

a more or less self adjusting pavement in terms of redistributing uneven stress distributions. So depending upon various costs: tendon, construction, concrete, and site requirements, it may make more sense to use transverse dams, or tendons. In order to post-compress the slabs transversely a force would have to be generated between one of the transverse dams and the side of the pavement. This can be done with hydraulic rams at evenly spaced intervals. Then while under hydraulic pressure a shim could be wedged between the dam and the pavement side face. The shim would have clearance slots for the hydraulic rams. Once the shims are in place the rams could be removed. This process could walk down the length of longitudinally prestressed roadway. Near the longitudinal dams there would be a conflict between the orthogonal prestressing directions. So near the longitudinal dams there could be a length of transverse tendons with no transverse dams at that local.

Another sub-option related to transverse retention dams is to eliminate both longitudinal retention dams, and tilt-up prestressing. This proposal is to prestress the pavement slabs longitudinally with temporary cables and then to clamp the prestressed slabs in place with the transverse retention dams as described above, thereby prestressing both directions simultaneously. This could be done in extended lengths of pavement.

Yet another sub-option would be to use longitudinal dams but without tilt-up prestressing. If the longitudinal dams are not spaced too far apart the longitudinal post compressing could be done hydraulically, pushing off against the dams and slabs. Then the prestressing held with shim wedges between the dams and the end slab faces as described above.

Another construction method option is multi-directional prestressing. This can be accomplished by using a diamond pattern of slabs: square slabs at a 45 degree angle to the direction of prestress loading, coupled with triangular elements, and retention dams on all sides but only needing compressive loading along one facet of the periphery. This would be appropriate for small pavement sections especially symmetric sections or pads.

However many different polygon pavement sections could utilize this technique, with various polygon slab combinations internal to the pavement section. Still only needing prestress loading applied to one facet. This technique could be especially applicable to odd pavement sections such as intersections or traffic circles. Traffic circles could be shaped as hexagonal or octagonal sections. Shear movements between slabs could create large residual shear stresses especially within the rubber layers; this could lead to high levels of uneven stress distributions. Lubrication at the joint interfaces along with key joint features such as toothed rubber, or MS joints, could more easily allow shear movements. Additionally vibration devices could be run over the pavement section after post tensioning to help even all internal stresses. This multi-direction prestressing could also be accomplished with tendons as the restraining devices, solely or in combination with retention dams.

For both the transverse and longitudinal prestressing there are a number of additional considerations and requirements:

For both tilt-up and flat clamping (post compressing):

There are a multitude of details concerning the manufacturing processes and materials, construction techniques and costs that can only be completely catalogued and reviewed through experimental trials of the proposals presented here. But there are some issues that can be easily anticipated. That is the issue of tolerances on components and assemblies, also due to material changes over time.

- ➔ Various soil and ground formations … remedy: utilize various construction options; such as different dam structures, MS joints Vs EB joints
- ➔ Permanent formation movement … remedy: Add or remove shims
- ➔ Initial component tolerances … remedy: Cast in place or shims
- ➔ Shrinkage … remedy: Thicker rubber or add shims at a later time
- ➔ Creep … remedy: same as above
- ➔ Fracture damage … remedy: Replace slab

➔ Normal Wear … remedy: Replace slab or resurface

➔ Corrosion … remedy: Grouting, epoxy coating, or replacement

The use of shims is a robust cost effective method of adjustment. The shims can be made of concrete shim blocks or metal shims can be used for fine adjustment. Also glass filled plastic can work well for shim material.

Another use of the rubber layer is the monitoring of the internal stress levels of the pavement. This can be done by examining the degree of rubber bulging at the exposed edges. This bulge can act as a compression gauge. Figure 61 illustrates the relationship between the compression of the rubber layer and the side bulge[6].

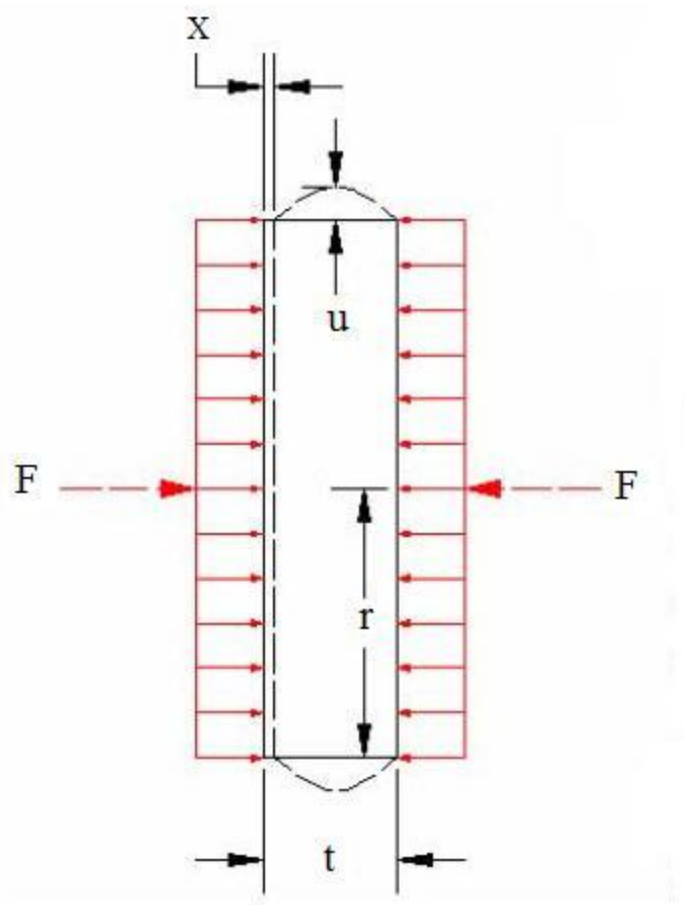

Figure 61. Rubber Layer Bulge Under Compression

$$u = \frac{3rx}{4t} \tag{6.17}$$

Where u is the peak distance that the rubber pad/layer bulges, x is the compressive deflection, r is the radius of the layer and t is the original thickness. F is the force per length perpendicular to the view of figure 61. And if the rubber is assumed to be linearly elastic:

$$\frac{F}{2r} = \frac{x}{t} E_R \tag{6.18}$$

This is essentially the same as equation 6.7. Compression set can be included in the same way as equation 6.10. In order to evaluate the degree of compression set there could be removable inspection blocks on the non-bonded sides of the EB joints. These blocks could be bolted into place such that their joint surface is coplanar to the adjacent joint surface. Once an inspection block is removed a special gauge can be pressed against the rubber layer to check the degree of compression set that has occurred. These inspection blocks can be placed in portions of the pavement that see little or no traffic loading so that the rubber bulges are not worn down. Also remotely monitored sensors could be attached to the joints such that they could sense the degree of rubber bulging. These electronic sensing devices could transmit their measurements to remote receiving devices, which in turn could notify engineering staff with alarms for major deviations in stress levels.

For tilt-up Prestressing:

Skid plates are likely needed to prevent the lower corners of the tilted slabs from digging into the roadbed base material. Not only will this cause damage to the surface continuity of the base but could cause material entrapment within the joint. Small High Density Polyethylene (HDPE) strips or rails can be embedded into the base under the slab corner edges. A small rounded edge on the concrete would help the bearing interactions here as well. Only a 0.8in long plastic strip would be needed for 7.56 degree tilted plates.

Tension adjustments may be required for the tendons at the construction site. Adjustments shims on transverse tendons could be applied. These shims could take the form of c-clip washers of various thicknesses. They could be inserted into the tendon anchor ends which could increase the tendon deflection along with the tendon loading. Threaded anchors with adjustment nuts could also serve the same function although likely at a higher cost than shims. The adjustment process would entail lifting the

flattened slabs after checking the internal compressive stress of the pavement; after the initial flattening. This could be done by measuring the rubber layer bulge. And then adding shims if required.

Tendon grouting for transverse prestressing has its benefits, although it is not necessarily a requirement. These benefits were discussed in section 3.2. There are additional beneficial aspects as well for the tilt-up prestressing. That is, depending upon the depth of the tendon into the slab, the tendon clearance grooves can significantly weaken the slab especially in the longitudinal direction. For the precast slabs the process of grouting would be to simply grout around the tendons after the slabs are flattened. The grout could be pumped through channels at the top of the slab and the grout could bond well with the groove walls. However it would help with the flatness of the bottoms, and hence the sliding of the slabs, if tape was adhered to the bottom of the grooves to seal them for grouting. This could be done by having the tape under the tendons at the beginning of the tilt-up operation and upon flattening the tape would automatically be adhered to the bottom. Another option instead of tape is to use wedge inserts, which were discussed above in section 6.2.1. In general tilt-up slabs do not require tendon ducts because ducts produce a tunnel for routing tendons through the concrete after casting, prior to post tensioning. For the majority of the prestressing process the tendons are outside/below the slabs. Also ducts help to reduce friction between the concrete elements and the tendons. Again the tendons for the most part do not contact the slabs during the majority of the prestressing process. However there is a case where a duct or at least a partial duct will aid in the tilt-up prestressing process. That is, when the slabs are cast in place prior to tilting up. There needs to be a device to create a groove in the concrete for the tendons to escape from the bottom of the slab, when the middles of the slabs are lifted for anchoring the tendon ends to the side faces. This device can be a duct or partial casting barrier/form covering each tendon during the casting process.

Ganging of precast slabs together at the casting plant could aid in the efficiency of manufacturing and transportation. Two or three slabs tied together with transverse tendons could be transported together to the road construction site. For a two lane road, two slabs ganged together would save in the transportation steps and time and would make for more robust elements for hoisting into place. At the precasting plant either pretensioning or post tensioning could be used for prestressing the ganged slabs.

Retention Dams:

The retention dams' function is to hold back the compressive forces on the pavement slabs. Only a portion of the structures large enough to interface with the slab edges are required above the ground. Most current ground anchoring structures/devices are required to resist forces and moments in many directions however for the proposed pavement structures it is only in one lateral direction, parallel to the ground that is required. "End restraints" are common pavement structures used in continuous concrete pavements that act much as the longitudinal dams however they are not specifically designed to provide any specific prestressing load. In general they are simple longitudinal ground anchors.

There is a wide variety of ground anchoring devices which are suited to various types of soil or ground formation. In general, because of the variability of ground structure and content, there will be a large amount of variability in the strength of any particular type of in situ anchor. Therefore in situ testing of the retention dams under load needs to be part of any construction project in order to detect yield or excessive creep[20].

Longitudinal Dams:

The dam structure shown in figure 47 is a formed concrete footing joined to a slab, but many other forms of footings or anchors could be candidates for the retention

dam structures. Grouted stakes or piers are good candidates because numbers of them can be inserted through holes in the slab into the ground to the required depth. Subsequently grout under high pressure could be pumped down through them into the ground adjacent to the piers or stakes.

When prestressing loads are imposed upon a dam the degree of deflection would need to be monitored. And if too much movement is detected an additional dam structure can be added as incorporated into an adjacent - subsequent slab.

Transverse Dams:

The same alternatives and issues face the transverse retention structures as do the longitudinal. However the longitudinal retention dams are anchored to ground that is generally well known and consistent being that it is the roadbed strata. The transverse dams however would be anchored to the side boundaries of the roadbed and the compressive loading from the slabs would flow outward from the roadbed. Often the ground adjacent to a road drops off at an abrupt slope. For many circumstances this is due to the native topography which the roadbed is embedded into or to facilitate good drainage away from the road. These drop offs would significantly reduce the potential strength of a submerged footing. So for retrofitting an existing road, transverse dams may not be applicable. For initial pavement projects the requirements for the transverse dams could be more easily incorporated into the design. However in-situ testing is still required to adjust the degree of anchoring if necessary.

One method for mitigating weak spots along the transverse dam structures could be to remove slabs next to the failing dam structure section. Then run a number of tension elements, steel bars or tendons across the roadbed, tying the opposite transverse retention dams together. The tension elements could be fine adjusted with threaded ends and nuts-anchors. The tension bars would be buried just below the top surface of the base layer. Then the slabs would be replaced and the dams retested.

Depending upon the ground formation (and number of lanes) the cost or complexity could make transverse dams impractical. The more lanes the better the business case is for using side clamping. If the cost of the transverse dam methods is higher than tendon post tensioning then the tendons would make the most sense.

Figure 63 is a cross section of one proposed transverse retention dam structure. For this work a trencher could be used to make the cut for burying the footing. The structure could be precast or cast in place. If precast it would be advisable to grout the footing in place thereby improving both the positional accuracy and the coupling to the ground. During the grouting, a frame acting as a grouting jig could span across the lanes of the roadway to hold the dams in precise position and distance across.

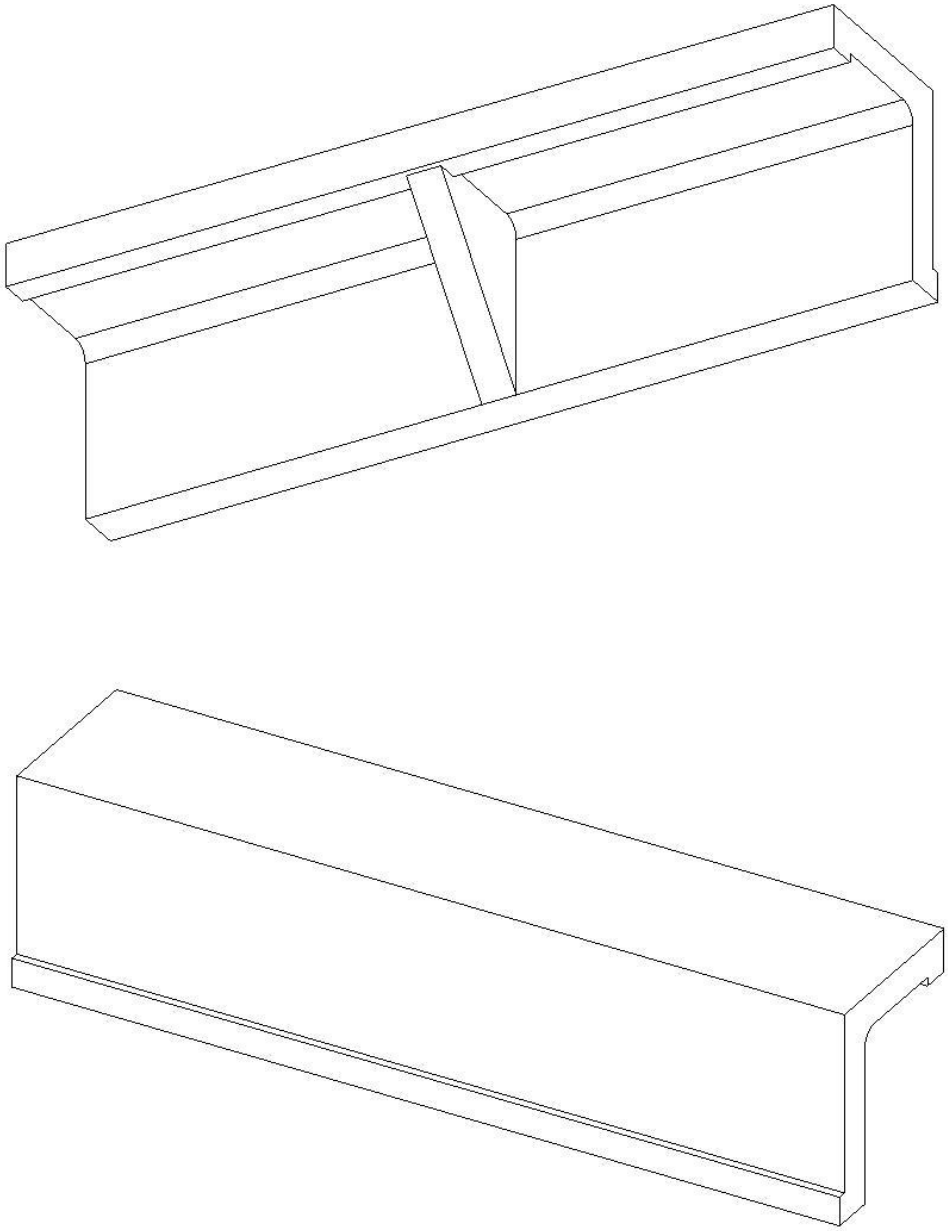

Figure 62. Transverse Retention Dam Section

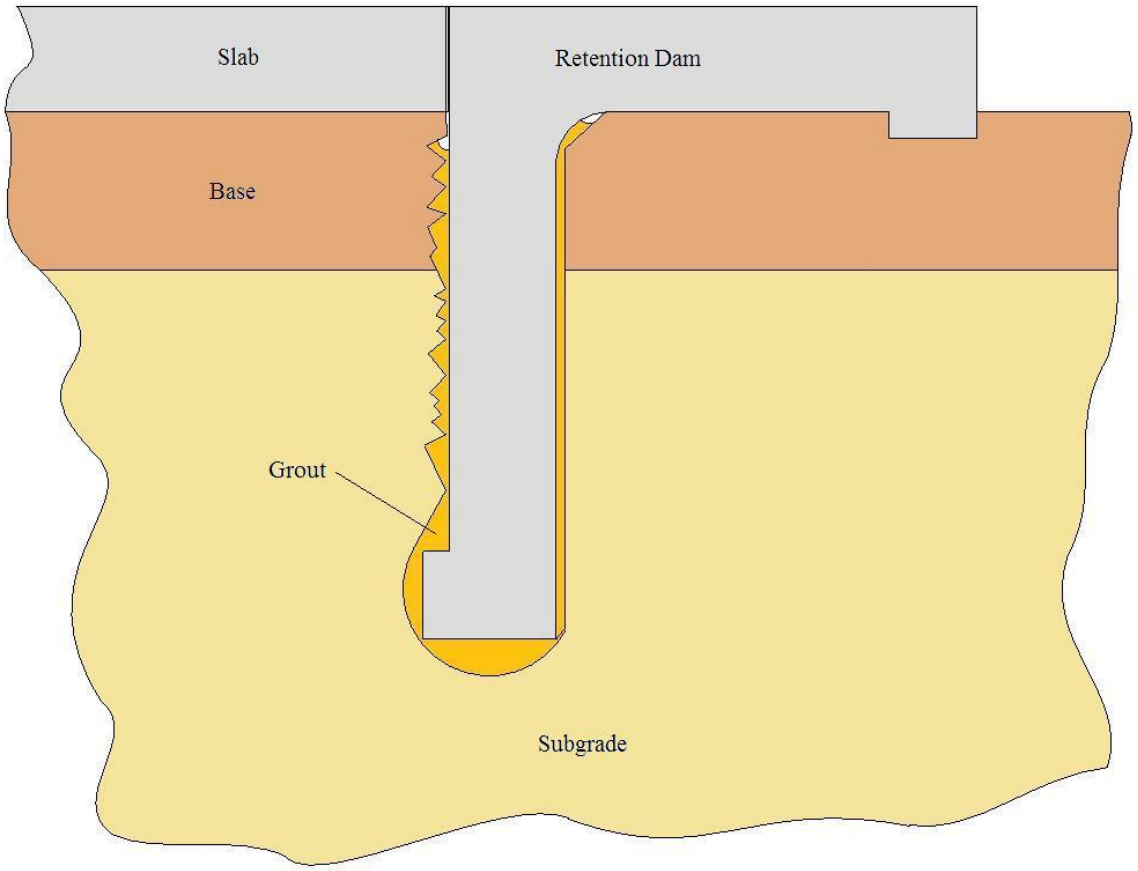

Figure 63. Transverse Retention Dam Cross Section

In the longitudinal direction the transverse dam structures could be composed of segmental elements, joined together via the joining systems proposed here (MS and EB joints). This could make the structures more robust and lessen the material requirements.

Cast In Place

Cast in place methods can be utilized in most of the above proposals. As previously mentioned it can facilitate with road transitions thru match-casting. Large: d^2y/dx^2, d^2z/dx^2 (Turning, hills, dips and banks) can be accommodated. During the prestressing interspersed adjustment shims may be required to keep match-cast slabs in their optimal positions through the post tensioning process, as the longitudinal deflections may become significant. Initial prestressing can cause maximum longitudinal deflections of 33.5mm for 30 slab long sections.

For cast in place slabs, the side clamping could be applicable as well as the tilt-up prestressing. This would represent a construction cost improvement over precast however slab quality would be more consistent with precasting. As mentioned above, for cast in place tilt-up prestressing there needs to be a means for creating the grooves for the tendons.

The time between casting and prestressing is the cure time for the concrete. There must be enough cure time to assure that the concrete has reached the required strength to withstand the tilt-up process, and that there is not excessive shrinkage after prestressing. Concrete shrinkage is a much greater concern than with precast and would need to be included in the design optimization equations.

For large pavement construction projects cast in place coupled with side clamping could potentially be cost competitive with CRCP or JRCP pavement methods. Especially when considering pavement life and repair. The various cost advantages for clamped cast in place pavement over conventional CRCP or JRCP are:

- ➔ Thinner concrete, concrete material savings
- ➔ Very little reinforcement steel, such as rebar
- ➔ No dowels
- ➔ No expansion joints

- ➔ Longer life
- ➔ Less, and easier, repair

The cost disadvantages are:

- ➔ Retention Dams, especially for side clamping
- ➔ Prestressing costs, the process for the clamping method
- ➔ Shims, material and time
- ➔ Special testing and monitoring, such as the rubber bulge sensors

What is more or less equivalent:

- ➔ Joint setup Vs rebar and dowel setup
- ➔ Roadbed
- ➔ Casting process
- ➔ No slab lifting and handling

One additional advantage is that casting could be easily interrupted for the proposed EB jointed pavement. For CRCP this can be a problem. Although a doweled joint can act as an EB joint in this capacity, allowing for breaks in the continuous casting process. If there are no joints in a continuously cast pavement then a stoppage in casting can cause a severe discontinuity in the slab integrity, that is, an unbonded interface between the two casts; as poured concrete will not readily bond to previously cured concrete.

Miscellaneous Construction Configuration Considerations

For the precast slabs and tilt-up cast in place slabs, lifting of the slabs is required. This generally entails cranes and rigging. For the precast slabs this would be for lifting off the truck to place into position on the roadbed. For tilt-up: lifting would be needed for

positioning the slabs in their tilted position. However the previously mentioned flattening trucks could also be the devices used for doing the initial slab tilting. Often lifting eyes are bolted onto the slabs for lifting, but another alternative lifting device is the vacuum hoist. Vacuum hoists are regularly used for slab handling in precast plants because they put far less stress on the slabs than a rigging system does, and are much quicker to engaged and disengage to the slabs. They could be incorporated into the flattening truck system. Potentially they could be used for lifting precast slabs or retention dams off of the transportation trucks.

The joint bearing plates between the concrete and rubber have so far been presented as sheet metal, namely steel. This need not be the case. Through the analysis of the sign post and pavement proposals it can be seen that the sheet steel bearing plates are always well below yield. This fact points to the possibility of using other materials than steel for the bearing plates. One strong candidate is the use of plastic. Plastic made from virgin resins is usually not less expensive than steel however the use of recycled plastic presents an inexpensive alternative. Plastic can have creep issues but the creep can be mitigated with fiber fill reinforcement, the most common fill material being glass. For unreinforced Polyethylene Terephthalate (PET) the typical compressive strength is 90.7MPa. As can be seen from figure 52 the bearing plate stresses are a small fraction of the PET yield stress. PET is a very commonly available used plastic material. Figure 64 illustrates a portion of one proposed plastic bearing plate configuration. The embossed pattern would help to register the plate to the rubber. The rubber layer will partially form into this pattern, through the rubber compression set, when the joint is under prestress loading. The plastic plates could be used for both sides of the joint: the side with the rubber layer bonded to it, and the opposing side.

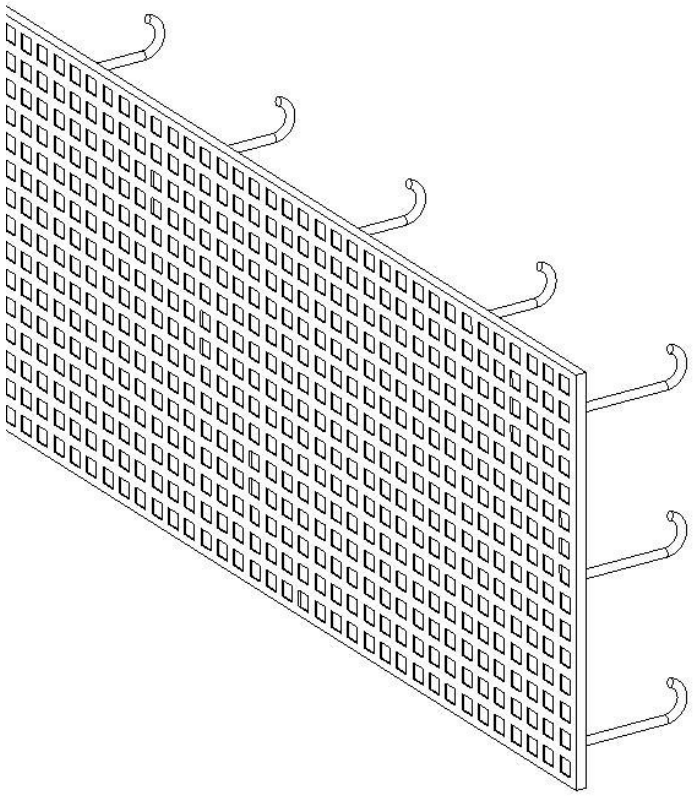

Figure 64. Plastic EB Joint Bearing Plate with Nail Anchors

Anchor wires, or nails, are shown in the figure 64 coming out the back of the bearing plate. These anchors wires would help securely attach the bearing plates to the ends faces of the concrete and can be applied to the sheet metal plates as well. For the plastic plates the wires can be inserted into the plastic during the molding process; commonly referred to as insert molding. The inserted portions could have nail head features buried in the plastic. A good molding process would be compression molding which is good for very large surface area parts. For sheet metal plates the anchor nails could be spot welded to the plates. Adhesives between the bearing plates and the concrete could also be used.

Adhesives compatible with both the concrete and bearing plates may be sufficient for securely bonding the concrete and plate, especially if the adhesive penetrates deeply into the concrete. A waffle pattern on the back of the plate would help with the bonding as well.

Key slots can be part of an EB joint. Much as doweled joints act to transfer shear loading from slab to slab in current systems, there can be various mechanical interlocking between the bearing plates and the rubber layers within an EB joint. To rely on purely frictional interlocking through the EB joint maybe risky under different conditions. As discuss previously extreme cold conditions could lead to zero pressure or disconnection between slabs at the rubber layers to bearing plates. Extreme overloading or road base degradation could likewise do the same. Also "walking out" can occur where over time the rubber to bearing plate becomes displaced parallel to the plane of contact. This condition is especially prevalent when lubricant is present[6]. To insure the joint surfaces remain properly registered to each other some means of key joints or slots can be provided. Because of the nature of the EB joint pavement system, misregistration forces should be minor and transitory. This is because there is a large degree of elastic deflection available from the rubber layers which will help maintain the prestressing pressure. Therefore unlike doweled pavement, where the full shear load transfer must often be handled by the dowels for the life of the pavement, an EB joint should rarely or only partially need to handle poorly prestressing conditions. So the keying features within EB joints need not be very large. Some options for keying are:

- ➔ Compression set rubber into a bearing plate pattern
- ➔ Toothed rubber into ribbed bearing plates
- ➔ The nail heads (part of the bearing plate anchors) could extend outwardly through corresponding holes in the rubber layer; or even further into the opposite bearing plate under the rubber layer

- ➔ Adhesive bonding between the rubber and opposing plate, near the central-neutral plane only. An adhesive bond near the outer surfaces would setup tensile stresses which could cause concrete failure
- ➔ For tendon prestressed slabs the tendons (especially grouted) can act as load transfer and registration elements

To reduce the rubber costs and open up options for the shape factor, the rubber layers can be broken up into strips. For the transverse direction the prestress pressure would be lower than the longitudinal direction and therefore would not optimally need as much rubber. The rubber could be broken into strips running along the top and bottom of the joints. This would increase the compression set but this would not be a big concern in the transverse direction if tendons are used, as the tendons store a large amount of strain energy in them and the tendons are closely matched to the concrete in thermal expansion and contraction.

The possibilities for slab element shape are broad. They could be square, hex, triangular, or mixed with circular shapes. And with various combinations of color and texture patterns, such as is done in brick or tile construction. This adds esthetic options which cannot be utilized in continuous forms of pavement.

Another configuration option that could help with reducing costs is to hollow out the concrete slabs. This can be done in multiple ways: by longitudinally coring the slabs with channels running the length of the slabs, or removing much of the bottom material in cavities such as in an egg carton structure. Looking at the maximum stress conditions depicted in figures 50 and 52 it can be seen that there is still a good margin between the stress levels and the concrete yield. So some amount of material can be removed without weakening the slabs too much. Care must be taken to maintain the proper factors of safety especially in regard to handling and tilt-up requirements. Shape optimization software could help with this investigation.

Concerning the costs of the proposed pavement structures verses current technology, there needs to be a lot more information collected especially in regards to pavement life. The additional costs of post tensioning (longitudinal and transverse) could easily be offset by reduced repair costs and longer life pavement.

6.3 Rapid Road Repair

In various Departments of Transportation across the country there are requirements for repairing pavements within overnight, or weekend hours so that high traffic roads are not shut down or narrowed during peak usage times. When considering the comprehensive costs due to traffic slow down or stoppage ("user cost") then there is ample motivation and financial incentive for much more expensive forms of pavement if they can achieve repairs within the required timeframes. User costs are indirect costs to the users of the roadway. These costs include those associated with traffic delays (e.g., longer commute time and increased fuel consumption). Precast pavement construction could minimize, or even eliminate, these traffic delays and, hence, user costs imposed by construction[14]. The following focuses on the repair of CRCP pavement and how it can be rapidly repaired with the proposed joint systems as applied to pavement.

A long existing method for CRCP repair is cast in place concrete. However in order to construct patches during the times allowed for limited lane closures, high early strength concretes are used. The durability of patches can be compromised to meet high early strength requirements. This is because high cement content in high early strength concrete patches increases the chance of cracking due to thermal effects and shrinkage[21].

A number of developments pertinent to rapid road repair include various studies conducted in the past two decades. One Japanese study had good results with smaller sized precast slabs on stabilized bases, with no prestressing. The slab sizes ranged from

1m x 2m, 2m x 2m, and 3m x 2m, all of the panels were approximately 150 mm thick; this points to smaller segments being more robust[14]. This would make sense in relation to the fact that the longer and more slender a beam element, the higher the tensile stresses within the beam for any given loading. A common small sized segmental pavement is concrete pavers which are not bonded together. However they do use joint sand between pavers to secure them. The smaller any pavement segments are the more the speed of repair would be a problem, especially time for assembly. However the use of smaller segmental units would help with adapting to deviations from straight patterned and planar pavement (significant d^2y/dx^2, d^2z/dx^2)[22].

Another group of studies have been conducted that focused on drop-in precast slabs with unique methods of joining the slabs to the existing pavement. These use no prestressing. These types of systems have been used in a number of studies and are attractive for their simplicity and speed of installation. Super Slab and FHWA CPTP are two systems that both use dowels into slots[21]. The Super Slab system has the slots opened downward (for the most part) with grout holes above each dowel. Two adjacent slab edges are slotted while the other two edges have dowels precast into them. For the joints that are bound to the existing pavement, dowels must be joined/inserted to the existing pavement into drilled holes[23]. The FHWA CPTP system has the dowel slots opened upward. Dowels are precast into the drop-in slabs while slots are cut into the existing pavement. The FHWA CPTP system is the easiest and fastest between the two systems because no drilling is required and the grouting process is easier. Unfortunately there is evidence that the asymmetrical grouting surrounding the dowels, due to the open slot structure, can be a source of stress concentrations that can lead to destruction of the grout at the open end of the slots. FEA studies could help confirm this hypothesis however the experimental results from studies at the Virginia Transportation Research Council show ample evidence of this type of failure (see figure 66)[21, 23].

Other systems studied for rapid road repairs include: The Uretek system that has been widely used, according to the developer, for intermittent repairs. This system requires the use of expansion joints if a series of adjoining panels is used. The Kwik Slab system has also been used on a limited basis in Hawaii. This system behaves similarly to long jointed reinforced concrete pavement sections[23]. All the above systems utilize precast slabs without prestressing.

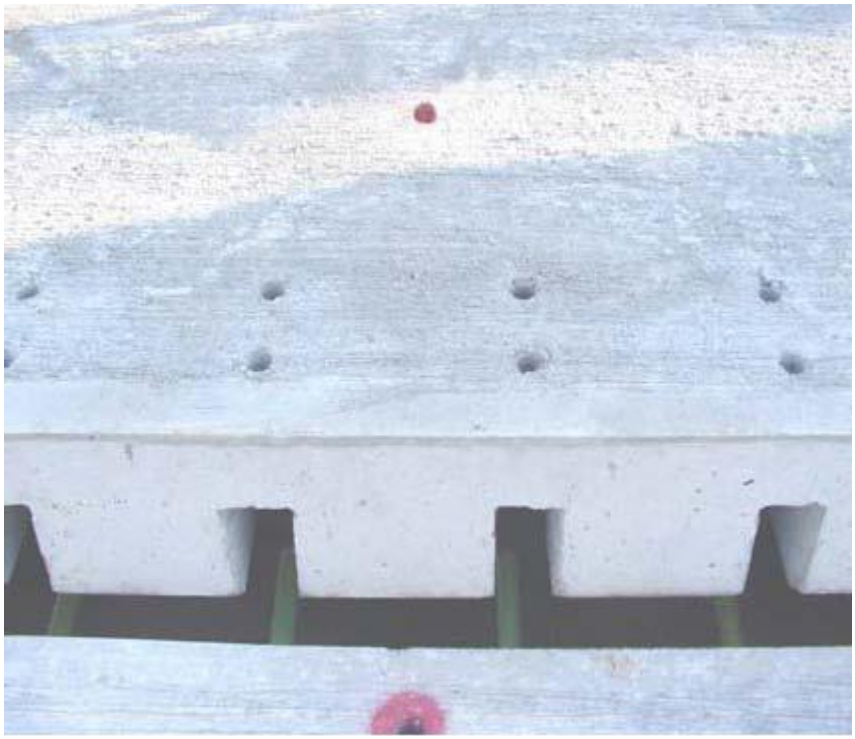

Figure 65. Super Slab Joint[24]

Figure 66. FHWA CPTP Slab Joint, with Early Grout Damage[21]

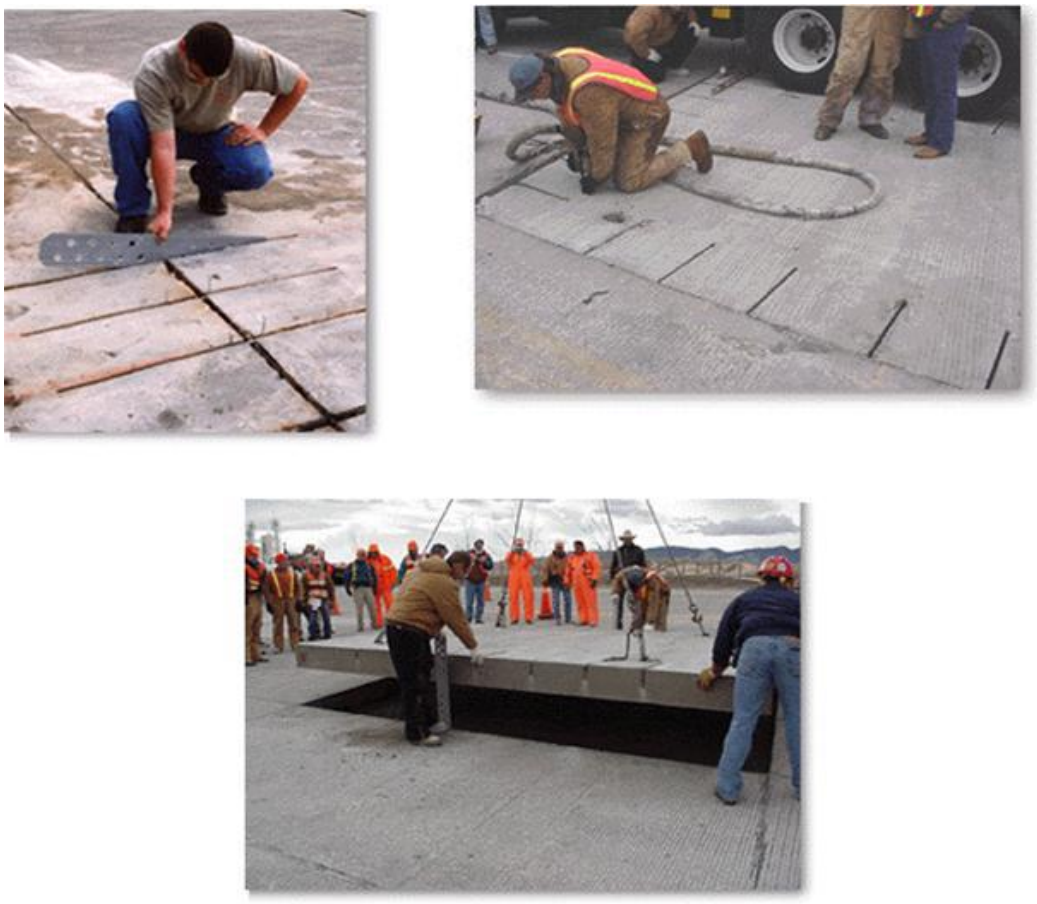

Figure 67. Uretek's Stitch-In-Time Slab Joint[23]

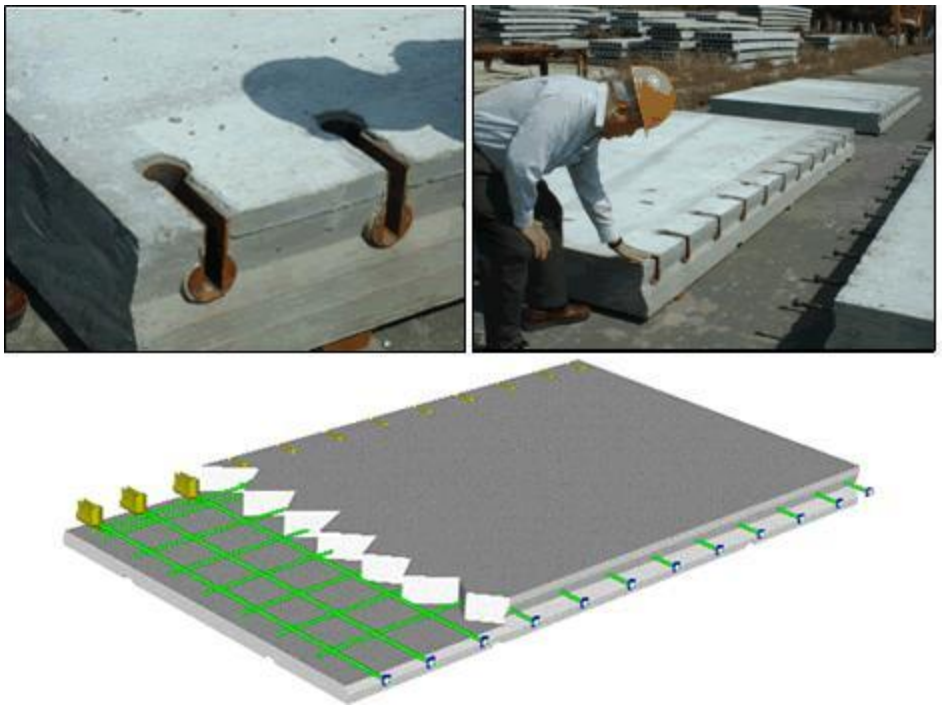

Figure 68. Kwik Slab System[33]

Many popular concrete pavement repair methods use drop-in slab patches that are considerably stronger than the original concrete. This is a concern in the fact that the original cause of the damaged pavement is often likely associated with the location of the damage or defect. And the inserted slab can act as a stress concentration. The repair location may be a site of stress concentration due to:

- ➔ Weak or defective roadbed
- ➔ Water ingress or collection
- ➔ Poor thermal strain relief (from defective expansion joints (too narrow or debris contamination))
- ➔ Susceptibility to freeze thaw cycling

- ➔ Abrupt change in friction coefficient between concrete and base
- ➔ Thermal-material properties
- ➔ Formation faults or earth movements
- ➔ Surrounding pavement affects/defects
    - o Neck downs in pavement thickness
    - o Poor or abrupt changes in concrete mixture properties (aggregate with poor bonding properties (river gravel or quartz), contaminants, too dry or too wet mixtures, etc.)
- ➔ Poor or abrupt changes in concrete curing due to weather
- ➔ Poor, or abrupt changes in, reinforcement due to rebar quality
- ➔ Poor, or abrupt changes in, bond between rebar and concrete
- ➔ Defective dowel joints (no lubrication or misalignment)
- ➔ Horizontal cracking (below surface…often due to above causes)

So a patch may need to be expanded much further than the area of damage because the patch can act to increase strain relief at the patch site. When using the existing pavement for retention, with low (or zero) prestress levels, that can concentrate more stress on neighboring pavement causing future damage. However restraint anchors could be added to the surrounding pavement in the form of grouted piers that are formed through holes drilled into and under the existing pavement; similar to the retention dam structures.

There is a recent example of a precast and post-tensioned pavement study: conceived by Neil Cable working together with the Center for Transportation Research (CTR). It is considered an option for rapid road repair but not for patches, rather for extended pavement sections. It consists of a body of various configuration options. Overall it is a combination of various well established post tensioning methods applied to pavement. It also contains a number of innovative details. In order to save on costs as

well as improve speed of construction relatively low levels of prestressing were used, especially in the longitudinal direction. Longitudinally the stress levels were set at 120psi maximum. An experimental study funded by a Federal Highway Administration (FHWA) was conducted by CTR, which resulted in the construction of a 701m long precast prestressed concrete pavement pilot project near Georgetown, Texas, in spring 2002[23]. A total of 339 panels were used. Each panel was 10 ft long, some were full width (11.0 m) and others were partial width. Panels were post-tensioned in 76.2m sections. Each 76.2m section took about 6 hours to place on two inch hot-mix asphalt (HMA) leveling course covered with polyethylene sheeting for friction reduction. These slabs achieved acceptable ride quality, and diamond grinding was not needed. This study had failures due to longitudinal cracking in the full width panels. The second FHWA funded demonstration project was conducted in California. A total of 31 panels were placed for a roadway 75.6m long. The length of the slabs was 8ft to facilitate transportation[23]. Slabs were set on a lean concrete base and then covered with polyethylene sheeting to reduce friction. Placement of the 37.8m post- tensioned section took about 3 hours. The surface was then diamond ground for smoothness. The primary differences between the proposal pavements, composed of the EB and MS joint systems, and the Neil Cable system are the joints and means of prestressing; as well as the prestressing pressure level[24]. The Neil Cable joint is a grouted key joint and as discussed in section 1.2, if the grout fails the joint is not designed to open. It is simply meant to aid in permanently bonding two slabs together. As opposed to the proposed joints they cannot aid in tensile stress relief or in reducing compressive stress concentrations as the proposed joint can. Also because the MS and EB joints are not bonded post-compression is a prestressing option open to these new systems.

The following factors need to be considered when assessing the use of precast concrete pavement as a viable candidate for rapid repair of concrete pavements:

1. Fabricating the precast concrete panels at a nearby plant, to reduce cost and to reduce traffic disruptions
2. Site access for heavy cranes
3. Rapid removal of old pavement
4. Rapid preparation of the base/subgrade
5. Installing precast concrete panel on finished base/foundation
8. Matching adjacent pavement surface grade as closely as possible.
9. Interconnecting precast concrete panels and existing pavement using a mechanical load transfer system/joint
10. Injecting bedding grout to firmly seat panels, as applicable.

Considering the base, or bedding and slab seating, one successful method is to pump grout under the precast elements after they are placed and held in precise position as the grout cures. A means of holding the precast slabs in position is with leveling frames set above the slabs that are coplanar with the adjacent slabs.

In order to implement rapid road repair with precast elements it is necessary to have as much of the pavements materials prepared in advance prior to starting the repair work. Also all the tools, equipment and personnel must be prepared and deployed efficiently. Given the short repair timeframes any delays or errors could be very costly.

The following is a square patch proposal using the concepts developed above in the previous section, using EB and MS joining, as applied to pavement repair. Figure 70 illustrates this proposal and the assembly steps for the square pavement patch. This proposal is composed of four triangular slabs which mate to the existing pavement via MS joints and mate to each other along the other edges, running from corners to center, with EB joints. The process of assembly is similar to that of other current methods of drop-in slab repair.

Firstly the damaged area is cut from the pavement within a square section. The cut is done with a diamond saw with the aid of a saw cutting jig in order to make a precision cut. Next the edges of the hole would be ground to form chamfers on all eight edges. This grinding would likewise need to be done with a precision grinding jig. Then the MS joint end cap plates would be fitted to the cut hole faces. The end caps are secured to the concrete with a series of anchor studs. The end cap plates are predrilled to act as a drilling jig for the anchors. Before drilling, all four plates would be clamped into precise alignment to the top surface of the pavement, and to each other. After drilling the anchor studs are installed into the concrete. Then the backs of the plates are buttered with fast curing grout before being replaced into position, again with alignment clamps. After sufficient time has elapsed for the grout to cure, nuts and washers are tightened onto each anchor stud. Next the top of the base would be prepared by leveling and smoothing. Also self leveling bedding sand could be applied. Next the triangular slabs would be placed into the opening, either one at a time or ganged together. The slabs would be held in alignment to the top surface with a leveling frame. At this point one of the slabs would be forced into the other slabs in order to impart a post-compression pressure, in the same way as was described in the multi-directional prestressing process (section 6.2.4). A means of generating the compressive force would be to use a flat-jack bladder between the triangular slab concrete and the end cap which would also act as the rubber layer (see figure 71).

These types of flat-jacks are used in various structures currently. In the railroad track illustrated in figure 69, resin is pumped into the bladders beneath the rail support structures for precise-permanent leveling of the track. In the mining column example there is a bladder between the top of the support column and the mine ceiling which is being filled with grout at a prescribed pressure to preload the ceiling.

After the prestressing process, and while the leveling frame is still attached, bedding grout can be injected under the slabs in order to create a stronger and more

precise base. At this point the leveling frame is removed and the pavement is ready for regular use.

The leveling frame could also act as slab hoist, saw cut jig, chamfer grinding jig, peripheral end cap grouting fixture, and bedding sand leveling jig. This would be very helpful for speed of pavement repair. However this multipurpose device would be most applicable to smaller patch sizes. For larger extended sections many of these functions could be combined into a single framed device; however the end cap grout fixturing could be very difficult or not feasible.

On large patches with many elements, the slab elements themselves could be used for the alignment clamping during the peripheral end cap grouting. Temporary flat-jacks could be used to push the elements into their interlocked positions. Then only the peripheral elements would need to be temporarily removed in order to tighten the nuts onto to the anchor studs.

Part, or all, of the prestressing forces could be absorbed by tendons running through the triangular elements. If the patch is close to, or at the edge of the pavement then there would not be a way to generate a compressive/prestressing force between the patch slabs and the existing pavement, at least not in all directions. Therefore in many cases it would be necessary to use tendons to restrain the segments that make up a patch.

As shown in figure 70 grooved rubber layers along with grooved sheet metal would mate together to form the EB joint interfaces between all the interior joints. The rubber should be lubricated before the prestressing process. Soapy water could be a good candidate. However MS joints could be used throughout as well. The MS joints would need to be lubricated. High pressure grease could work for this application.

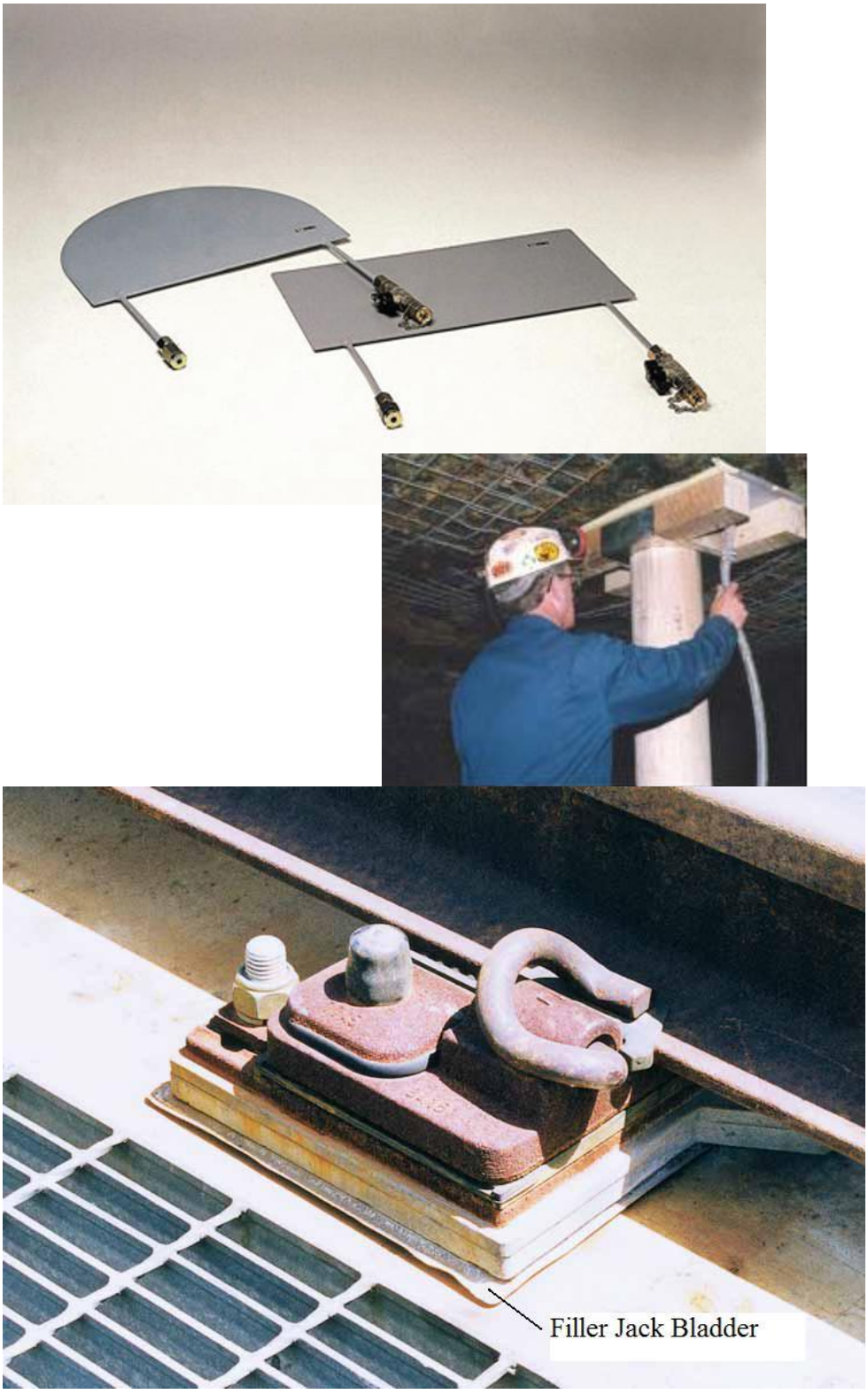

Figure 69. Flat-Jacks[34]

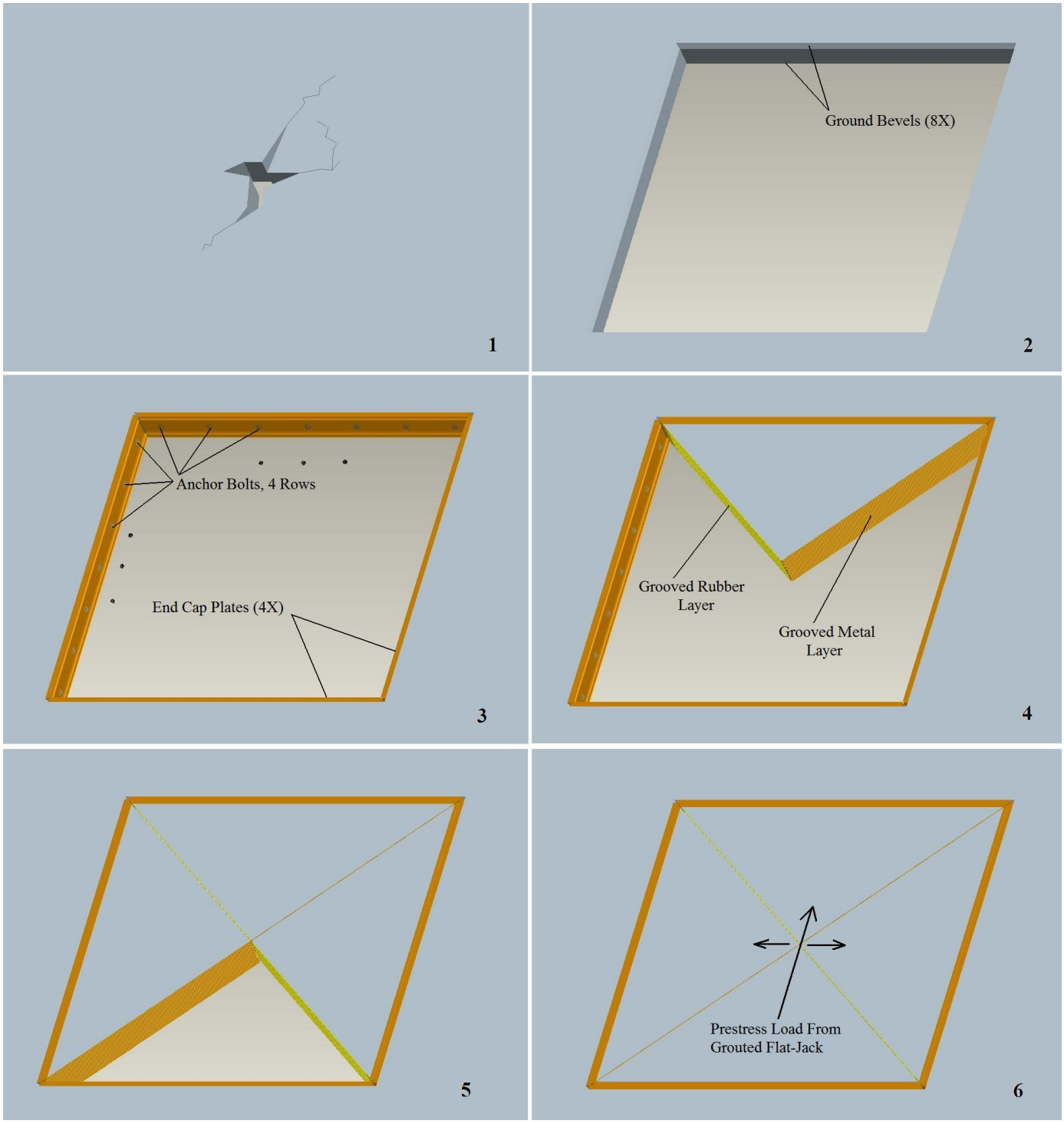

Figure 70. Square Patch Proposal

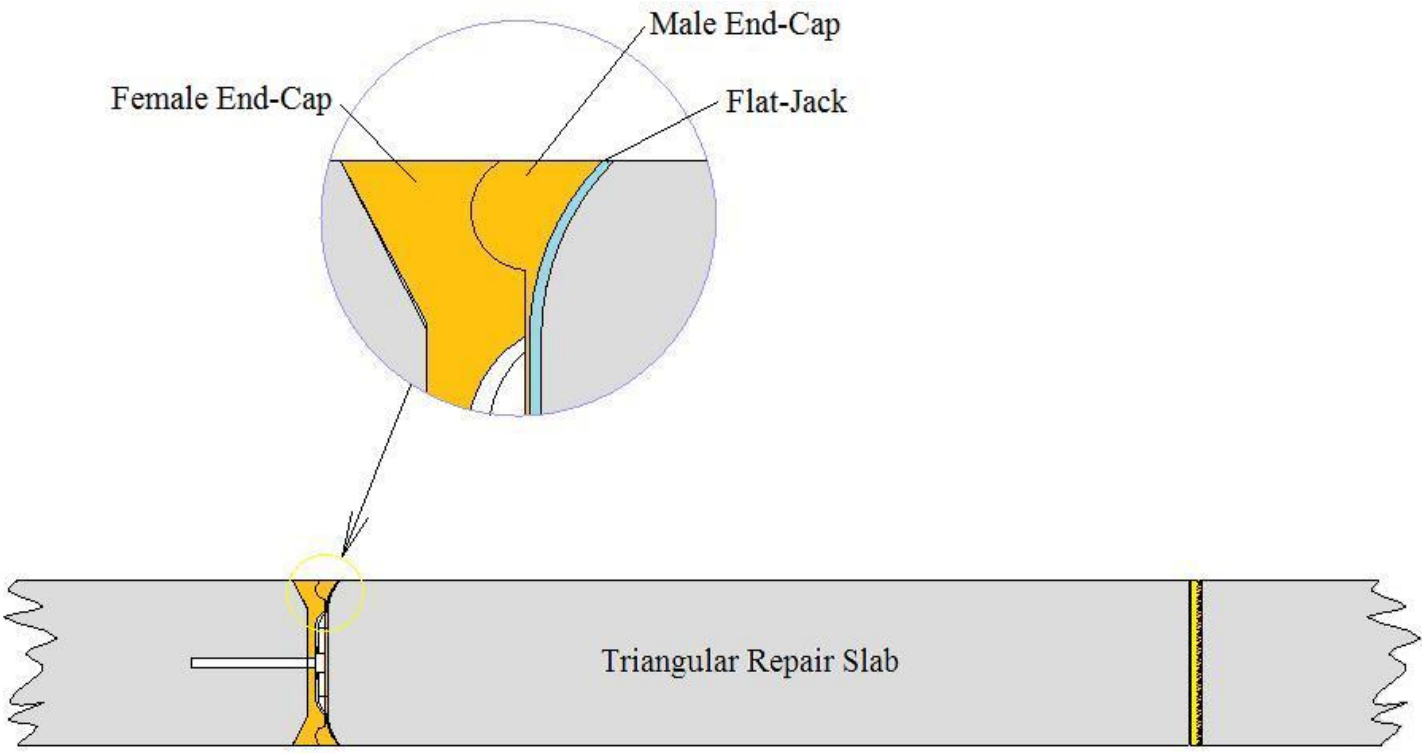

Figure 71. Square Patch Cross-Section, With Flat-Jack Detail

Chapter 7: Summary and Future Work

In conclusion a number of important advantages were revealed for the new proposed joint systems:

- ➔ Cost savings
- ➔ Increased strength
- ➔ Increased overload capabilities
- ➔ Longer life
- ➔ Ease of repair
- ➔ Applications to a broad variety of structures, many new to prestressed assemblies

From the results of the sign post study both hypotheses were proven. Essentially that the proposed joint systems achieve lower costs and higher strength, compared to current conventional prestressed concrete. The EB joint should improve strength by 54% or reduce costs by at least 13%, compared to current prestressed concrete structures. The MS joint structure should improve strength by 73% or reduce costs by at least 11%. These results provide a strong motivation to construct actual prototypes for poles, towers and columns, to test the joints experimentally. Subsequently other structural elements could be prototyped and evaluated, such as beams, slabs, and multidimensional blocks. These experimental trials could help to confirm the FEA results.

Worldwide many billions of dollars could be saved due to material costs alone. Based upon a rough estimate of worldwide concrete consumption of 2.3 billion tons/year or over $50 billion in concrete costs, there is a large amount of money that could be saved[25].

The proposed joining structures have a potential for much greater overload capabilities when compared to current conventional prestressed concrete structures; this is especially true for the MS joining system. Various extreme overload situations face a

large percentage of all concrete structures. Natural disasters such as wind storms, earthquakes and floods cause tremendous damage and are a constant threat. Hurricanes cause a mean annual property loss of approximately $5 billion, in the United States[26]. Losses associated with Earthquakes are $2.5 billion average annually[27]. The loss of human life is of course another very strong motivation for higher survivability structures.

Long term reliability can be vastly improved due to the elimination of typical reinforced concrete cracking and the cyclic deterioration that accompanies the typical cracks. The proposed joints provide stress relief as typical cracks do but without the detrimental effects. One of the primary motivations for current segmental structures is stress relief at the joints. For structures such as JCP where prestressing is not used joint integrity requires relatively expensive elements such as doweled joints or expansion joints. For the cases where the structures are prestressed such as with segmental post-tensioned bridges, the prestressing works to prevent tensile stresses which in turn help prevent cracking. However when the structures are overloaded to the point that tensile stresses develop, the typical bonded key joints provide poor, or no stress relief. The EB and MS joint structures provide stress relief along with prestressing.

Structural repair of segmental structures is inherently easier due to the ease of replacing segments. Depending upon the particular structure, removal and replacement of segments can be simple or difficult. Temporarily removing the prestressing within a section and then disengaging the connector elements between the segments will allow their removal. If these steps are simple then the repair can be done quickly and inexpensively. The post-compression pavement presented in chapter 6 offers a system where the prestressing can be quickly removed, and reapplied. And because there are no tendons running through the segments disconnecting the elements from each other is done simply by shifting the segments a small distance relative to each other after destressing. For more complex structures such as buildings which must remain in service

during repairs, the higher strength and resiliency of the proposed joint systems should aid greatly.

Large potential exists for further optimization of the joint geometries:
The results of the studies on the proposed joint systems indicate the potential for further material reduction, i.e. reduce costs further, and simultaneously improving structural strength. Automated geometric optimization can be performed to minimize costs while improving strength for all types of structures.

However there are a number of limitations in the analyses of this introductory study; they were listed in section 1.3. In future studies these limitations should be explored. An expanded cost model would be very useful in refining the economic attractiveness of the proposed systems. An accurate cost model is especially important in regard to the pavement costs and the novel structural elements. One novel set of elements are the retention dam concepts. Along with more detailed cost studies experimental trials could also be conducted. In the process of building functional, in service prototype installations, the costs and performance data can be collected. Later the experimental results can be compared to the prior analyses. For pavement proposals critical functional questions can be answered such as soil creep with retention dam installations, LTE's and vertical temperature gradient effects.

Future studies could explore Reactive Structures that utilize the various aspects of the proposed joint systems. One area to explore is the tendon positioning internally (as discussed in chapter 5), such as variable tendon eccentricity which could be controlled via solenoid locking at joints. That is the tendons could be locked to the central longitudinal axis but allowed to move off center towards the outer edges or pivots of the joints, under various loading conditions. This would allow variable compliance throughout a structure that could in turn aid in dynamic dampening.

An important new area of study is Performance Based Seismic Design (PBSD). PBSD is a building design approach which employs the concept *of performance*

objectives. A performance objective is the specification of an acceptable level of damage to a building if it experiences an earthquake of a given severity. This creates a "sliding scale" whereby a building can be designed to perform in a manner that meets the owner's economic and safety goals. A single performance objective that requires buildings remain operational even in the worst possible earthquakes will result in unreasonably high costs. On the other hand, a design where life safety is the only consideration may not adequately protect the economic interests of building stakeholders[38]. To achieve performance objectives required by the building owners, while simultaneously achieving their budget constraints, may be difficult or not possible with current construction technologies.

The proposed joint, and segment, systems may offer a series of construction options that could help achieve difficult performance objectives. The proposed systems offer various novel aspects of: widely distributed dampening, diverse segmentation options and, new forms of distributed variably reactive functions, mentioned above. Therefore the application of the proposed systems to the arena of PBSD holds a great potential for future study.

As discussed in chapter 5, stronger concrete could help allow the mechanistic mode in many MS joint structures. High Performance and Ultra-High Performance Concrete (UHPC) could help because many types of these new concretes offer considerably higher compressive and tensile strengths. If the casting process for the segments is done in a factory setting, then the use of these mixtures is greatly facilitated. The mixtures tend to be more difficult to make and to cast than conventional concrete. This is because of the very low water content as well as the need to achieve very good compaction during casting. From the FEA studies done in this dissertation it is evident that the stresses tend to develop on the outer surfaces of the concrete segmental elements. Therefore it may be possible to develop various methods of casting the high strength mixtures into just these outer surface areas while subsequently casting less costly

conventional mixtures into the interior zones. Centrifugal casting is often used for casting UHPC parts and could be utilized for distributing the UHPC mix onto the outer surfaces of the segment. First a relatively small shot of UHPC could be cast into the mold. Then the mold could be rapidly spun in various axes in order to distribute a layer of the UHPC against the interior surfaces of the mold. Then after a short time period of time a shot of conventional, low cost, concrete could be charged into the mold to complete the segment.

Table 5. A Typical UHPC composition[39]

Material	Amount (kg/m3 (lb/yd3))	Percent by Weight
Portland Cement	712 (1,200)	28.5
Fine Sand	1,020 (1,720)	40.8
Silica Fume	231 (390)	9.3
Ground Quartz	211 (355)	8.4
Superplasticizer	30.7 (51.8)	1.2
Accelerator	30.0 (50.5)	1.2
Steel Fibers	156 (263)	6.2
Water	109 (184)	4.4

Additional details to study further (MS joint systems):

- ➔ Lubrication
- ➔ Tendon Details, such as power cables verse 7-strand tendons
- ➔ Leash Details
- ➔ Tendon Networks

Future studies can have an expanded scope that includes virtually any structural application. Other future applications may include, but not limited to:

- ➔ Buildings
- ➔ Bridges
- ➔ Towers

- ➔ Vehicle frames
    - Cars
    - Aircraft
    - Trains
    - Ships
- ➔ Railroad: ties, composite rails…
- ➔ Robotics
- ➔ Crash Barriers
- ➔ Furniture
- ➔ Tunnel application: Currently large diameter tunnel walls are constructed of segments which often need sealing along all joints. EB joining can inherently accomplish the sealing and provide more robust tunnels; especially in regard to seismic loading.
- ➔ Artificial Bones and Joints: Interestingly there are a number of parallels between the proposed joining systems and biological skeletal systems. The most important similarity being between the elastomeric layers and hyaline cartilage. Hyaline cartilage is simple in structure, with no nerves or blood vessels. It has high elasticity and helps cushion and protect bones[29]. As can be seen in figure 72 the hyaline layers are at the interface of the joints and transmit the total stress loading. Other general similarities include:
    - Skeletal systems are segmental
    - The tensile elements are tendons; running mostly on the exterior of the bones
    - The bones act mostly as compressive elements. Compressive strength of bone is over twice its tensile strength[28].

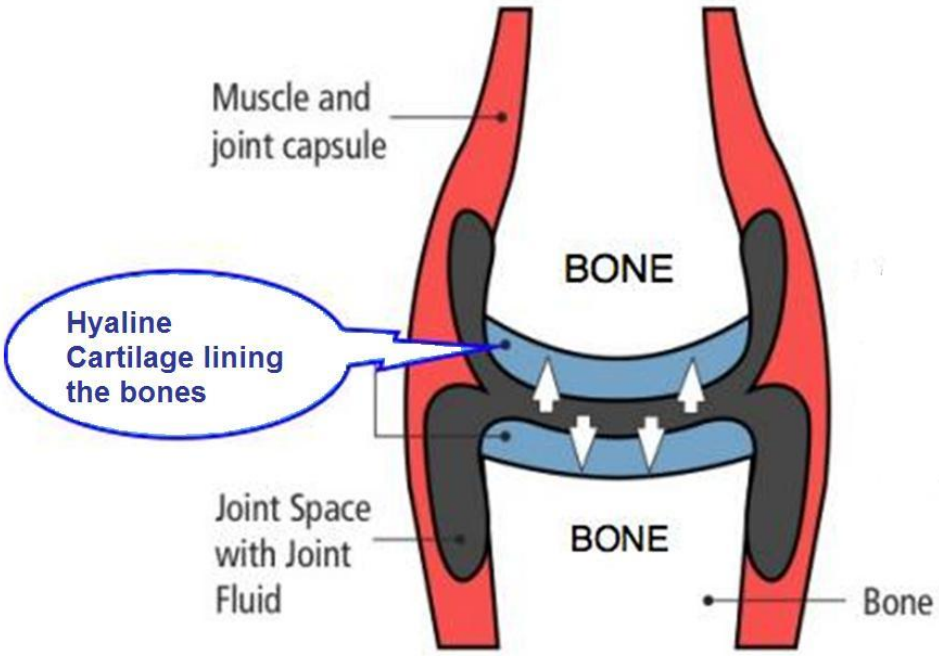

Figure 72. Cross Section of Human Skeletal Joint[34]

Appendix A:

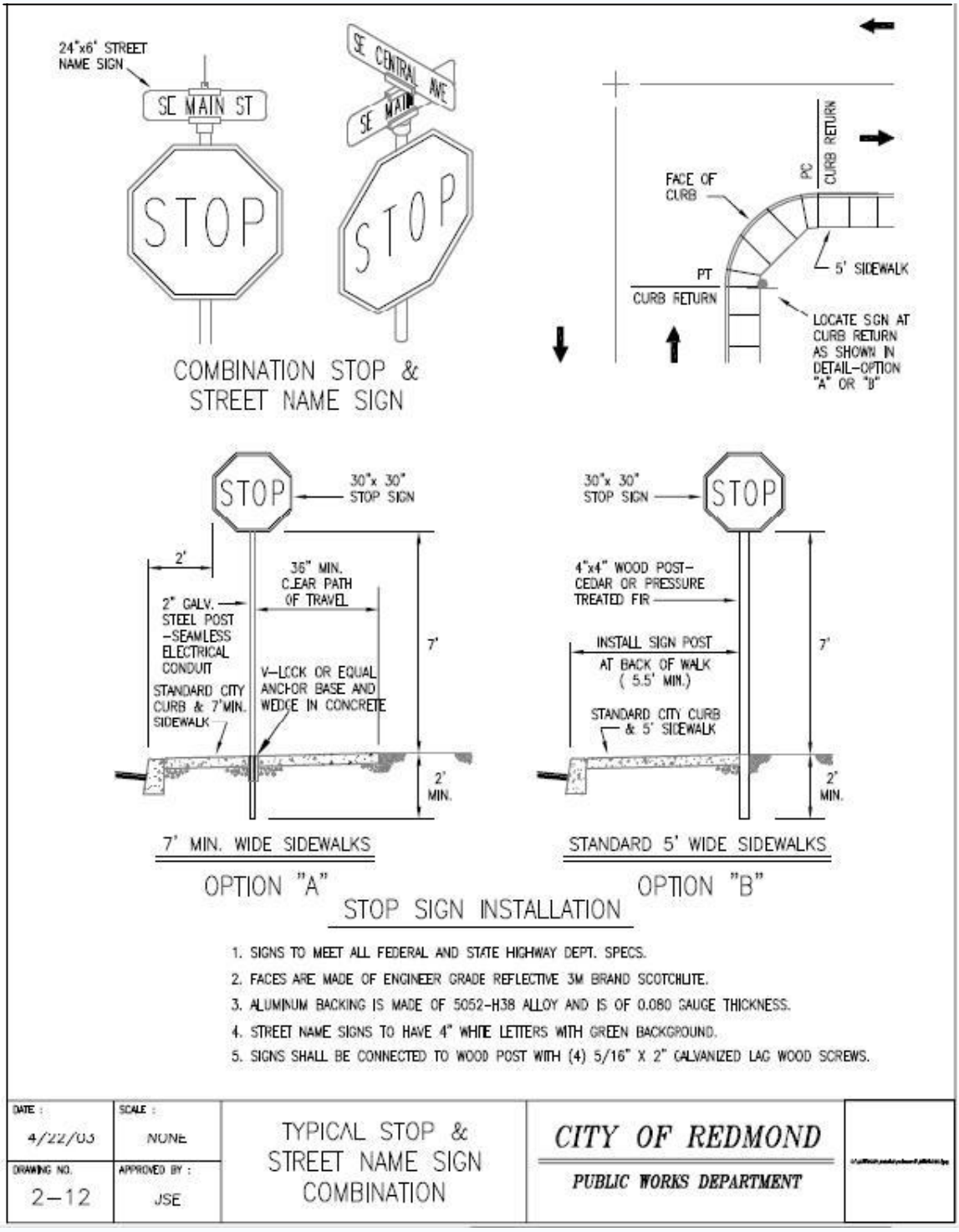

Antler Ridge – Phase 1, Details, Redmond Oregon

Appendix B:

$th_{R\_0} := 3$ $th_{R\_1} := 3$ $th_{R\_2} := 3$ $th_{R\_3} := 3$ $th_{R\_4} := 3$

$L_{c\_and\_steel\_1} := 3658$ $L_{c\_and\_steel\_2} := 3658$ $L_{c\_and\_steel\_3} := 3658$ $L_{c\_and\_steel\_4} := 3658$

$P_{C\_1} := 6.89476 \times 10^{6}$ $P_{C\_2} := 6.89476 \times 10^{6}$ $P_{C\_3} := 6.89476 \times 10^{6}$ $P_{C\_4} := 6.89476 \times 10^{6}$

$L_{T\_0} := 3661$ $L_{T\_f} := 3660$

$E_R := 0.1 \cdot 10^{9}$ $\alpha_C := 12 \cdot 10^{-6}$ $\Delta T := 25$ $E_C := 2.99922 \times 10^{10}$ $L_{c\_and\_steel\_0} := 3657.6$

Given

$th_{R\_0} < 10$

$P_{C\_4} < 1.10316 \times 10^{7}$

$P_{C\_3} > 34474$

$th_{R\_0} + L_{c\_and\_steel\_0} = L_{T\_0}$

$th_{R\_1} + L_{c\_and\_steel\_1} = L_{T\_f}$

$$P_{C\_1} = \frac{L_{c\_and\_steel\_0} - L_{c\_and\_steel\_1}}{L_{c\_and\_steel\_0}} \cdot E_C$$

$$P_{C\_1} = \frac{th_{R\_0} - th_{R\_1}}{th_{R\_0}} \cdot E_R$$

$th_{R\_2} + L_{c\_and\_steel\_2} = L_{T\_f}$

$$P_{C\_2} = \frac{L_{c\_and\_steel\_0} - L_{c\_and\_steel\_2}}{L_{c\_and\_steel\_0}} \cdot E_C$$

$$P_{C\_2} = 0.65 \cdot \frac{th_{R\_0} - th_{R\_2}}{th_{R\_0}} \cdot E_R$$

$th_{R\_3} + L_{c\_and\_steel\_3} = L_{T\_f}$

$P_{C\_3} = P_{C\_2} - \alpha_C \cdot \Delta T \cdot E_C$

$$th_{R\_4} + L_{c\_and\_steel\_4} = L_{T\_f}$$

$$P_{C\_4} = P_{C\_2} + \alpha_C \cdot \Delta T \cdot E_C$$

$$P_{C\_4} = 0.65 \cdot \frac{th_{R\_0} - th_{R\_4}}{th_{R\_0}} \cdot E_R$$

$$V := \text{Minerr}\left(th_{R\_0}, th_{R\_1}, th_{R\_2}, th_{R\_3}, th_{R\_4}, L_{c\_and\_steel\_1}, L_{c\_and\_steel\_2}, L_{c\_and\_steel\_3}, L_{c\_and\_steel\_4}, P_{C\_1}, P_{C\_2}, P_{C\_3}, P_{C\_4}, L_{T\_0}, L_{T\_f}\right)$$

$V =$

	0
0	3.251435
1	3.016206
2	2.926387
3	3.188533
4	2.62687
5	$3.656718 \cdot 10^3$
6	$3.656808 \cdot 10^3$
7	$3.656545 \cdot 10^3$
8	$3.657107 \cdot 10^3$
9	$7.234624 \cdot 10^6$
10	$6.498106 \cdot 10^6$
11	$1.257489 \cdot 10^6$
12	$1.248579 \cdot 10^7$
13	$3.660851 \cdot 10^3$
14	$3.659734 \cdot 10^3$

Appendix C:

Mooney-Rivlin form[11]

The form of the Mooney-Rivlin strain energy potential is

$$U = C_{10}(\overline{I}_1 - 3) + C_{01}(\overline{I}_2 - 3) + \frac{1}{D_1}(J^{el} - 1)^2,$$

where *U* is the strain energy per unit of reference volume; C_{10}, C_{01}, and D_1 are temperature-dependent material parameters; $\overline{I}_1$ and $\overline{I}_2$ are the first and second deviatoric strain invariants defined as

$$\overline{I}_1 = \overline{\lambda}_1^2 + \overline{\lambda}_2^2 + \overline{\lambda}_3^2 \qquad \text{and} \qquad \overline{I}_2 = \overline{\lambda}_1^{(-2)} + \overline{\lambda}_2^{(-2)} + \overline{\lambda}_3^{(-2)},$$

where the deviatoric stretches $\overline{\lambda}_i = J^{-\frac{1}{3}}\lambda_i$; *J* is the total volume ratio; J^{el} is the elastic volume ratio from thermal expansion (however thermal expansion was not included in any analysis); and λ_i are the principal stretches. The initial shear modulus and bulk modulus are given by

$$\mu_0 = 2(C_{10} + C_{01}), \qquad K_0 = \frac{2}{D_1}.$$

Bulk modulus (K) • Young's modulus (E) • Lamé's first parameter (λ) • Shear modulus (G) • Poisson's ratio (ν) • P-wave modulus (M)

$$K = \frac{2G(1+\nu)}{3(1-2\nu)}$$

Using ν = 0.4942 for Neoprene or EPDM.

Midwest ANSYS Users Group
May 18, 2005
Analyzing Hyperelastic Materials *w/ Some Practical Considerations, 2005*

Prepared by: Paris Altidis; Borg Warner
Updated by: Vince Adams; IMPACT

Mooney Rivlin Parameters - METRIC

Shore-A [°]	Young's Modulus [N/mm2]	Shear Mod (G [N/mm2]	C10 [N/mm2]	C01 [N/mm2]
35	1.102	0.406	0.162	0.041
36	1.148	0.407	0.163	0.041
37	1.199	0.412	0.165	0.041
38	1.255	0.421	0.168	0.042
39	1.315	0.435	0.174	0.044
40	1.381	0.452	0.181	0.045
41	1.452	0.473	0.189	0.047
42	1.530	0.496	0.198	0.050
43	1.613	0.523	0.209	0.052
44	1.703	0.551	0.220	0.055
45	1.800	0.581	0.232	0.058
46	1.904	0.613	0.245	0.061
47	2.015	0.647	0.259	0.065
48	2.134	0.682	0.273	0.068
49	2.261	0.718	0.287	0.072
50	2.397	0.755	0.302	0.076
51	2.540	0.793	0.317	0.079
52	2.693	0.832	0.333	0.083
53	2.855	0.872	0.349	0.087
54	3.026	0.914	0.366	0.091
55	3.207	0.956	0.382	0.096
56	3.398	0.999	0.400	0.100
57	3.599	1.043	0.417	0.104
58	3.811	1.089	0.436	0.109
59	4.034	1.136	0.454	0.114
60	4.268	1.185	0.474	0.118
61	4.513	1.236	0.494	0.124
62	4.771	1.289	0.516	0.129
63	5.040	1.345	0.538	0.135
64	5.322	1.403	0.561	0.140
65	5.616	1.465	0.586	0.147
66	5.924	1.531	0.612	0.153
67	6.244	1.600	0.640	0.160
68	6.579	1.675	0.670	0.168
69	6.927	1.754	0.702	0.175
70	7.289	1.839	0.736	0.184

$E\ (psi) = 11.427*A - 0.4445*A^2 + 0.0071*A^3$

References

1. Buyukozturk O et al. *Shear behavior of joints in precast concrete segmental bridges*. ASCE Journal of Structural Engineering 1990; 3380–401.

2. Bashir,M. (2007). *Development of Design Method of Connection (Steel Box Filled with Concrete) by using 3-D Finite Element Analysis*. Unpublished thesis, University of Engineering & Technology, Lahore.

3. Arnold, Stuart et al. *A test method and deterioration model for joints and cracks in concrete slabs*. Cement and Concrete Research (December 2005), 35 (12), pg. 2371-2383.

4. Englekirk, Robert E. (2003). *Seismic design of reinforced and precast concrete buildings*. Hoboken, NJ : Wiley.

5. Yazdani N, Eddy S, Cai CS. *Effect of bearing pads on precast prestressed concrete bridges*. Journal of Bridge Engineering ASCE 2000;5(3):224–32.

6. FDOT, 2009. *Stiffness Evaluation of Neoprene Bearing Pads Under Long Term Loads*. Report No. BD545 RPWO #39, Florida Department of Transportation.

7. MODOT, 2003. *Bearing Pads for Structures*. Section 1038, Missouri Department of Transportation.

8. Othman AB. *Property profile of a laminated rubber bearing*. Polym Test 2001;20:159–66.

9. Carr, A.J., Cooke, N., Moss, P.J. *Compression behavior of bridge bearings used for seismic isolation.* Eng. Struct. 1996:18, 351–362.

10. Libby JR. (1990). *Modern prestressed concrete: design principles and construction methods.* New York: Chapman and Hall.

11. ABAQUS Manual 6.8.

12. Everard, Noel J. (1993). *Reinforced Concrete Design, 3rd Edition, Schaum's Outlines.* New York: McGraw-Hill.

13. Stern, Sylvan P. (1959). *Elements of reinforced concrete.* Englewood Cliffs, N. J.: Prentice-Hall.

14. FHWA, 2000. *The Feasibility of Using Precast Concrete Panels to Expedite Highway Pavement Construction.* Research Report Number 1517-1, Federal Highway Administration.

15. Polak, E. (1997). *Optimization: algorithms and consistent approximations*. New York: Springer-Verlag.

16. Janoo, V., Irwin, L., Haehnel, R., 2003. *Pavement subgrade performance study.* ERDC/CRREL TR-03-5. U.S. Army Engineer Research and Development Center, Cold Regions Research and Engineering Laboratory, Hanover, New Hampshire.

17. FDOT, 2009. *Impact of Wide-Base Single Tires on Pavement Damage*. Research Report No. 09-528. Florida Department of Transportation.

18. Harvey, John et al. *Performance of Dowel Bar Retrofitted Concrete Pavement Under HVS Loading.* Paper No. 03-4161. Transportation Research Board 2003

19. USACE, 1999. *Lubricant and Hydraulic Fluids*. Pub. Number EM 1110-2-1424. US Army Corps of Engineers.

20. USACE, 1975. *On The Theory of Ground Anchors*. Document No. AD/A-O06 582. US Army Corps of Engineers.

21. Hossain, Shabbir et al. *Evaluation of Concrete Pavement Repair Using Precast Technology in Virginia.* National Conference on Preservation, Repair, and Rehabilitation of Concrete Pavements 2009; Part 5.

22. Burak, R. J. *Segmental Concrete Pavements for Municipal and Heavy Use Industrial or Port Applications.* 2nd Material Specialty Conference of the Canadian Society for Civil Engineering, Montreal, 2002

23. FHWA, 2004. *Using Precast Concrete Panels for Pavement Construction in Indiana*. Publication No.: FHWA/IN/JTRP-2003/26, SPR-2779, Federal Highway Administration.

24. Tayabji, Shiraz et al. *Precast Concrete Pavement for Intermittent Concrete Pavement Repair Applications*. National Conference on Preservation, Repair, and Rehabilitation of Concrete Pavements 2009; Part 5.

25. Block, Ben (2010). *Life-Cycle Studies: Concrete* (Worldwatch Institute). Retrieved from http://www.worldwatch.org/node/6412

26. Pielke, R. A. et al. *Evaluation of catastrophe models using normalized historical records*. Journal of Insurance Regulation (1999), Vol. 18, No. 2, 177-194.

27. Vranes, Kevin. *Normalized Earthquake Damage and Fatalities in the United States: 1900–2005*. Natural Hazards Rev (August 2009). Volume 10, Issue 3, pp. 84-101

28. Evans, F. Gaynor and Lissner, Herbert R**.** *Tensile and Compressive Strength of Human Parietal Bone*. J Appl Physiol (1957). 10: 493-497

29. Jeffrey, D. R. *Imaging hyaline cartilage*. The British Journal of Radiology (2003). Volume 76, pp. 777-787.

30. James M. Kelly and Juan C. Simo. *Finite element analysis of the stability of multilayer elastomeric bearings*. Engineering Structures (July 1984). Volume 6, Issue 3, 162-174

31. C. W. Macosko. (1994). *Rheology: principles, measurement and applications*. Weinheim Germany: VCH Publishers.

32. TABLE C-l Friction Coefficient for Concrete Cast on Soil (references 4). (2011). Retrieved from http://www.tpub.com/content/USACETechnicalletters/ETL-1110-3-446/ETL-1110-3-4460006.htm

33. Kwik Slab – Interlocking Roadway Systems. (2011). Retrieved from http://www.kwikslab.com/applications.htm

34. Google Images. (2011). Public domain off Google Images http://www.google.com/imghp?hl=en&tab=wi

35. Horn, John R. 2004, *Extendible hinge*, US Patent 6766562**.**

36. Mahoney, Thomas H. 2007, *Basketball breakaway goal release apparatus*, US Patent 7214148.

37. Li, Ran 2002, *Prestressed pavement system*, US Patent 6409423.

38. FEMA, 2007. *Action Plan for Performance Based Seismic Design*. Publication No.: FEMA 349, Federal Emergency Management Agency.

39. FHWA, 2006. *Structural Behavior of Ultra-High Performance Concrete Prestressed I-Girders*. Publication No.: FHWA-HRT-06-115, Federal Highway Administration.

Curriculum Vita

Ralph Jensen earned his Bachelor of Engineering degree in Mechanical Engineering from the University of Texas at El Paso in 1987. He received his Master of Science degree in Mechanical Engineering in 2005 from the University of Texas at El Paso. In 2005 he joined the doctoral program for Infrastructures Engineering.

Dr. Jensen has been the recipient of numerous honors and awards such as receiving an Amoco Academic scholarship, a member of the Dean's list, Honors Society and the Marshal of the Graduate School of Engineering in 2005.
He also maintained a 4.0 GPA throughout his Master's and PhD studies.

While pursuing his degree, Dr. Jensen worked as the Global Director of Engineering for Axxion Corporation. He also worked as an RA and instructor at UTEP.

Dr. Jensen's dissertation entitled, "Improved Joining Method for Segmental Prestressed Structures," was supervised by Dr. Louis Everett. He intends on continued post-doctoral work to further the development of his research.

Permanent Address: 1712 Lazy Lane
El Paso, Texas 79902